ESAIM: M2AN 60 (2026) 1177–1215
https://doi.org/10.1051/m2an/2026031

ESAIM: Mathematical Modelling and Numerical Analysis
www.esaim-m2an.org

HYBRID HIGH-ORDER METHOD FOR THE EXTENDED FISHER-KOLMOGOROV AND THE FISHER-KOLMOGOROV EQUATIONS

Raman Kumar[1,2] and Neela Nataraj[1,*]

Abstract. This article analyzes hybrid high-order method for space discretization and *backward Euler* and *Crank-Nicolson schemes* for time discretization of the nonlinear extended Fisher-Kolmogorov and the Fisher-Kolmogorov equations. The critical parameter $\gamma > 0$ is incorporated in the stabilization term of the HHO method. Error estimate of order $\mathscr{O}(h^{k+1} + \Delta t)$ (resp. $\mathscr{O}(h^{k+1} + (\Delta t)^2)$ in the energy-norm for the *backward Euler* (resp. *Crank-Nicolson*) *scheme* is obtained when polynomials of order $k+2$ (resp. k) with $k \geq 0$ are utilized to approximate the exact solution in the interior of the polygon and its traces on the boundary of the polygon (resp. normal derivative on the mesh faces). The HHO discretization for the Fisher-Kolmogorov equation, that is, when the parameter $\gamma = 0$, leads to a convergence rate of $\mathscr{O}(h^{k+2})$ in the space variable. The results of the numerical experiments validate the theoretical results.

Mathematics Subject Classification. 65N30, 65N15.

Received November 11, 2024. Accepted March 28, 2026.

1. Introduction

This article analyzes hybrid high-order (HHO) method for the numerical approximation of the extended Fisher-Kolmogorov (EFK) and the Fisher-Kolmogorov (FK) equations. The EFK model seeks $u(x,t)$ such that

$$\begin{aligned} &u_t + \gamma\Delta^2 u - \Delta u + f(u) = 0 && \text{for all } (x,t) \in \Omega \times (0,T], \\ &u = \gamma\partial_{\mathbf{n}} u = 0 && \text{for all } (x,t) \in \partial\Omega \times (0,T], \\ &u(x,0) = u_0(x) && \text{for all } x \in \Omega. \end{aligned} \tag{1.1}$$

Here Ω is an open, bounded, polygonal, Lipschitz domain in $\mathbb{R}^2$, with boundary $\partial\Omega$, the critical parameter γ lies in $[0,1]$, $f(u) = u^3 - u$, $0 < T < \infty$, T is the final time, $\mathbf{n}$ denotes the unit outward normal to $\partial\Omega$, and $u_0(x)$ represents the initial state of the system. The choice $\gamma = 0$ in (1.1) leads to the FK equation [2]. The second boundary condition is scaled by γ so that when $\gamma = 0$, (1.1) leads to the FK equation with Dirichlet boundary condition.

The model problem (1.1) for $0 < \gamma \leq 1$, introduced as an extension of the FK equation for analyzing front propagation between equilibrium states in bistable systems was proposed in [11, 16]. Some bistable systems exhibit deviations from the smooth transition between equilibria, such as uneven or periodic wave-like transitions

Keywords and phrases. Extended Fisher-Kolmogorov, hybrid high-order, backward Euler, Crank-Nicolson.

[1] Department of Mathematics, Indian Institute of Technology Bombay, Powai, Mumbai 400076, India.
[2] IMAG, CNRS, University of Montpellier, Montpellier, France.
*Corresponding author: neela@math.iitb.ac.in, nataraj.neela@gmail.com

referred to as kinks. For $\gamma \leq 1/8$, it has been noted that the solutions of the EFK equation closely resemble those of the FK equation, see for example, [2, 10, 33, 34]. But if $\gamma > 1/8$, discernible differences emerge in the solutions of these equations. The EFK equation has applications in phase transitions of binary systems [29], domain wall propagation in liquid crystals [28], and traveling waves in reaction-diffusion systems [2].

Conforming and non-standard finite element methods (FEMs) have been studied in the literature for the EFK equation. We refer to [12] for conforming FEM, [26] for the C^0 interior penalty method, [13] for the Morley finite element method, and [32] for the virtual element method. More recently, [14] discusses a mixed finite element method and [15] presents a unified approach for nonstandard FEMs using lowest-order piecewise P_2 polynomials for discretization in space variable and *backward Euler scheme* for time discretization. To the best of our knowledge, the analysis in existing literature holds when the parameter $\gamma > \frac{1}{8}$ and does not include the case $\gamma = 0$ in (1.1) that leads to the second-order FK equation.

The benefits of HHO methods are well-known: they are dimension-independent in their construction, support general meshes, include general polytopal mesh cells and non-matching interfaces, and are computationally efficient. The HHO methods were introduced in the last decade and have found applications in linear elasticity [18], diffusion [20], biharmonic problems [23, 24], Stokes problem [21], Navier–Stokes equations [3, 19], singularly perturbed problems [22], and magnetostatics [8]. Furthermore, the method is explored for quasilinear and nonlinear PDEs in [27, 31], poroelasticity [4], hyperelastic materials [1], and Leray-Lions problems [17]. For time-dependent problems, HHO methods have been developed for Sobolev equations [38], Cahn–Hillard equations [7], and wave equation [5, 6].

The HHO methods utilize discrete unknowns in the cells and the faces. The cell unknowns are locally eliminated using the static condensation techniques. The two fundamental ingredients for the HHO methods are a *reconstruction operator* that locally reconstructs a displacement field or its gradient from the local cell and face unknowns and a *stabilization operator* that weakly enforces consistency between the local face unknowns and the trace of the cell unknowns on each mesh face.

In [23], two HHO schemes are designed for the biharmonic clamped plate problems and optimal order error estimates in the energy norm are derived. The HHO-A scheme employs unequal-order HHO elements to approximate unknowns. The cell unknowns are approximated in $\mathscr{P}_{k+2}(K)$, the traces of unknown on the faces in $\mathscr{P}_{k+1}(F)$, and normal derivative of the unknowns on the faces in $\mathscr{P}_k(F)$, where $k \geq 0$, K is the polytopal element, F denotes the faces of K, and $\mathscr{P}_r(K)$ and $\mathscr{P}_r(F)$ denote polynomials of degree less than or equal to r defined on K and F, respectively. The HHO-B scheme approximates the cell unknowns in $\mathscr{P}_{k+2}(K)$, face unknowns in $\mathscr{P}_{k+2}(F)$, and the normal derivatives of the unknowns on the faces in $\mathscr{P}_k(F)$. This article adopts the HHO-B scheme [22] to handle semilinear problems with lower-order terms. The boundary conditions are weakly imposed by means of a Nitsche-boundary penalty technique [22].

The novel contributions of this article can be outlined as follows:

- The time-dependent semilinear EFK and FK equations are analyzed using the HHO scheme for space discretization and two-time discretization schemes. To the best of our knowledge, this is the *first work* that provides a unified framework for EFK and FK equations that hold for the entire range of the critical parameter, that is, $0 \leq \gamma \leq 1$.
- The existence and uniqueness of the solution to the nonlinear discrete system obtained using *HHO space* discretization and *backward Euler* (resp. *Crank-Nicolson*) time discretization scheme is established using the Brouwer's fixed point theorem.
- The *HHO space* discretization and *backward Euler* time discretization provide error estimates of order $\mathscr{O}(h^{k+1} + \Delta t)$(resp. $\mathscr{O}(h^{k+2} + \Delta t)$) in the energy-norm for the EFK (resp. FK) equation.
- The *HHO space* discretization and *Crank-Nicolson* time discretization provide error estimates of order $\mathscr{O}(h^{k+1} + (\Delta t)^2)$(resp. $\mathscr{O}(h^{k+2} + (\Delta t)^2)$) in the energy-norm for the EFK (resp. FK) equation.
- The numerical experiments validate the theoretical findings and are presented for different choices of $0 \leq \gamma \leq 1$. Optimal order convergence rates in L^2(energy) and L^∞(energy)-norms are obtained for the HHO in space and backward Euler (Crank-Nicolson) in time for EFK and FK equations.

– Though the theoretical results in this paper are designed for smooth data, the numerical experiments illustrate the adaptability of the schemes to handle non-smooth initial data.

Standard notation for Lebesgue and Sobolev spaces apply throughout the paper. For $i := (i_1, i_2)$ with $i_1, i_2 \geq 0$ and $|i| := i_1 + i_2$, $v := v(x_1, x_2)$, let $D^i v := \frac{\partial^{|i|} v}{\partial x_1^{i_1} \partial x_2^{i_2}}$. For any $K \subset \mathbb{R}^2$ and any integer $r \geq 0$, define the Sobolev space $H^r(K) := \{v \in L^2(K) : \ D^i v \in L^2(K) \text{ for } 0 \leq |i| \leq r\}$. For $v \in H^r(K)$, the associated norm and seminorm are denoted by $\|v\|_{H^r(K)} = \big(\sum_{|i|\leq r} \|D^i v\|^2_{L^2(K)}\big)^{\frac{1}{2}}$ and $|v|_{H^r(K)} = \big(\sum_{|i|=r} \|D^i v\|^2_{L^2(K)}\big)^{\frac{1}{2}}$, respectively. In particular, $D^1 v = Dv$ and $D^2 v$ denote the gradient and Hessian, respectively. The L^2 inner product and norm defined on Ω are denoted by $(\cdot,\cdot)$ and $\|\cdot\|$, respectively. For any partition $\mathscr{T}_h$ of Ω, $H^r(\mathscr{T}_h) = \Pi_{K\in\mathscr{T}_h} H^r(K)$ and $\mathscr{P}_r(K)$, is the space of polynomials of degree at most r in each K. For $r = 0$ and any cell $X := K \in \mathscr{T}_h$ or any face $X := F$ of K, denote the inner product (resp. norm) by $(\cdot,\cdot)_X$ (resp. $\|\cdot\|_X$). Let Y denote a normed space with norm $\|\bullet\|_Y$ and seminorm $|\bullet|_Y$, respectively, and $g : (0,T) \to Y$ be a measurable function. For $1 \leq r \leq \infty$,

$$\|g\|^r_{L^r(0,T;Y)} := \int_0^T \|g(t)\|^r_Y \,\mathrm{d}t, \quad 1 \leq r < \infty \ \text{ and } \ \|g\|_{L^\infty(0,T;Y)} := \operatorname{ess}\sup_{0\leq t\leq T} \|g(t)\|_Y.$$

Let $L^r(0,T;Y) := \{g : (0,T) \to Y : \|g\|^r_{L^r(0,T;Y)} < \infty\}$. This paper frequently employs the Young's inequality given by

$$ab \leq \frac{a^2}{2\varepsilon} + \frac{\varepsilon b^2}{2} \quad \text{for} \quad a, b \geq 0 \ \text{ and } \ \varepsilon > 0. \tag{1.2}$$

The notation Δt denotes the time step, whereas Δv (resp. $\Delta^2 v$) denotes the Laplacian (resp. bi Laplacian) of v. This slight abuse of notation should be clear from the context. The rest of the paper is organized as follows: Section 2 discusses the preliminaries related to the hybrid-high order method. The main results of the article are stated in Section 3. Some approximation properties that are crucial for the analysis are presented in Section 4. Section 5 discusses the proof of the discrete energy estimate. The error analysis for the backward Euler and Crank Nicolson schemes are discussed in Sections 6 and 7, respectively. The numerical results that validate the theoretical estimates are presented in Section 8.

2. HHO PRELIMINARIES

This section discusses weak formulation and the discrete setting. The three important components in the HHO setting, namely, the *local and global reduction operators*, the *local reconstruction operator*, and the *stabilizer* are introduced.

Following [22], consider the Hilbert space $V := \gamma H^2_0(\Omega) + H^1_0(\Omega)$, which is a shortcut notation for $H^2_0(\Omega)$ if $\gamma > 0$ and $H^1_0(\Omega)$ if $\gamma = 0$. Recall that $f(u) = u^3 - u$. The **weak formulation** that corresponds to (1.1) seeks $u(\bullet, t) \in V$ such that

$$(u_t, v) + \gamma \int_\Omega D^2 u : D^2 v \,\mathrm{dx} + \int_\Omega Du \cdot Dv \,\mathrm{dx} + (f(u), v) = 0 \quad \text{for all } v \in V, \ u(x,0) = u_0(x). \tag{2.1}$$

For $\gamma > 0$, the existence, uniqueness, and regularity results for (2.1) are established under the assumption that $u_0 \in H^2_0(\Omega)$. We refer to Theorem 2.1 in [12], Theorem 2.1 in [13], Lemma 2.3 and proof of Theorem 5.3 in [15] for details of proofs. The existence, uniqueness, and regularity results for $\gamma = 0$ can be derived following similar arguments as in Theorems 2.1–2.2 in [12] under the regularity assumption that $u_0 \in H^1_0(\Omega)$.

We consolidate the regularity results in the lemma below.

Lemma 2.1. (a) *($\gamma > 0$) ([13], Thm. 2.1). Suppose $u_0 \in H^2_0(\Omega)$. Then for any finite time $T > 0$, there exists a unique weak solution u such that $\gamma^{1/2} u \in L^\infty(0,T;H^2_0(\Omega))$, $u \in L^\infty(0,T;H^1(\Omega)) \cap L^\infty(0,T;L^q(\Omega))$ $(1 \leq q < \infty)$, and $u_t \in L^2(0,T;L^2(\Omega))$.*

(b) *($\gamma = 0$) [35]. Suppose $u_0 \in H_0^1(\Omega)$. Then for any finite time $T > 0$, there exists a unique weak solution u that satisfies $u \in L^\infty(0,T;H_0^1(\Omega))$ and $u_t \in L^2(0,T;L^2(\Omega))$. Moreover, if $u_0 \in H_0^1(\Omega) \cap H^2(\Omega)$, then there exists unique u such that $u \in L^\infty(0,T;H_0^1(\Omega)) \cap L^2(0,T;H^2(\Omega))$ and $u_t \in L^2(0,T;L^2(\Omega))$.*

Moreover, Lemma 2.1 and the Sobolev embedding in 2D yield $u \in L^\infty(0,T;L^q(\Omega))$, where $1 \le q < \infty$ for $\gamma > 0$ and $\gamma = 0$.

2.1. Meshes

Following the notations from [18, 23], for every $h > 0$, let $\{\mathscr{T}_h\}_h$ be a mesh family such that each mesh $\mathscr{T}_h$ consists of a finite number of non-empty disjoint open polygonal cells K with planar faces that covers Ω exactly. We partition the boundary $\mathscr{F}_K$ of any mesh cell $K \in \mathscr{T}_h$ into interior and boundary faces: $\mathscr{F}_K^{\mathrm{i}} := \overline{\mathscr{F}_K \cap \Omega}$ and $\mathscr{F}_K^{\mathrm{b}} := \mathscr{F}_K \cap \partial\Omega$. We partition the mesh as $\mathscr{T}_h := \mathscr{T}_h^{\mathrm{i}} \cup \mathscr{T}_h^{\mathrm{b}}$. The presence of hanging nodes is possible in such meshes, and the mesh-size is defined by $h := \max_{K\in\mathscr{T}_h} K$, where h_K represents the diameter of cell K. A closed subset F of Ω is denoted as a mesh face if it is a subset of an affine hyperplane H_F with positive 1-dimensional Hausdorff measure and if either of the following two conditions holds: (I) There exist $K_1(F)$ and $K_2(F)$ in $\mathscr{T}_h$ such that $F \subset \partial K_1(F) \cap \partial K_2(F) \cap H_F$. In this case, F is termed an internal face. (II) There exists $K(F) \in \mathscr{T}_h$ such that $F \subset \partial K(F) \cap \partial\Omega \cap H_F$. Here, F is referred to as a boundary face. The mesh faces are collected in the set $\mathscr{F}_h$, which is split as $\mathscr{F}_h = \mathscr{F}_h^{\mathrm{i}} \cup \mathscr{F}_h^{\mathrm{b}}$, where $\mathscr{F}_h^{\mathrm{i}}$ is the collection of the interior faces (shared by two distinct mesh cells) and $\mathscr{F}_h^{\mathrm{b}}$ the collection of boundary faces. The mesh sequence $\mathscr{T}_h$ is assumed to be shape-regular in the conventional sense [18, 23]; for any $K \in \mathscr{T}_h$ and $F \in \mathscr{F}_K$, the diameter h_F is comparable to h_K, indicating that $2\rho^2 h_K \le h_F \le h_K$, where ρ is the mesh regularity parameter. In addition, there exists an integer M_∂ depending on ρ and dimension of the domain such that $\max_{K\in\mathscr{T}_h} \mathrm{card}(\mathscr{F}_K) \le M_\partial$. For all $K \in \mathscr{T}_h$, introduce a parameter σ_K [22] defined below that depends on the mesh to measure the local dominant operator in the EFK:

$$\sigma_K := \max\{1, \gamma h_K^{-2}\}. \tag{2.2}$$

2.2. Discrete spaces

For all $K \in \mathscr{T}_h$, and $k \ge 0$, the local HHO space is defined as

$$\widehat{V}_K := \mathscr{P}_{k+2}(K) \times \mathscr{P}_{k+2}(\mathscr{F}_K^{\mathrm{i}}) \times \mathscr{P}_k(\mathscr{F}_K^{\mathrm{i}})$$

with $\mathscr{P}_r(\mathscr{F}_K^{\mathrm{i}}) := \times_{F\in\mathscr{F}_K^{\mathrm{i}}} \mathscr{P}_r(F)$, where $\mathscr{P}_r(X)$ $(X = K, F)$ denotes the polynomial space of degree $r \ge 0$ defined on X. Note that there are no discrete unknowns introduced on boundary faces of the domain. A generic element in $\widehat{V}_K$ is denoted by $(v_K, v_{\mathscr{F}_K^{\mathrm{i}}}, \zeta_{\mathscr{F}_K^{\mathrm{i}}})$, where $v_K \in \mathscr{P}_{k+2}(K)$, $v_{\mathscr{F}_K^{\mathrm{i}}} \in \mathscr{P}_{k+2}(\mathscr{F}_K^{\mathrm{i}})$, $\zeta_{\mathscr{F}_K^{\mathrm{i}}} \in \mathscr{P}_k(\mathscr{F}_K^{\mathrm{i}})$, represent the solution inside the mesh cell, its trace on the interior part of the cell boundary, and its normal derivative of the interior part of the cell boundary along the direction of the outward unit normal $\mathbf{n}_K$, respectively.

Define the global HHO space with single-valued interface unknowns as

$$\widehat{V}_h := \mathscr{P}_{k+2}(\mathscr{T}_h) \times \mathscr{P}_{k+2}(\mathscr{F}_h^{\mathrm{i}}) \times \mathscr{P}_k(\mathscr{F}_h^{\mathrm{i}}).$$

A generic element of $\widehat{V}_h$ is denoted as $\widehat{v}_h := (v_h, v_{\mathscr{F}_h^{\mathrm{i}}}, \zeta_{\mathscr{F}_h^{\mathrm{i}}})$ with $v_h = (v_K)_{K\in\mathscr{T}_h}$, $v_{\mathscr{F}_h^{\mathrm{i}}} := (v_F)_{F\in\mathscr{F}_h^{\mathrm{i}}}$, $\zeta_{\mathscr{F}_h^{\mathrm{i}}} := (\zeta_F)_{F\in\mathscr{F}_h^{\mathrm{i}}}$, where ζ_F is meant to approximate the normal derivative in the direction of the unit normal vector $\mathbf{n}_F$ orienting F. The restriction of $\widehat{v}_h \in \widehat{V}_h$ to $K \in \mathscr{T}_h$ is denoted by $(v_K, v_{\mathscr{F}_K^{\mathrm{i}}}, \zeta_{\mathscr{F}_K^{\mathrm{i}}}) \in \widehat{V}_K$. Here, $v_{\mathscr{F}_K^{\mathrm{i}}}|_F := v_F \in \mathscr{P}_{k+2}(F)$ and $\zeta_{\mathscr{F}_K^{\mathrm{i}}}|_F := (\mathbf{n}_K \cdot \mathbf{n}_F)\zeta_F \in \mathscr{P}_{k+2}(F)$; v_K, v_F, and ζ_F are polynomials in the interior of element K, normal derivative at the faces F of K, respectively.

2.3. Local and global reduction operators

For any integer $s \ge 0$ and given $X = K \in \mathscr{T}_h$ or $F \in \mathscr{F}_h$, the L^2-projection $\Pi_X^s : L^2(X) \to \mathscr{P}_s(X)$ is defined as follows: For any $v \in L^2(X)$,

$$(\Pi_X^s(v), w)_X = (v, w)_X \quad \text{for all } w \in \mathscr{P}_s(X). \tag{2.3}$$

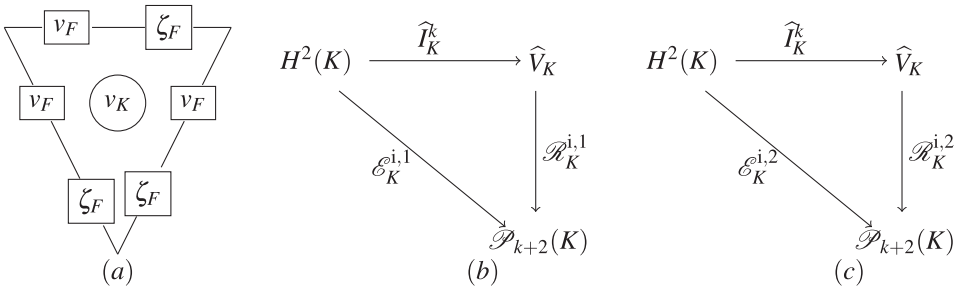

FIGURE 1. (a) $\widehat{v}_K \in \widehat{V}_K$ for $K \in \mathscr{T}_h$. (b) (resp. (c)). Commuting diagrams for $\mathscr{R}_K^{\mathrm{i},1} \circ \widehat{I}_K^k = \mathscr{E}_K^{\mathrm{i},1}$ (resp. $\mathscr{R}_K^{\mathrm{i},2} \circ \widehat{I}_K^k = \mathscr{E}_K^{\mathrm{i},2}$).

For given $K \in \mathscr{T}_h$, and for all $v \in H^2(K)$, the *local reduction operator* $\widehat{I}_K^k : H^2(K) \to \widehat{V}_K$ is defined by

$$\widehat{I}_K^k(v) := (\Pi_K^{k+2}(v), \Pi_{\mathscr{F}_K^{\mathrm{i}}}^{k+2}(v), \Pi_{\mathscr{F}_K^{\mathrm{i}}}^{k}(\mathbf{n}_K \cdot Dv)).$$

For all $v \in H^2(\Omega)$, the *global reduction operator* $\widehat{I}_h^k : H^2(\Omega) \to \widehat{V}_h$ is defined by

$$\widehat{I}_h^k(v) := (\Pi_h^{k+2}(v), \Pi_{\mathscr{F}_h^{\mathrm{i}}}^{k+2}(v), \Pi_{\mathscr{F}_h^{\mathrm{i}}}^{k}(\partial_{\mathbf{n}} v)),$$

where $\Pi_h^{k+2}(v)|_K = \Pi_K^{k+2}(v)$, $\Pi_{\mathscr{F}_h^{\mathrm{i}}}^{k+2}(v)|_F = \Pi_F^{k+2}(v)$, and $\Pi_{\mathscr{F}_h^{\mathrm{i}}}^{k}(\partial_{\mathbf{n}} v)|_F = \Pi_F^{k}(\mathbf{n}_F \cdot Dv)$,

2.4. Local reconstruction operators

The *local reconstruction operators* $\mathscr{R}_K^{\mathrm{i},j} : \widehat{V}_K \to \mathscr{P}_{k+2}(K)$ $(j = 1, 2)$ for the gradient and Hessian, respectively, are such that $\mathscr{R}_K^{\mathrm{i},j}(\widehat{v}_K) \in \mathscr{P}_{k+2}(K)$ and are defined as follows: For given $\widehat{v}_K = (v_K, v_{\mathscr{F}_K^{\mathrm{i}}}, \zeta_{\mathscr{F}_K^{\mathrm{i}}}) \in \widehat{V}_K$ and for any $K \in \mathscr{T}_h$,

$$\begin{aligned}(D\mathscr{R}_K^{\mathrm{i},1}(\widehat{v}_K), Dw)_K &:= (Dv_K, Dw)_K + \sum_{F \in \mathscr{F}_K^{\mathrm{i}}} (v_F - v_K, \partial_{\mathbf{n}} w)_F \\ &\quad - \sum_{F \in \mathscr{F}_K^{\mathrm{b}}} (v_K, \partial_{\mathbf{n}} w)_F \quad \text{for all } w \in \mathscr{P}_{k+2}(K), \qquad (2.4)\\ (\mathscr{R}_K^{\mathrm{i},1}(\widehat{v}_K), 1)_K &:= (v_K, 1)_K,\end{aligned}$$

and

$$\begin{aligned}(D^2\mathscr{R}_K^{\mathrm{i},2}(\widehat{v}_K), D^2 w)_K &:= (D^2 v_K, D^2 w)_K + \sum_{F \in \mathscr{F}_K^{\mathrm{i}}} (v_K - v_F, \partial_{\mathbf{n}} \Delta w)_F - \sum_{F \in \mathscr{F}_K^{\mathrm{i}}} (\partial_{\mathbf{n}} v_K - \zeta_F, \partial_{\mathbf{nn}} w)_F \\ &\quad - \sum_{F \in \mathscr{F}_K^{\mathrm{i}}} (\partial_{\mathbf{t}}(v_K - v_F), \partial_{\mathbf{nt}} w)_F + \sum_{F \in \mathscr{F}_K^{\mathrm{b}}} (v_K, \partial_{\mathbf{n}} \Delta w)_F - \sum_{F \in \mathscr{F}_K^{\mathrm{b}}} (Dv_K, D^2 w \mathbf{n}_K)_F \quad \text{for all } w \in \mathscr{P}_{k+2}(K), \qquad (2.5)\\ (\mathscr{R}_K^{\mathrm{i},2}(\widehat{v}_K), \phi)_K &:= (v_K, \phi)_K \quad \text{for all } \phi \in \mathscr{P}_1(K).\end{aligned}$$

In comparison with [22], we have two reconstruction operators: $\mathscr{R}_K^{\mathrm{i},1}(\bullet)$ for gradient operator and $\mathscr{R}_K^{\mathrm{i},2}(\bullet)$ for the Hessian operator. This approach avoids the parameter γ in the reconstruction operators. The index i in $\mathscr{R}_K^{\mathrm{i},1}(\bullet)$ indicates that the local reconstruction operator does not involve boundary terms.

Note that $\sum_{F \in \mathscr{F}_K^{\mathrm{b}}} (Dv_K, D^2 w \mathbf{n}_K)_F := \sum_{F \in \mathscr{F}_K^{\mathrm{b}}} ((\partial_{\mathbf{n}} v_K, \partial_{\mathbf{nn}} w)_F + (\partial_{\mathbf{t}} v_K, \partial_{\mathbf{nt}} w)_F)$. The operators $\mathscr{E}_K^{\mathrm{i},j}$ for $j = 1, 2$ are defined as $\mathscr{E}_K^{\mathrm{i},j} := \mathscr{R}_K^{\mathrm{i},j} \circ \widehat{I}_K^k : H^2(K) \to \mathscr{P}_{k+2}(K)$ operators (see Figs. 1b and 1c), respectively.

These operators do not involve boundary terms when $K \in \mathscr{T}_h^{\mathrm{b}}$ and certain boundary contributions are excluded from the definition of the reconstruction operators. To address this, define the *lifting operators* $\mathscr{L}_K^j : H^2(K) \to \mathscr{P}_{k+2}(K)$ $(j = 1, 2)$ for all $K \in \mathscr{T}_h$ such that, for all $v \in H^2(K)$ and all ([22], Sect. 4.2)

$$w \in \mathscr{P}_{k+2}(K)^{\perp} := \{w \in \mathscr{P}_{k+2}(K) : (w, \zeta) = 0 \text{ for all } w \in \mathscr{P}_{k+1}(K)\},$$
$$(D\mathscr{L}_K^1 v, Dw)_K := \sum_{F \in \mathscr{F}_K^{\mathrm{b}}} (v, \partial_{\mathbf{n}} w)_F, \tag{2.6}$$
$$(D\mathscr{L}_K^2 v, Dw)_K := -\sum_{F \in \mathscr{F}_K^{\mathrm{b}}} ((v, \partial_{\mathbf{n}} \Delta w)_F - (\partial_{\mathbf{n}} v, \partial_{\mathbf{nn}} w)_F - (\partial_{\mathbf{t}} v, \partial_{\mathbf{nt}} w)_F), \tag{2.7}$$

together with the condition $(\mathscr{L}_K^j(v), 1)_K = 0$. Note that $\mathscr{L}_K^j(v) = 0$ for all $K \in \mathscr{T}_h^{\mathrm{i}}$. Now, we define the operator $\mathscr{E}_K^j : H^2(K) \to \mathscr{P}_{k+2}(K)$ such that $\mathscr{E}_K^j := \mathscr{E}_K^{\mathrm{i},j} + \mathscr{L}_K^j(v)$ for $j = 1, 2$. It should be noted that $\mathscr{E}_K^j$ no longer display H^2-elliptic properties. However, they still maintain the approximation characteristics of H^2-elliptic projections (for further details, see [22, 23]).

2.5. Stabilizer

For all $\widehat{v}_K = (v_K, v_{\mathscr{F}_K^{\mathrm{i}}}, \zeta_{\mathscr{F}_K^{\mathrm{i}}})$, $\widehat{w}_K = (w_K, w_{\mathscr{F}_K^{\mathrm{i}}}, \chi_{\mathscr{F}_K^{\mathrm{i}}})$ with $\widehat{v}_K, \widehat{w}_K \in \widehat{V}_K$, the *local stabilization* bilinear form $\mathscr{S}_K : \widehat{V}_K \times \widehat{V}_K \to \mathbb{R}$ is defined as $\mathscr{S}_K(\bullet, \bullet) := \mathscr{S}_K^{\mathrm{i}}(\bullet, \bullet) + \mathscr{S}_K^{\mathrm{b}}(\bullet, \bullet)$ such that

$$\mathscr{S}_K^{\mathrm{i}}(\widehat{v}_K, \widehat{w}_K) := \sum_{F \in \mathscr{F}_K^{\mathrm{i}}} \sigma_K h_K^{-1} (v_F - v_K, w_F - w_K)_F + \sum_{F \in \mathscr{F}_K^{\mathrm{i}}} \sigma_K h_K (\Pi_F^k(\zeta_F - \partial_{\mathbf{n}} v_K), \Pi_F^k(\chi_F - \partial_{\mathbf{n}} w_K))_F. \tag{2.8}$$
$$\mathscr{S}_K^{\mathrm{b}}(\widehat{v}_K, \widehat{w}_K) := \sum_{F \in \mathscr{F}_K^{\mathrm{b}}} \sigma_K h_K^{-1} (v_K, w_K)_F + \sum_{F \in \mathscr{F}_K^{\mathrm{b}}} \gamma h_K^{-1} (Dv_K, Dw_K)_F. \tag{2.9}$$

Note that the local stabilization form is composed of a contribution on $\mathscr{F}_K^{\mathrm{i}}$ and $\mathscr{F}_K^{\mathrm{b}}$.

2.6. Bilinear form

For all $\widehat{v}_h, \widehat{w}_h \in \widehat{V}_h$, the *bilinear form* $a_h : \widehat{V}_h \times \widehat{V}_h \to \mathbb{R}$ is defined by $a_h(\widehat{v}_h, \widehat{w}_h) := \sum_{K \in \mathscr{T}_h} a_K(\widehat{v}_K, \widehat{w}_K)$, where

$$a_K(\widehat{v}_K, \widehat{w}_K) := \gamma(D^2 \mathscr{R}_K^{\mathrm{i},2}(\widehat{v}_K), D^2 \mathscr{R}_K^{\mathrm{i},2}(\widehat{w}_K))_K + (D\mathscr{R}_K^{\mathrm{i},1}(\widehat{v}_K), D\mathscr{R}_K^{\mathrm{i},1}(\widehat{w}_K))_K + \mathscr{S}_K(\widehat{v}_K, \widehat{w}_K).$$

The bilinear form $a_h(\bullet, \bullet)$ is coercive and continuous on $\widehat{V}_h$ (see Lem. 3.1).

2.7. Norms

For $\widehat{v}_K = (v_K, v_{\mathscr{F}_K^{\mathrm{i}}}, \zeta_{\mathscr{F}_K^{\mathrm{i}}}) \in \widehat{V}_K$, define a seminorm on $\widehat{V}_K$ by $|\widehat{v}_K|_{\widehat{V}_K}$ by

$$|\widehat{v}_K|_{\widehat{V}_K}^2 := \gamma \|D^2 v_K\|_K^2 + \|Dv_K\|_K^2 + \sum_{F \in \mathscr{F}_K^{\mathrm{i}}} \sigma_K h_K^{-1} \|v_F - v_K\|_F^2 + \sum_{F \in \mathscr{F}_K^{\mathrm{i}}} \sigma_K h_K \|\zeta_F - \partial_{\mathbf{n}} v_K\|_F^2 + \sum_{F \in \mathscr{F}_K^{\mathrm{b}}} \sigma_K h_K^{-1} \|v_K\|_F^2 + \sum_{F \in \mathscr{F}_K^{\mathrm{b}}} \gamma h_K^{-1} \|Dv_K\|_F^2. \tag{2.10}$$

With an abuse of notation, for all $\widehat{v}_h \in \widehat{V}_h$, let the seminorm on $\widehat{V}_h$ be denoted by $\|\widehat{v}_h\|_{\widehat{V}_h}$ and be defined as $\|\widehat{v}_h\|_{\widehat{V}_h} := \big(\sum_{K \in \mathscr{T}_h} |\widehat{v}_K|_{\widehat{V}_K}^2\big)^{1/2}$. Note that the seminorm is a norm for $v_h \in \widehat{V}_h$.

Next, for any $K \in \mathscr{T}_h$ and a given function $w \in H^{2+r}(K)$ with $r > \frac{3}{2}$, introduce the following seminorm:

$$\|w\|_{\#,K}^2 := \gamma\|D^2 w\|_K^2 + \|Dw\|_K^2 + \sum_{F\in\mathscr{F}_K} \gamma\big(h_K^3\|\partial_{\mathbf{n}}\Delta w\|_F^2 + h_K\|\partial_{\mathbf{nn}} w\|_F^2 + h_K\|\partial_{\mathbf{nt}} w\|_F^2\big) + \sum_{F\in\mathscr{F}_K} h_K\|\partial_{\mathbf{n}} w\|_F^2. \quad (2.11)$$

Moreover, define the seminorm in $H^r(\mathscr{T}_h)$ as $|v|_{H^r(\mathscr{T}_h)} = \sum_{K\in\mathscr{T}_h} |v|_{H^r(K)}$ for $r > 0$.

2.8. Integration by parts formula

The *integration by parts* formulae ([23], Sect. 2.1) stated next are used extensively in the sequel. For any $K \in \mathscr{T}_h$ and for sufficiently smooth functions v and w, it holds

$$\text{(a) } (\Delta^2 w, v)_K = (D^2 w, D^2 v)_K + \sum_{F\in\mathscr{F}_K^{\mathrm{i}}} \big((v, \partial_{\mathbf{n}}\Delta w)_F - (\partial_{\mathbf{n}} v, \partial_{\mathbf{nn}} w)_F - (\partial_{\mathbf{t}} v, \partial_{\mathbf{nt}} w)_F\big) \quad (2.12)$$

$$+ \sum_{F\in\mathscr{F}_K^{\mathrm{b}}} (v, \partial_{\mathbf{n}}\Delta w)_F - \sum_{F\in\mathscr{F}_K^{\mathrm{b}}} (Dv, D^2 w\mathbf{n}_K)_F. \quad (2.13)$$

$$\text{(b) } (\Delta w, v)_K = -(Dw, Dv)_K + \sum_{K\in\mathscr{F}_h^{\mathrm{i}}} (v, \partial_{\mathbf{n}} w)_F + \sum_{K\in\mathscr{F}_h^{\mathrm{b}}} (v, \partial_{\mathbf{n}} w)_F. \quad (2.14)$$

3. Main results

This section first defines a projection operator and states its properties that will be useful for error analysis. The proofs are provided in Section 5. Two time discretization schemes are discussed for (1.1): the main results for the backward Euler scheme are stated in Lemma 3.3 and Theorem 3.4 and that for the Crank-Nicolson scheme in Lemma 3.5 and Theorem 3.6. The proofs are provided in Section 6 and Section 7, respectively.

3.1. Projection operator

Let $\mathscr{Y} = \{w \in H^2(\Omega) : B(w) := \gamma\Delta^2 w - \Delta w \in L^2(\Omega)\}$. Motivated by Ern and Steins [25], for a fixed time $t \in (0, T]$, define the projection operator $\widehat{E}_h : \mathscr{Y} \to \widehat{V}_h$ as

$$a_h(\widehat{E}_h(w), \widehat{v}_h) = \mathscr{L}_h(\widehat{v}_h) \quad \text{for all } \widehat{v}_h \in \widehat{V}_h, \quad (3.1)$$

where the definition of the $\mathscr{L}_h(\widehat{v}_h)$ (see (5.1)) is motivated by the consistency error analysis (see the proof of Thm. 3.2). The well-posedness of the operator $\widehat{E}_h$ follows from the next lemma.

Lemma 3.1 (Boundedness and coercivity)**.** *For all $\widehat{v}_K \in \widehat{V}_K$ and $K \in \mathscr{T}_h$ it holds that $|\widehat{v}_K|_{\widehat{V}_K}^2 \lesssim a_K(\widehat{v}_K, \widehat{v}_K) \lesssim |\widehat{v}_K|_{\widehat{V}_K}^2$. A summation over all $K \in \mathscr{T}_h$ leads to $C_a\|\widehat{v}_h\|_{\widehat{V}_h}^2 \le a_h(\widehat{v}_h, \widehat{v}_h) \le C_A\|\widehat{v}_h\|_{\widehat{V}_h}^2$ for all $\widehat{v}_h \in \widehat{V}_h$. The constants in $\lesssim$ depend on the constants from Theorem 4.1(a), (b), and (d). Moreover, the norms $\|\widehat{v}_h\|_{a,h} := \big(a_h(\widehat{v}_h, \widehat{v}_h)\big)^{1/2}$ and $\|\widehat{v}_h\|_{\widehat{V}_h}$ are equivalent in $\widehat{V}_h$.*

The proof of the lemma follows from arguments in from Lemma 4.1 of [22].

Theorem 3.2 (Discrete energy estimate)**.** *For any $w \in H^{2+r}(\Omega)$ with $r > \frac{3}{2}$, it holds*

$$\|\widehat{I}_h^k(w) - \widehat{E}_h(w)\|_{a,h} \lesssim \sum_{K\in\mathscr{T}_h} \|w - \Pi_K^{k+2}(w)\|_{\#,K},$$

where $\widehat{I}_h^k(w) := (\Pi_h^{k+2}(w), \Pi_{\mathscr{F}_h^{\mathrm{i}}}^{k+2}(w), \Pi_{\mathscr{F}_h^{\mathrm{i}}}^{k}(\partial_{\mathbf{n}} w))$ is the global reduction operator from Section 2.3 and $\widehat{E}_h$ is the projection operator from (3.1).

The proof of Theorem 3.2 is discussed in Section 5.

3.2. Backward Euler scheme

Divide the interval $[0,T]$ into m sub-intervals of equal length $\Delta t = \frac{T}{m}$ with equidistant grid-points $t^n = n\Delta t$ for $0 \le n \le m$. Adopt the notation u^n for $u(x,t^n)$ and let $\bar\partial u_h^n := \frac{u_h^n - u_h^{n-1}}{\Delta t}$. For $1 \le n \le m$, the *fully-discrete backward Euler HHO scheme* that corresponds to (1.1) seeks $\widehat{u}_h^n = (u_h^n, u_{\mathscr{F}_h^{\mathrm{i}}}^n, \sigma_{\mathscr{F}_h^{\mathrm{i}}}^n) \in \widehat{V}_h$ such that

$$(\bar\partial u_h^n, v_h) + a_h(\widehat{u}_h^n, \widehat{v}_h) + (f(u_h^n), v_h) = 0 \quad \text{for all } \widehat{v}_h = (v_h, v_{\mathscr{F}_h^{\mathrm{i}}}, \zeta_{\mathscr{F}_h^{\mathrm{i}}}) \in \widehat{V}_h \text{ and } \widehat{u}_h^0 = \widehat{I}_h^k(u_0). \tag{3.2}$$

Define $F(v) := \frac{1}{4}(1-v^2)^2$ and note that $F'(v) = f(v)$. The discrete Lyapunov functional [13] reads

$$L(\widehat{u}_h^n) := \frac{1}{2} a_h(\widehat{u}_h^n, \widehat{u}_h^n) + (F(u_h^n), 1) \ \text{ for } \ 0 \le n \le m. \tag{3.3}$$

Lemma 3.3. (a) (Stability). *Let $\widehat{u}_h^n$ $(1 \le n \le m)$ denote the solution of the discrete formulation (3.2), $u_0 \in H_0^2(\Omega)$, and let $0 < \Delta t < \frac{1}{2}$. Then there exists a (generic) positive constant C that depends on γ and u_0 with dependency shown below such that*

$$\text{(i) } L(\widehat{u}_h^n) \le L(\widehat{u}_h^0) \ \text{ for all } n \ge 1 \text{ and (ii) } \|\widehat{u}_h^n\|_{a,h} \le C(|u_0|_{H^1(\mathscr{T}_h)}, \gamma^{\frac{1}{2}}|u_0|_{H^2(\mathscr{T}_h)}, |\Omega|).$$

(iii) *Moreover, $\|u_h^n\|_{L^q(\Omega)} \le C(|u_0|_{H^1(\mathscr{T}_h)}, \gamma^{\frac{1}{2}}|u_0|_{H^2(\mathscr{T}_h)}, |\Omega|)$, where $1 \le q < \infty$.*

(b) (Existence and uniqueness). *Given $\widehat{u}_h^0, \widehat{u}_h^1, \cdots, \widehat{u}_h^{n-1}$, there exists a unique solution $\widehat{u}_h^n$ to the fully-discrete hybrid high-order scheme (3.2).*

The notation $C(|u_0|_{H^1(\mathscr{T}_h)}, \gamma^{\frac{1}{2}}|u_0|_{H^2(\mathscr{T}_h)}, |\Omega|)$ above means that constant C depends on $|u_0|_{H^1(\mathscr{T}_h)}$, $\gamma^{\frac{1}{2}}|u_0|_{H^2(\mathscr{T}_h)}$, and the area of Ω, $|\Omega|$. This terminology of indicating the dependency of the constant on the data is followed throughout the paper.

Theorem 3.4 (Discrete energy estimates). *Let u (resp. $\widehat{u}_h^n$ $(1 \le n \le m)$) solve (1.1) (resp. (3.2)) for $0 \le \gamma \le 1$ and let u satisfy the global regularity $u \in L^\infty(0,T;H^{2+r}(\Omega))$ with $r > 3/2$. Under the additional regularity assumptions*

- *$u, u_t \in L^\infty(0,T;H^{k+3}(\mathscr{T}_h))$, $u_{tt} \in L^2(0,T;H^{k+3}(\mathscr{T}_h))$ for $k \ge 1$,*
- *$u, u_t \in L^\infty(0,T;H^{3+\beta}(\mathscr{T}_h))$, $u_{tt} \in L^2(0,T;H^{3+\beta}(\mathscr{T}_h))$ with $\beta := \min(r-1,1) \in (1/2,1]$ for $k=0$, it holds*

$$\text{(a)} \ \max_{1\le n\le m} \|u^n - u_h^n\| + \left(\Delta t \sum_{n=1}^{m} \left(\sum_{K\in\mathscr{T}_h} \left(\gamma \|D^2(u^n - \mathscr{R}_K^2(\widehat{u}_K^n))\|_K^2 + \|D(u^n - \mathscr{R}_K^1(\widehat{u}_K^n))\|_K^2\right)\right)^{1/2}\right)$$
$$= \begin{cases} \mathscr{O}\big(\Delta t + \sum_{K\in\mathscr{T}_h} h^{k+2}\sigma_K^{\frac{1}{2}}\big) & \text{for } k \ge 1, \\ \mathscr{O}\big(\Delta t + \sum_{K\in\mathscr{T}_h} h^2(1+h^\beta)\sigma_K^{\frac{1}{2}}\big) & \text{for } k = 0, \end{cases} \qquad \text{for } 0 < \Delta t < 1/2,$$

$$\text{(b)} \ \max_{1\le n\le m} \left(\sum_{K\in\mathscr{T}_h} \left(\gamma^{\frac{1}{2}} \|D^2(u^n - \mathscr{R}_K^2(\widehat{u}_K^n))\|_K + \|D(u^n - \mathscr{R}_K^1(\widehat{u}_K^n))\|_K\right)\right)$$
$$= \begin{cases} \mathscr{O}\big(\Delta t + \sum_{K\in\mathscr{T}_h} h^{k+2}\sigma_K^{\frac{1}{2}}\big) & \text{for } k \ge 1, \\ \mathscr{O}\big(\Delta t + \sum_{K\in\mathscr{T}_h} h^2(1+h^\beta)\sigma_K^{\frac{1}{2}}\big) & \text{for } k = 0, \end{cases} \qquad \text{for sufficiently small } \Delta t.$$

3.3. Crank-Nicolson scheme

For $1 \le n \le m$, define $u^{n-\frac{1}{2}} := \frac{u^n + u^{n-1}}{2}$ and $\widehat{u}_h^{n-\frac{1}{2}} = \frac{\widehat{u}_h^n + \widehat{u}_h^{n-1}}{2}$. Recall that $F(v) := \frac{1}{4}(1-v^2)^2$. For $\widetilde{f}(z,w) := \frac{1}{4}(z^3+z^2w+zw^2+w^3) - \frac{1}{2}(z+w)$, elementary manipulations show $\widetilde{f}(z,w) = \begin{cases} \frac{F(z)-F(w)}{z-w}, & \text{for } z \ne w, \\ F'(z), & \text{for } z = w. \end{cases}$

That is, $\widetilde{f}(z,w) \to f(w)$ as $z \to w$.

For $1 \le n \le m$, the *Crank-Nicolson HHO scheme* that corresponds to (1.1) seeks $\widehat{u}_h^n = (u_h^n, u_{\mathscr{F}_h^i}^n, \sigma_{\mathscr{F}_h^i}^n) \in \widehat{V}_h$ such that

$$(\bar{\partial} u_h^n, v_h) + a_h(\widehat{u}_h^{n-\frac{1}{2}}, \widehat{v}_h) + (\widetilde{f}(u_h^{n-1}, u_h^n), v_h) = 0 \quad \text{for all } \widehat{v}_h \in \widehat{V}_h \text{ and } \widehat{u}_h^0 = \widehat{I}_h^k(u_0). \tag{3.4}$$

Lemma 3.5. (a) (Stability). *Let $\widehat{u}_h^n$ $(1 \le n \le m)$ denote solution of the discrete formulation (3.4). Then there exists a positive constant C that depends on γ and u_0 such that*

$$\text{(i) } L(\widehat{u}_h^n) \le L(\widehat{u}_h^0) \quad \text{for all } n \ge 1 \text{ and (ii) } \|\widehat{u}_h^n\|_{a,h} \le C(|u_0|_{H^1(\mathscr{T}_h)}, \gamma^{\frac{1}{2}}|u_0|_{H^2(\mathscr{T}_h)}, |\Omega|).$$

(iii) *Moreover, $\|u_h^n\|_{L^q(\Omega)} \le C(|u_0|_{H^1(\mathscr{T}_h)}, \gamma^{\frac{1}{2}}|u_0|_{H^2(\mathscr{T}_h)}, |\Omega|)$ where $1 \le q < \infty$.*

(b) (Existence and uniqueness). *Given $\widehat{u}_h^0, \widehat{u}_h^1, \cdots, \widehat{u}_h^{n-1}$, there exists a unique solution $\widehat{u}_h^n$ to the fully-discrete Crank-Nicolson hybrid high-order scheme (3.4).*

Theorem 3.6. *Let u (resp. $\widehat{u}_h^n$ $(1 \le n \le m)$) solve (1.1) (resp. (3.4)) for $0 \le \gamma \le 1$ and let u satisfy the regularity assumption $u \in L^\infty(0,T; H^{2+r}(\Omega))$, $r > 3/2$. Under the additional regularity assumptions*

- $u, u_t, u_{tt} \in L^\infty(0,T; H^{k+3}(\mathscr{T}_h))$, $u_{ttt} \in L^2(0,T; H^{k+3}(\mathscr{T}_h))$ for $k \ge 1$,
- $u, u_t, u_{tt} \in L^\infty(0,T; H^{3+\beta}(\mathscr{T}_h))$, $u_{ttt} \in L^2(0,T; H^{3+\beta}(\mathscr{T}_h))$ *with* $\beta := \min(r-1, 1) \in (\frac{1}{2}, 1]$ for $k = 0$,

$$\max_{1 \le n \le m} \left(\sum_{K \in \mathscr{T}_h} \left(\gamma^{\frac{1}{2}} \|D^2(u^n - \mathscr{R}_K^2(\widehat{u}_K^n))\|_K + \|D(u^n - \mathscr{R}_K^1(\widehat{u}_K^n))\|_K \right) \right)$$
$$= \begin{cases} \mathscr{O}\big((\Delta t)^2 + \sum_{K \in \mathscr{T}_h} h^{k+2} \sigma_K^{\frac{1}{2}}\big) & \text{for } k \ge 1, \\ \mathscr{O}\big((\Delta t)^2 + \sum_{K \in \mathscr{T}_h} h^2(1 + h^\beta) \sigma_K^{\frac{1}{2}}\big) & \text{for } k = 0, \end{cases} \qquad \text{for sufficiently small } \Delta t.$$

Remark 3.7 (Regularity in Thms. 3.4 and 3.6)**.** The global regularity $u \in H^{2+r}(\Omega)$ with $r > 3/2$ ensures that for all $K \in \mathscr{T}_h$, $\partial_{\mathbf{n}} \Delta u$, $\partial_{\mathbf{nn}} u$, $\partial_{\mathbf{nt}} u$, and $\partial_{\mathbf{n}} u$ are single-valued and are $L^2(\partial K)$ functions across the mesh-interfaces. This is intrinsic in the proof of bound for consistency error in Lemma 5.1. The consistency error bound is further employed in the proofs of Theorems 3.2, 3.4, and 3.6. The additional regularity estimates in Theorems 3.4 and 3.6 are used to derive the explicit error bounds.

Remark 3.8 (Alternate assumption)**.** In Theorems 3.4–3.6 the regularity of the global solution of the problem (1.1) is assumed to be $u \in H^{2+r}(\Omega)$, $r > 3/2$ to derive the optimal bounds for the HHO scheme in the space direction. However similar estimates can be achieved for the HHO scheme with $u \in H_0^2(\Omega) \cap H^4(\mathscr{T}_h)$.

4. Approximation properties

In this section, we discuss some useful estimates: discrete inverse, trace and Sobolev inequalities, Poincare inequality, and approximation properties that are critical for the proofs of the main results.

Theorem 4.1. *Let $\mathscr{T}_h$ be a shape-regular mesh sequence, let $k \ge 0$ and recall that $\Omega \subset \mathbb{R}^2$. For each $K \in \mathscr{T}_h$ and $F \in \mathscr{F}_K$, the following estimates hold.*

(a) (Discrete trace, discrete inverse, discrete inverse inequalities on faces). *For all $w_h \in \mathscr{P}_k(K)$,*

$$\|w_h\|_F \lesssim h_K^{-\frac{1}{2}} \|w_h\|_K, \quad \|Dw_h\|_K \lesssim h_K^{-1} \|w_h\|_K, \quad \text{and} \quad \|\partial_{\mathbf{t}} w_h\|_F \lesssim h_K^{-1} \|w_h\|_F \text{ for all } w_h \in \mathscr{P}_k(K).$$

(b) (Poincaré inequality on cell). *Let $H^2(K)^\perp := \{w \in H^2(K) : (w, \zeta)_K = 0 \quad \text{for all } \zeta \in \mathscr{P}_1(K)\}$. For all $v \in H^2(K)^\perp$, $h_K^{-2}\|v\|_K + h_K^{-1}\|Dv\|_K \lesssim \|D^2 v\|_K$.*

(c) (Trace inequality). *For all $v \in H^s(K)$, $s \in (\frac{1}{2}, 1]$, $\|v\|_F \lesssim \big(h_K^{-\frac{1}{2}}\|v\|_K + h_K^{s-\frac{1}{2}}|v|_{H^s(K)}\big)$.*

(d) (An approximation property). *For all* $v \in H^r(K)$, $r \in [0, s+1]$, $m \in \{0, \ldots, \lfloor r \rfloor\}$, *and* $s \geq 0$, $|v - \Pi_K^s(v)|_{H^m(K)} \lesssim h_K^{r-m}|v|_{H^r(K)}$ for all $v \in H^r(K)$.

(e) (Discrete Sobolev embedding). *For* $1 \leq q < \infty$, *it holds* $\|v_h\|_{L^q(\Omega)} \lesssim \|\widehat{v}_h\|_{1,2,h}$ *for all* $\widehat{v}_h \in \widehat{V}_h$, *where* $v_h = (v_K)_{K\in\mathscr{T}_h}$, $\|\widehat{v}_h\|_{1,2,h} = \big(\sum_{K\in\mathscr{T}_h} \|\widehat{v}_K\|_{1,2,K}^2\big)^{\frac{1}{2}}$ *with* $\|\widehat{v}_K\|_{1,2,K} = \big(\|Dv_K\|_K^2 + \sum_{F\in\mathscr{F}_K} h_K^{-1}\|v_F - v_K\|_F^2\big)^{\frac{1}{2}}$.

(f) (A boundedness result). *For all* $\widehat{v}_h = (v_h, v_{\mathscr{F}_h^{\mathrm{i}}}, \zeta_{\mathscr{F}_h^{\mathrm{i}}}) \in \widehat{V}_h$, *it holds that*

$$\|v_h\|_{L^q(\Omega)} \leq C_b \|\widehat{v}_h\|_{\widehat{V}_h}, \quad \text{where } 1 \leq q < \infty.$$

The constants in $\lesssim$ *in the above inequalities depend on the shape-regularity of the mesh, the polynomial degree* k, *and* s *in (c) and (d).*

We refer to Lemma 2.2 and (2.8) (resp. Lem. 2.4) [23] for the proof of (a) (resp. (b)) and Lemma 2.2 of [9] for the proof of (c). For the proof of (d), see Lemma 2.5 of [9]. The proof of (e) follows from Proposition 5.4 of [17]. The proof of (f) follows form (e) and Lemma 3.1.

An application of Theorem 4.1(a) leads to the following inequalities that are frequently used in the article. For all $\widehat{v}_K \in \widehat{V}_K$,

$$\begin{aligned} \|\partial_{\mathbf{n}}\Delta v_K\|_F \lesssim h_K^{-3/2}\|D^2 v_K\|_K,\ \|\partial_{\mathbf{nn}} v_K\|_F \lesssim h_K^{-1/2}\|D^2 v_K\|_K, \\ \|\partial_{\mathbf{t}}(v_K - v_F)\|_F \lesssim h_K^{-1}\|v_K - v_F\|_F, \text{ and } \|\partial_{\mathbf{nt}} v_K\|_F \lesssim h_K^{-1/2}\|D^2 v_K\|_K. \end{aligned} \tag{4.1}$$

Lemma 4.2 (Temporal approximation properties [38]). *For all* $v_{tt} \in L^2(t^{n-1}, t^n; H^2(\mathscr{T}_h))$, *it holds*

$$\begin{aligned} &\|v_t^n - \bar{\partial} v^n\| \lesssim (\Delta t)^{\frac{1}{2}}\|v_{tt}\|_{L^2(t^{n-1},t^n;L^2(\Omega))},\ \|D(v_t^n - \bar{\partial} v^n)\| \lesssim (\Delta t)^{\frac{1}{2}}\|v_{tt}\|_{L^2(t^{n-1},t^n;H^1(\mathscr{T}_h))}, \\ &\text{and } \|\Delta(v_t^n - \bar{\partial} v^n)\| \lesssim (\Delta t)^{\frac{1}{2}}\|v_{tt}\|_{L^2(t^{n-1},t^n;H^2(\mathscr{T}_h))}. \end{aligned}$$

Lemma 4.3 (Bounds for projectors and stabilizer). *Any* $v \in H^{2+r}(K)$ *with* $r > \frac{3}{2}$, *where* $K \in \mathscr{T}_h$ *satisfies*

$$\begin{aligned} &\text{(a) } \gamma^{\frac{1}{2}}\|D^2(v - \mathscr{E}_K^2(v))\|_K \lesssim \|v - \Pi_K^{k+2}(v)\|_{\#,K},\ \text{(b) } \gamma^{\frac{1}{2}}\|D^2(\Pi_K^{k+2}(v) - \mathscr{E}_K^2(v))\|_K \lesssim \|v - \Pi_K^{k+2}(v)\|_{\#,K}, \\ &\text{(c) } \|D(v - \mathscr{E}_K^1(v))\|_K \lesssim \|v - \Pi_K^{k+2}(v)\|_{\#,K}, \\ &\text{and (d) } \mathscr{S}_K^{\mathrm{i}}(\widehat{I}_K^k(v), \widehat{I}_K^k(v))^{\frac{1}{2}} + \mathscr{S}_K^{\mathrm{b}}(v - \Pi_K^{k+2}(v), v - \Pi_K^{k+2}(v))^{\frac{1}{2}} \lesssim \|v - \Pi_K^{k+2}(v)\|_{\#,K}. \end{aligned}$$

The proof of (a)–(d) follow from Lemma 4.3 of [22] with minor modifications and hence is skipped.

Lemma 4.4 (Error bound for L^2 projection). *For* $K \in \mathscr{T}_h$, *the error bound for the* L^2 *projection reads*

$$\|v - \Pi_K^{k+2}(v)\|_{\#,K} \lesssim \begin{cases} \sigma_K^{\frac{1}{2}} h_K^{k+2}|v|_{H^{k+3}(K)}, & \text{for } k \geq 1 \text{ and } v \in H^{k+3}(K), \\ \sigma_K^{\frac{1}{2}} h_K(h_K|v|_{H^3(K)} + h_K^{1+\beta}|v|_{H^{3+\beta}(K)}), & \text{for } k = 0 \text{ and } v \in H^{3+\beta}(K) \text{ with } \beta \in (\tfrac{1}{2}, 1]. \end{cases}$$

The proof utilizes Theorem 4.1 and (2.11) and is skipped.

Lemma 4.5 (Boundedness of local projection). *For any* $v \in H^2(K)$, $\widehat{I}_K^k(v) \in \widehat{V}_K$ *satisfies* $|\widehat{I}_K^k(v)|_{\widehat{V}_K} \lesssim |v|_{H^1(K)} + \gamma^{\frac{1}{2}}|v|_{H^2(K)}$. *A summation over all* $K \in \mathscr{T}_h$ *leads to* $\|\widehat{I}_h^k(v)\|_{\widehat{V}_h} \lesssim |v|_{H^1(\mathscr{T}_h)} + \gamma^{\frac{1}{2}}|v|_{H^2(\mathscr{T}_h)}$.

5. Proof of Theorem 3.2

In this section, the proof of Theorem 3.2 is presented. The proof depends heavily on a bound for the consistency error presented in Lemma 5.1.

Recall that $B(w) := \gamma\Delta^2 w - \Delta w \in L^2(\Omega)$ for all $w \in H^2(\Omega)$ from Section 3.1. The definition of lifting operators (2.6) and (2.7) and definition of the boundary stabilization (2.9) yield

$$\mathscr{L}_h(\widehat{v}_h) := (B(w), v_h) - \sum_{K\in\mathscr{T}_h} \big(\gamma(D^2\mathscr{L}_K^2(w), D^2\mathscr{R}^{\mathrm{i},2}(\widehat{w}_K))_K + (D\mathscr{L}_K^1(w), D\mathscr{R}^{\mathrm{i},1}(\widehat{v}_K))_K + \mathscr{S}_K^{\mathrm{b}}(w, \widehat{v}_K)\big). \quad (5.1)$$

For $\widehat{I}_h^k(w) \in \widehat{V}_h$, $\delta_h(w) \in (\widehat{V}_h)'$, and the duality pairing between $(\widehat{V}_h)'$ and $\widehat{V}_h$ denoted by $\langle\cdot,\cdot\rangle$, define the *consistency error* equation by

$$\begin{aligned}\langle\delta_h(w), \widehat{v}_h\rangle := (B(w), v_h) - \sum_{K\in\mathscr{T}_h} \big(&\gamma(D^2\mathscr{E}_K^2(w), D^2\mathscr{R}^{\mathrm{i},2}(\widehat{w}_K))_K + (D\mathscr{E}_K^1(w), D\mathscr{R}^{\mathrm{i},1}(\widehat{v}_K))_K + \mathscr{S}_K^{\mathrm{i}}(\widehat{I}_K^k(w), \widehat{v}_K)\\ &- \mathscr{S}_K^{\mathrm{b}}(\Pi_K^{k+2}(w) - w, \widehat{v}_K)\big) \text{for all } \widehat{v}_h = (v_h, v_{\mathscr{F}_h^{\mathrm{i}}}, \zeta_{\mathscr{F}_h^{\mathrm{i}}}) \in \widehat{V}_h. \end{aligned} \quad (5.2)$$

Lemma 5.1 (Bound for consistency error)**.** *For any $w \in H^{2+r}(\Omega)$ with $r > 3/2$, it holds*

$$\|\delta_h(w)\|_* := \sup_{\widehat{v}_h\in\widehat{V}_h} \frac{|\langle\delta_h(w), \widehat{v}_h\rangle|}{\|\widehat{v}_h\|_{\widehat{V}_h}} \lesssim \left(\sum_{K\in\mathscr{T}_h} \|w - \Pi_K^{k+2}(w)\|_{\#,K}^2\right)^{\frac{1}{2}}.$$

Proof. Recall the definition of *consistency error* from (5.2). The first three terms on the right-hand side of *consistency error* are simplified next. An integration by parts from (2.13) and (2.14) and the symmetry of $(\bullet,\bullet)_F$ lead to

$$\begin{aligned}(B(w), v_K)_K = \gamma(D^2 w, D^2 v_K)_K + (Dw, Dv_K)_K + \sum_{F\in\mathscr{F}_K^{\mathrm{i}}} \gamma(\partial_{\mathbf{n}}\Delta w, v_K)_F - \sum_{F\in\mathscr{F}_K^{\mathrm{i}}} \gamma(\partial_{\mathbf{nn}} w, \partial_{\mathbf{n}} v_K)_F\\ - \sum_{F\in\mathscr{F}_K^{\mathrm{i}}} \gamma(\partial_{\mathbf{nt}} w, \partial_{\mathbf{t}} v_K)_F - \sum_{F\in\mathscr{F}_K^{\mathrm{i}}} (\partial_{\mathbf{n}} w, v_K)_F + \sum_{F\in\mathscr{F}_K^{\mathrm{b}}} \gamma(\partial_{\mathbf{n}}\Delta w, v_K)_F - \sum_{F\in\mathscr{F}_K^{\mathrm{b}}} \gamma(\partial_{\mathbf{nn}} w, \partial_{\mathbf{n}} v_K)_F\\ - \sum_{F\in\mathscr{F}_K^{\mathrm{b}}} \gamma(\partial_{\mathbf{nt}} w, \partial_{\mathbf{t}} v_K)_F - \sum_{F\in\mathscr{F}_K^{\mathrm{b}}} (\partial_{\mathbf{n}} w, v_K)_F. \end{aligned} \quad (5.3)$$

The symmetry of $\mathscr{R}_K^{\mathrm{i},2}$, (2.5), and elementary algebra reveal

$$\begin{aligned}(D^2\mathscr{E}_K^2(w), D^2\mathscr{R}_K^{\mathrm{i},2}(\widehat{v}_K))_K &= (D^2 v_K, D^2 w)_K - (D^2 v_K, D^2(w - \mathscr{E}_K^2(w)))_K\\ &+ \sum_{F\in\mathscr{F}_K^{\mathrm{i}}} \big((v_K - v_F, \partial_{\mathbf{n}}\Delta\mathscr{E}_K^2(w))_F - (\partial_{\mathbf{n}} v_K - \zeta_F, \partial_{\mathbf{nn}}\mathscr{E}_K^2(w))_F - (\partial_{\mathbf{t}}(v_K - v_F), \partial_{\mathbf{nt}}\mathscr{E}_K^2(w))_F\big)\\ &+ \sum_{F\in\mathscr{F}_K^{\mathrm{b}}} \big((v_K, \partial_{\mathbf{n}}\Delta\mathscr{E}_K^2(w))_F - (Dv_K, D^2\mathscr{E}_K^2(w)\mathbf{n}_K)_F\big). \end{aligned} \quad (5.4)$$

The symmetry of $\mathscr{R}_K^{\mathrm{i},1}$, (2.4), and elementary algebra show

$$\begin{aligned}(D\mathscr{E}_K^1(w), D\mathscr{R}_K^{\mathrm{i},1}(\widehat{v}_K))_K &= (Dv_K, Dw)_K - (Dv_K, D(w - \mathscr{E}_K^1(w)))_K\\ &- \sum_{F\in\mathscr{F}_K^{\mathrm{i}}} (v_K - v_F, \partial_{\mathbf{n}}\mathscr{E}_K^1(w))_F - \sum_{F\in\mathscr{F}_K^{\mathrm{b}}} (v_K, \partial_{\mathbf{n}}\mathscr{E}_K^1(w))_F. \end{aligned} \quad (5.5)$$

A substitution of (5.3)–(5.5) in (5.2), Cauchy–Schwarz inequality, and a reorganisation of the terms show

$$|\langle\delta_h^{(w)}, \widehat{v}_h\rangle| \lesssim \sum_{K\in\mathscr{T}_h} \Big(\gamma\|D^2 v_K\|_K\|D^2(w - \mathscr{E}_K^2(w))\|_K + \|Dv_K\|_K\|D(w - \mathscr{E}_K^1(w))\|_K$$

$$
\begin{aligned}
&+\sum_{F\in\mathscr{F}_K^{\mathrm{i}}}\gamma\|v_K-v_F\|_F\|\partial_{\mathbf{n}}\Delta(w-\mathscr{E}_K^2(w))\|_F+\sum_{F\in\mathscr{F}_K^{\mathrm{i}}}\gamma\|\partial_{\mathbf{n}}v_K-\zeta_F\|_F\|\partial_{\mathbf{nn}}(w-\mathscr{E}_K^2(w))\|_F\\
&+\sum_{F\in\mathscr{F}_K^{\mathrm{i}}}\gamma\|\partial_{\mathbf{t}}(v_K-v_F)\|_F\|\partial_{\mathbf{nt}}(w-\mathscr{E}_K^2(w))\|_F+\sum_{F\in\mathscr{F}_K^{\mathrm{i}}}\|v_K-v_F\|_F\|\partial_{\mathbf{n}}(w-\mathscr{E}_K^1(w))\|_F\\
&+\sum_{F\in\mathscr{F}_K^{\mathrm{b}}}\big(\|v_K\|_F\|\partial_{\mathbf{n}}(w-\mathscr{E}_K^1(w))\|_F+\|v_K\|_F\|\partial_{\mathbf{n}}\Delta(w-\mathscr{E}_K^2(w))\|_F+\|Dv_K\|_F\|D^2(w-\mathscr{E}_K^2(w))\|_F\big)\\
&+\mathscr{S}_K^{\mathrm{i}}(\widehat{I}_K^k(w),\widehat{I}_K^k(w))^{\frac12}\mathscr{S}_K^{\mathrm{i}}(\widehat{v}_K,\widehat{v}_K)^{\frac12}+\mathscr{S}_K^{\mathrm{b}}(\Pi_K^{k+2}(w)-w,\Pi_K^{k+2}(w)-w)^{\frac12}\mathscr{S}_K^{\mathrm{b}}(\widehat{v}_K,\widehat{v}_K)^{\frac12}\Big).
\end{aligned}
\tag{5.6}
$$

Next the terms on the right-hand side of (5.6) are controlled. The definition of $|\widehat{v}_K|_{\widehat{V}_K}$ from (2.10) and Lemma 4.3(a), (c) controls the first two terms of (5.6) inside the summation as

$$
\gamma\|D^2v_K\|_K\|D^2(w-\mathscr{E}_K^{\mathrm{i},2}(w))\|_K+\|Dv_K\|_K\|D(w-\mathscr{E}_K^{\mathrm{i},1}(w))\|_K\lesssim|\widehat{v}_K|_{\widehat{V}_K}\|w-\Pi_K^{k+2}(w)\|_{\#,K}.
$$

Recall (2.2) and (2.10) to bound the third term on the right-hand side of (5.6) as

$$
\begin{aligned}
\gamma\|v_K-v_F\|_F\|\partial_{\mathbf{n}}\Delta(w-\mathscr{E}_K^2(w))\|_F&\le\big(\gamma^{\frac12}h_K^{-\frac32}\|v_K-v_F\|_F\big)\big(\gamma^{\frac12}h_K^{\frac32}\|\partial_{\mathbf{n}}\Delta(w-\mathscr{E}_K^2(w))\|_F\big)\\
&\lesssim\gamma^{\frac12}h_K^{\frac32}|\widehat{v}_K|_{\widehat{V}_K}\|\partial_{\mathbf{n}}\Delta(w-\mathscr{E}_K^2(w))\|_F.
\end{aligned}
$$

An application of triangle inequality leads to

$$
\gamma^{\frac12}h_K^{\frac32}\|\partial_{\mathbf{n}}\Delta(w-\mathscr{E}_K^2(w))\|_F\le\gamma^{\frac12}h_K^{\frac32}\|\partial_{\mathbf{n}}\Delta(w-\Pi_K^{k+2}(w))\|_F+\gamma^{\frac12}h_K^{\frac32}\|\partial_{\mathbf{n}}\Delta(\Pi_K^{k+2}(w)-\mathscr{E}_K^2(w))\|_F.
$$

The definition of $\|\bullet\|_{\#,K}$ from (2.11) controls the first term in the right-hand side of the above inequality by $\|w-\Pi_K^{k+2}(w)\|_{\#,K}$. An application of (4.1) and Lemma 4.3(b) yields

$$
\gamma^{\frac12}h_K^{\frac32}\|\partial_{\mathbf{n}}\Delta(\Pi_K^{k+2}(w)-\mathscr{E}_K^2(w))\|_F\lesssim\gamma^{\frac12}\|D^2(\Pi_K^{k+2}(w)-\mathscr{E}_K^2(w))\|_K\lesssim\|w-\Pi_K^{k+2}(w)\|_{\#,K}.
$$

A combination of the above results prove

$$
\gamma\|v_K-v_F\|_F\|\partial_{\mathbf{n}}\Delta(w-\mathscr{E}_K^2(w))\|_F\lesssim|\widehat{v}_K|_{\widehat{V}_K}\|w-\Pi_K^{k+2}(w)\|_{\#,K}
$$

with (2.10) in the last step. The fourth-fifth (resp. sixth) terms on the right-hand side of (5.6) are also estimated analogously: first the powers of h_K,γ,σ_K are adjusted such that the term that involves $\widehat{v}_K$ is absorbed in $|\widehat{v}_K|_{\widehat{V}_K}$. A triangle inequality is applied to the terms involving w and are further controlled utilizing the definition of $\|\bullet\|_{\#,K}$ from (2.11) and Theorem 4.1(a) (resp. for the sixth term). We provide the final estimates below.

$$
\begin{aligned}
\gamma\|\partial_{\mathbf{n}}v_K-\zeta_F\|_F\|\partial_{\mathbf{nn}}(w-\mathscr{E}_K^2(w))\|_F&\lesssim|\widehat{v}_K|_{\widehat{V}_K}\|w-\Pi_K^{k+2}(w)\|_{\#,K},\\
\gamma\|\partial_{\mathbf{t}}(v_K-v_F)\|_F\|\partial_{\mathbf{nt}}(w-\mathscr{E}_K^2(w))\|_F&\lesssim|\widehat{v}_K|_{\widehat{V}_K}\|w-\Pi_K^{k+2}(w)\|_{\#,K},\\
\text{and }\|\partial_{\mathbf{n}}v_K-v_F\|_F\|\partial_{\mathbf{n}}(w-\mathscr{E}_K^1(w))\|_F&\lesssim|\widehat{v}_K|_{\widehat{V}_K}\|w-\Pi_K^{k+2}(w)\|_{\#,K}.
\end{aligned}
$$

The seventh term on the right-hand side is also controlled by $|\widehat{v}_K|_{\widehat{V}_K}\|w-\Pi_K^{k+2}(w)\|_{\#,K}$ by using the similar arguments as above. The last two-terms on the right-hand side of (5.6) is controlled by Cauchy–Schwarz inequality followed by Lemmas 4.3(d) and 3.1 as

$$
\begin{aligned}
&\mathscr{S}_K^{\mathrm{i}}(\widehat{I}_K^k(w),\widehat{I}_K^k(w))^{\frac12}\mathscr{S}_K^{\mathrm{i}}(\widehat{v}_K,\widehat{v}_K)^{\frac12}+\mathscr{S}_K^{\mathrm{b}}(\Pi_K^{k+2}(w)-w,\Pi_K^{k+2}(w)-w)^{\frac12}\mathscr{S}_K^{\mathrm{b}}(\widehat{v}_K,\widehat{v}_K)^{\frac12}\\
&\quad\le(\mathscr{S}_K^{\mathrm{i}}(\widehat{I}_K^k(w),\widehat{I}_K^k(w))^{\frac12}+\mathscr{S}_K^{\mathrm{b}}(\Pi_K^{k+2}(w)-w,\Pi_K^{k+2}(w)-w)^{\frac12})a_K(\widehat{v}_K,\widehat{v}_K)^{\frac12}\lesssim\|w-\Pi_K^{k+2}(w)\|_{\#,K}|\widehat{v}_K|_{\widehat{V}_K}.
\end{aligned}
$$

A combination of all the estimates in (5.6) and the definition of $\|\bullet\|_*$ concludes the proof. □

Proof of Theorem 3.2. To prove this, choose $\widehat{v}_h = \widehat{I}_h^k(w) - \widehat{E}_h(w)$ in (5.2) and then apply Lemma 3.1 to deduce

$$\begin{aligned}\|\widehat{I}_h^k(w) - \widehat{E}_h(w)\|_{a,h}^2 &\lesssim a_h(\widehat{I}_h^k(w) - \widehat{E}_h(w), \widehat{I}_h^k(w) - \widehat{E}_h(w)) = -\langle \delta_h^{(w)}, \widehat{I}_h^k(w) - \widehat{E}_h(w)\rangle \\ &\lesssim \|\delta_h(w)\|_* \|\widehat{I}_h^k(w) - \widehat{E}_h(w)\|_{\widehat{V}_h} \lesssim \|\delta_h(w)\|_* \|\widehat{I}_h^k(w) - \widehat{E}_h(w)\|_{a,h}.\end{aligned}$$

The inequality above and Lemma 5.1 establish that $\|\widehat{I}_h^k(w) - \widehat{E}_h(w)\|_{a,h} \lesssim \sum_{K\in\mathscr{T}_h} \|w - \Pi_K^{k+2}(w)\|_{\#,K}$. This concludes the proof. □

6. Backward Euler scheme

This section has three subsections: the proof of Lemma 3.3 is presented in Section 6.1, Theorems 3.4(a) and 3.4(b) are proved in Sections 6.2 and 6.3, respectively.

Recall the *fully-discrete backward Euler HHO scheme* from Section 3.2: For $1 \le n \le m$ and for all $\widehat{v}_h = (v_h, v_{\mathscr{F}_h^{\mathrm{i}}}, \zeta_{\mathscr{F}_h^{\mathrm{i}}}) \in \widehat{V}_h$, seek $\widehat{u}_h^n = (u_h^n, u_{\mathscr{F}_h^{\mathrm{i}}}^n, \sigma_{\mathscr{F}_h^{\mathrm{i}}}^n) \in \widehat{V}_h$ such that

$$(\bar{\partial} u_h^n, v_h) + a_h(\widehat{u}_h^n, \widehat{v}_h) + (f(u_h^n), v_h) = 0 \ \text{ and } \ \widehat{u}_h^0 = \widehat{I}_h^k(u_0). \tag{6.1}$$

6.1. Proof of Lemma 3.3

Proof of the Lemma 3.3(a) (i). It is enough to establish that $L(\widehat{u}_h^n)$ is a decreasing sequence for all $0 \le n \le m$. The choice $\widehat{v}_h^n = \bar{\partial}\widehat{u}_h^n$ in (6.1) leads to $\|\bar{\partial} u_h^n\|^2 + a_h(\widehat{u}_h^n, \bar{\partial}\widehat{u}_h^n) + (f(u_h^n), \bar{\partial} u_h^n) = 0$. Recall that $F(v) := \frac{1}{4}(1-v^2)^2$. A Taylor series expansion shows

$$(F(u_h^n) - F(u_h^{n-1}), 1) = (f(u_h^n), u_h^n - u_h^{n-1}) - \frac{1}{2}(F''(\varrho_h^n)(u_h^n - u_h^{n-1})^2, 1),$$

where $\widehat{\varrho}_h^n$ is a point on the line connecting $\widehat{u}_h^n$ and $\widehat{u}_h^{n-1}$. The above displayed identity and elementary algebra lead to

$$\|\bar{\partial} u_h^n\|^2 + \frac{1}{2}\bar{\partial} a_h(\widehat{u}_h^n, \widehat{u}_h^n) + \frac{\Delta t}{2} a_h(\bar{\partial}\widehat{u}_h^n, \bar{\partial}\widehat{u}_h^n) + (\bar{\partial} F(u_h^n), 1) = -\frac{\Delta t}{2}(F''(\varrho_n)(\bar{\partial} u_h^n)^2, 1). \tag{6.2}$$

The observation $F''(\bullet) = f'(\bullet) \ge -1$ leads to $-\frac{1}{2}(F''(\varrho_n)(\bar{\partial} u_h^n)^2, 1) \le \frac{1}{2}\|\bar{\partial} u_h^n\|^2$. Since $\frac{\Delta t}{2} a_h(\bar{\partial}\widehat{u}_h^n, \bar{\partial}\widehat{u}_h^n)$ is non-negative from Lemma 3.1, it follows that $(1-\frac{\Delta t}{2})\|\bar{\partial} u_h^n\|^2 + \frac{1}{2}\bar{\partial} a_h(\widehat{u}_h^n, \widehat{u}_h^n) + (\bar{\partial} F(u_h^n), 1) \le 0$. Hence for $0 < \Delta t \le \frac{1}{2}$, from (3.3), we obtain

$$\bar{\partial} L(\widehat{u}_h^n) \le \left(\frac{\Delta t}{2} - 1\right)\|\bar{\partial} u_h^n\|^2 \le 0.$$

□

Proof of the Lemma 3.3(a) (ii). The definition of $L(\bullet)$ from (3.3) and (i) lead to $\frac{1}{2} a_h(\widehat{u}_h^n, \widehat{u}_h^n) + (F(u_h^n), 1) \le \frac{1}{2} a_h(\widehat{u}_h^0, \widehat{u}_h^0) + (F(u_h^0), 1)$. Since $F(u_h^n) = \frac{1}{4}(1 - (u_h^n)^2)^2 \ge 0$ and $(F(u_h^0), 1) = \frac{1}{4}(\|u_h^0\|_{L^4(\Omega)}^4 - 2\|u_h^0\|^2 + |\Omega|)$, an application of Theorem 4.1(f) establishes $\|\widehat{u}_h^n\|_{a,h}^2 \lesssim \|\widehat{u}_h^0\|_{a,h}^2 + |\Omega|$. Lemmas 3.1 and 4.5 with $\widehat{u}_h^0 = \widehat{I}_h^k(u_0)$ conclude the proof of (ii). □

Proof of the Lemma 3.3(a) (iii). Theorem 4.1(f) and (ii) establish $\|u_h^n\|_{L^q(\Omega)} \le C(|u_0|_{H^1(\mathscr{T}_h)}, \gamma^{\frac{1}{2}}|u_0|_{H^2(\mathscr{T}_h)}, |\Omega|)$. □

Proof of Lemma 3.3(b) The proof follows from Theorem 5.2 of [13] and is presented for continuity of reading. The existence proof utilizes the lemma stated below which is a consequence of the Brouwer's fixed point theorem.

Lemma 6.1 ([30], pp. 219 and [36]). *Let H be a finite dimensional Hilbert space with inner-product $(\bullet,\bullet)_H$ and the induced norm $\|\bullet\|_H$. Further, let $\mathscr{N}: H \to H$ be a continuous mapping defined and be such that $(\mathscr{N}(v), v)_H \geq 0$ for all $v \in H$ with $\|v\|_H = \beta > 0$. Then there exists $v^* \in H$ with $\|v^*\|_H \leq \beta$ such that $\mathscr{N}(v^*) = 0$.*

Settings. Choose $H := \widehat{V}_h$ equipped with norm $|||\widehat{v}_h^n|||_{\widehat{V}_h}^2 := \Delta t a_h(\widehat{v}_h^n, \widehat{v}_h^n) + \frac{1}{4}\|v_h^n\|^2$ for all $\widehat{v}_h^n := (v_h^n, v_{\mathscr{F}_h^{\mathrm{i}}}^n, \zeta_{\mathscr{F}_h^{\mathrm{i}}}^n)$ with $v_h^n = (v_K^n)_{K\in\mathscr{T}_h}$. Then, define $\widetilde{\mathscr{N}}: \widehat{V}_h \to \mathbb{R}$ by

$$\widetilde{\mathscr{N}}(\widehat{w}_h) := (v_h^n, w_h) + \Delta t a_h(\widehat{v}_h^n, \widehat{w}_h) + \Delta t(f(v_h^n), w_h) - (v_h^{n-1}, w_h) \ \text{ for all } \widehat{w}_h \in \widehat{V}_h, \tag{6.3}$$

for given $\widehat{v}_h^{n-1} \in \widehat{V}_h$ (this is indeed the datum $\widehat{u}_h^{n-1}$ will be clear towards the end of the proof of the existence). The Riesz representation theorem yields $\mathscr{N}(\widehat{v}_h^n) \in \widehat{V}_h$ such that $(\mathscr{N}(\widehat{v}_h^n), \widehat{w}_h)_{\widehat{V}_h} := \widetilde{\mathscr{N}}(\widehat{w}_h)$ for all $\widehat{w}_h \in \widehat{V}_h$.

Existence. Note that $(f(v_h^n), v_h^n) = ((v_h^n)^3 - v_h^n, v_h^n) = \|v_h^n\|_{L^4(\Omega)}^4 - \|v_h^n\|^2 \geq -\|v_h^n\|^2$. This, the definition of $\|\bullet\|_{\widehat{V}_h}$, Cauchy–Schwarz inequality, the Young's inequality from (1.2), and elementary manipulations show

$$\begin{aligned}(\mathscr{N}(\widehat{v}_h^n), \widehat{v}_h^n)_{\widehat{V}_h} &\geq (1-\Delta t)\|v_h^n\|^2 + \Delta t a_h(\widehat{v}_h^n, \widehat{v}_h^n) - \|v_h^{n-1}\|\|v_h^n\| \\ &\geq \left(\frac{1}{2} - \Delta t\right)\|v_h^n\|^2 + |||\widehat{v}_h^n|||_{\widehat{V}_h}^2 - \|v_h^{n-1}\|^2 \geq |||\widehat{v}_h^n|||_{\widehat{V}_h}^2 - \|v_h^{n-1}\|^2\end{aligned}$$

for $0 < \Delta t < 1/2$. Hence for $\widehat{v}_h^n \in \widehat{V}_h$ with $|||\widehat{v}_h^n|||_{\widehat{V}_h} = \beta := (\|v_h^{n-1}\|^2 + 1)^{1/2}$, $(\mathscr{N}(\widehat{v}_h^n), \widehat{v}_h^n)_{\widehat{V}_h} \geq 0$.

Thus the hypothesis of Lemma 6.1 holds true and hence there exists $(\widehat{v}_h^n)^*$ such that $\mathscr{N}(\widehat{v}_h^n)^* = 0$. In particular, $(\widehat{v}_h^n)^* = \widehat{u}_h^n$ satisfies Lemma 6.1 and $\widehat{v}_h^{n-1} = \widehat{u}_h^{n-1}$. This concludes the proof of the existence.

Uniqueness. If possible, let $\widehat{p}_h^n$ and $\widehat{q}_h^n$ denote two distinct discrete solutions of (6.1). Define $\widehat{\Upsilon}_h^n := \widehat{p}_h^n - \widehat{q}_h^n$ with $\widehat{\Upsilon}_h^n = (\Upsilon_h^n, \Upsilon_{\mathscr{F}_h^{\mathrm{i}}}^n, \xi_{\mathscr{F}_h^{\mathrm{i}}}^n) \in \widehat{V}_h$. This yields

$$(\bar{\partial}\Upsilon_h^n, v_h) + a_h(\widehat{\Upsilon}_h^n, \widehat{v}_h) + (f(p_h^n) - f(q_h^n), v_h) = 0 \ \text{ for all } \widehat{v}_h \in \widehat{V}_h \text{ and } \widehat{\Upsilon}_h^0 = \widehat{0}_h. \tag{6.4}$$

Choose $\widehat{v}_h = \widehat{\Upsilon}_h^n$ in (6.4). The first-term is then controlled as $(\bar{\partial}\Upsilon_h^n, \Upsilon_h^n) \geq \frac{1}{2}\bar{\partial}\|\Upsilon_h^n\|^2$. The coercivity of a_h from Lemma 3.1 shows that $a_h(\widehat{\Upsilon}_h^n, \widehat{\Upsilon}_h^n) \geq 0$. The mean value theorem reveals $(f(p_h^n) - f(q_h^n), \Upsilon_h^n) = (f'(\varrho_n)\Upsilon_h^n, \Upsilon_h^n)$, where ϱ_n is the point on the line joining p_h^n and q_h^n. Since $f'(\bullet) \geq -1$, we obtain $(f(p_h^n) - f(q_h^n), \Upsilon_h^n) \geq -\|\Upsilon_h^n\|^2$.

All this in (6.4) leads to $\frac{1}{2}\bar{\partial}\|\Upsilon_h^n\|^2 - \|\Upsilon_h^n\|^2 \leq 0$. The definition of $\bar{\partial}$ and elementary algebra reveal $(1 - 2\Delta t)\|\Upsilon_h^n\|^2 \leq \|\Upsilon_h^{n-1}\|^2$. An inductive process shows $\Upsilon_h^n = 0_h$, *i.e.*, $p_h^n = q_h^n$ for all $0 \leq n \leq m$ with $0 < \Delta t < \frac{1}{2}$ This, the choice $\widehat{v}_h = \widehat{\Upsilon}_h^n$ in (6.4), and Lemma 3.1 lead to $\|\widehat{\Upsilon}_h^n\|_{a,h} = 0$. Hence, $\widehat{p}_h^n = \widehat{q}_h^n$. This contradiction establishes the uniqueness of the discrete solution.

6.2. Proof of Theorem 3.4 (a)

The proof of Theorem 3.4 is divided into eight steps below. The constants C_1, C_2, C_3 in Steps 3–5 are independent of γ but may depend on the constants from the discrete trace, discrete inverse, discrete Poincaré inequalities from Theorem 4.1 and ε in the Young's inequality.

Step 1: Settings**.** Recall the projection operator $\widehat{E}_h$ from Section 3.1. Define

$$\chi(v^n) := \bar{\partial}v^n - v_t^n \tag{6.5}$$

and let $\widehat{E}_h(u_0) := \widehat{I}_h^k(u_0)$. Introduce the split

$$\widehat{e}_h^n := \widehat{\eta}_h^n + \widehat{\theta}_h^n, \text{ where } \widehat{\eta}_h^n = \widehat{I}_h^k(u^n) - \widehat{E}_h(u^n),\ \widehat{\theta}_h^n = \widehat{E}_h(u^n) - \widehat{u}_h^n. \tag{6.6}$$

Also $\widehat{e}_h^n := \widehat{I}_h^k(u^n) - \widehat{u}_h^n = (e_h^n, e_{\mathscr{F}_h^{\mathrm{i}}}^n, \kappa_{\mathscr{F}_h^{\mathrm{i}}}^n)$ with $\widehat{e}_h^n|_K = \widehat{I}_K^k(u^n) - \widehat{u}_K^n := \widehat{e}_K^n = (e_K^n, e_{\mathscr{F}_K^{\mathrm{i}}}^n, \kappa_{\mathscr{F}_K^{\mathrm{i}}}^n)$. Recall that $\mathscr{E}_K^{\mathrm{i},1} := \mathscr{R}_K^{\mathrm{i},1} \circ \widehat{I}_K^k$ and $\mathscr{E}_K^{\mathrm{i},2} := \mathscr{R}_K^{\mathrm{i},2} \circ \widehat{I}_K^k$. Introduce a local split for the reconstruction errors as

$$\begin{aligned} u^n - \mathscr{R}_K^{\mathrm{i},1}(\widehat{u}_K^n) - \mathscr{L}_K^1(u^n) &= u^n - \mathscr{E}_K^1(u^n) + \mathscr{R}_K^{\mathrm{i},1}(\widehat{e}_K^n) \\ \text{and } u^n - \mathscr{R}_K^{\mathrm{i},2}(\widehat{u}_K^n) - \mathscr{L}_K^2(u^n) &= u^n - \mathscr{E}_K^2(u^n) + \mathscr{R}_K^{\mathrm{i},2}(\widehat{e}_K^n). \end{aligned} \tag{6.7}$$

We set the notation as $\mathscr{R}_K^j(\widehat{u}_K) := \mathscr{R}_K^{\mathrm{i},j}(\widehat{u}_K^n) + \mathscr{L}_K^j(u^n)$ $j = 1, 2$. Note that $\mathscr{L}^j(u)$ is non-zero only on the boundary cells where it is fully computable from the boundary cells.

Step 2: Error equation**.** The combination of HHO formulation (6.1) and (1.1) lead to

$$(\bar{\partial} u_h^n, \widehat{v}_h) + a_h(\widehat{u}_h^n, \widehat{v}_h) + (f(u_h^n), v_h) = (u_t^n + \gamma \Delta^2 u^n - \Delta u^n + f(u^n), v_h) \text{ for all } \widehat{v}_h \in \widehat{V}_h.$$

The definition of $\widehat{e}_h^n$ from Step 1 with $\widehat{I}_h^k(u^n) := (\Pi_h^{k+2}(u^n), \Pi_{\mathscr{F}_h^{\mathrm{i}}}^{k+2}(u^n), \Pi_{\mathscr{F}_h^{\mathrm{i}}}^k(\partial_{\mathbf{n}} u^n))$ and elementary manipulations reveal

$$\begin{aligned} (\bar{\partial} e_h^n, v_h) + a_h(\widehat{e}_h^n, \widehat{v}_h) &= a_h(\widehat{I}_h^k(u^n), \widehat{v}_h) - \gamma(\Delta^2 u^n, v_h) + (\Delta u^n, \widehat{v}_h) + (\bar{\partial}\Pi_h^{k+2}(u^n) - u_t^n, v_h) + (f(u_h^n) - f(u^n), v_h) \\ &= \langle \delta_h(u^n), \widehat{v}_h \rangle + (\bar{\partial}\Pi_h^{k+2}(u^n) - u_t^n, \widehat{v}_h) + (f(u_h^n) - f(u^n), v_h), \end{aligned}$$

where the definition of $\delta_h(u^n)$ from (5.2) used in the last step. The choice $\widehat{v}_h = \widehat{e}_h^n$ in above equation, the definition of $\bar{\partial}$, and elementary manipulations lead to

$$\begin{aligned} \|e_h^n\|^2 + \Delta t a_h(\widehat{e}_h^n, \widehat{e}_h^n) = \Delta t \big(&\langle \delta_h(u^n), \widehat{e}_h^n \rangle + (\bar{\partial}\Pi_h^{k+2}(u^n) - u_t^n, e_h^n) \\ &+ (f(u_h^n) - f(u^n), e_h^n) \big) + (e_h^n, e_h^{n-1}) := \Delta t \sum_{i=1}^{3} Q_i + Q_4. \end{aligned} \tag{6.8}$$

Step 3: Control of Q_1**.** Lemma 5.1 with $w = u^n$ (resp. $\widehat{v}_h = \widehat{e}_h^n$) yields $Q_1 \lesssim \sum_{K \in \mathscr{T}_h} \|\widehat{e}_K^n\|_{\widehat{V}_K} \|u^n - \Pi_K^{k+2}(u^n)\|_{\#,K}$. An application of Lemma 3.1 and (1.2) with $\varepsilon = 1/3$ leads to

$$Q_1 \leq \frac{1}{6} \|\widehat{e}_h^n\|_{a,h}^2 + C_1 \sum_{K \in \mathscr{T}_h} \|u^n - \Pi_K^{k+2}(u^n)\|_{\#,K}^2.$$

Step 4: Control of Q_2**.** Introduce an intermediate term to rewrite Q_2 as $(\bar{\partial}\Pi_h^{k+2}(u^n) - \bar{\partial} u^n, e_h^n) + (\chi(u^n), e_h^n)$, where $\chi(u^n) := \bar{\partial} u^n - u_t^n$. Elementary algebra using the definitions of $\bar{\partial}$ and the projection Π_h^{k+2} shows that the first term in this expression vanishes. The second term can be controlled using Cauchy–Schwarz inequality, Theorem 4.1(f), and (1.2) with $\varepsilon = 1/3$ and we obtain

$$Q_2 = (\chi(u^n), e_h^n) \leq \|\chi(u^n)\| \|e_h^n\| \leq C_2 \|\chi(u^n)\|^2 + \frac{1}{6} \|\widehat{e}_h^n\|_{a,h}^2.$$

Step 5: Control of Q_3**.** Rewrite Q_3 as $(f(\Pi_h^{k+2}(u^n)) - f(u^n), e_h^n) - (f(\Pi_h^{k+2}(u^n)) - f(u_h^n), e_h^n)$. The mean value theorem shows $f(\Pi_h^{k+2}(u^n)) - f(u^n) = f'(u_\alpha^n)(\Pi_h^{k+2}(u^n) - u^n)$, where $u_\alpha^n = (1-\alpha)u^n + \alpha \Pi_h^{k+2}(u^n)$ for some $\alpha \in (0,1)$. The definition of f' and Cauchy–Schwarz inequality yield

$$\begin{aligned} (f(\Pi_h^{k+2}(u^n)) - f(u^n), e_h^n) &= ((3(u_\alpha^n)^2 - 1)(\Pi_h^{k+2}(u^n) - u^n), e_h^n) \\ &\leq \big(3\|(u_\alpha^n)^2 e_h^n)\| + \|e_h^n\| \big) \|\Pi_h^{k+2}(u^n) - u^n\|. \end{aligned} \tag{6.9}$$

A generalized Holder's inequality shows $\|u_\alpha^n\|_{L^8(\Omega)}^2 \leq \tilde{C_3^1} \big(\|u^n\|_{L^8(\Omega)}^2 + \|\Pi_h^{k+2}(u^n)\|_{L^8(\Omega)}^2 \big)$ and

$$\|(u_\alpha^n)^2 e_h^n\| \leq \|u_\alpha^n\|_{L^8(\Omega)}^2 \|e_h^n\|_{L^4(\Omega)} \leq \tilde{C_3^1} \big(\|u^n\|_{L^8(\Omega)}^2 + \|\Pi_h^{k+2}(u^n)\|_{L^8(\Omega)}^2 \big) \|e_h^n\|_{L^4(\Omega)}. \tag{6.10}$$

The regularity of u^n and a Sobolev embedding result show $\|u^n\|_{L^8(\Omega)} \leq \tilde{C}_3^2$. Theorem 4.1(f) and Lemma 3.1 reveal

$$\|\Pi_h^{k+2}(u^n)\|_{L^8(\Omega)} \lesssim \|\widehat{I}_h^k(u^n)\|_{a,h} \lesssim \|\widehat{I}_h^k(u^n)\|_{\widehat{V}_h} \lesssim |u^n|_{H^1(\Omega)} + |u^n|_{H^2(\Omega)} \leq \tilde{C}_3^3$$

with Lemma 4.5, $\gamma \leq 1$, and the regularity of u^n utilized in the last step. Theorem 4.1(f) applied once again shows

$$\|e_h^n\|_{L^4(\Omega)} \leq \tilde{C}_3^4 \|\widehat{e}_h^n\|_{a,h} \text{ and } \|e_h^n\| \leq \tilde{C}_3^5 \|\widehat{e}_h^n\|_{a,h}. \tag{6.11}$$

A combination of these bounds in (6.9) show

$$(f(\Pi_h^{k+2}(u^n)) - f(u^n), e_h^n) \leq \widehat{C}_3 \|\widehat{e}_h^n\|_{a,h} \|\Pi_h^{k+2}(u^n) - u^n\| \quad \text{with } \widehat{C}_3 = 3\tilde{C}_3^1 \tilde{C}_3^4 ((\tilde{C}_3^2)^2 + (\tilde{C}_3^3)^2) + \tilde{C}_3^5. \tag{6.12}$$

Use (1.2) with $\varepsilon = 1/3$ in (6.12) to show

$$(f(\Pi_h^{k+2}(u^n)) - f(u^n), e_h^n) \leq C_3 \|\Pi_h^{k+2}(u^n) - u^n\|^2 + \frac{1}{6}\|\widehat{e}_h^n\|_{a,h}^2$$

with $C_3 = \frac{3}{2}\big(\widehat{C}_3\big)^2$. The mean value theorem applied once more shows $f(\Pi_h^{k+2}(u^n)) - f(u_h^n) = f'(\varrho_n)e_h^n$, where $\varrho_n = (1-\alpha)u_h^n + \alpha\Pi_h^{k+2}(u^n)$ for some $\alpha \in (0,1)$. Utilize $f'(\bullet) \geq -1$ and Cauchy–Schwarz inequality to obtain

$$-(f(\Pi_h^{k+2}(u^n)) - f(u_h^n), e_h^n) = -(f'(\varrho_n)e_h^n, e_h^n) \leq \|e_h^n\|^2.$$

A combination of the last two displayed inequalities yield

$$Q_3 \leq C_3 \|\Pi_h^{k+2}(u^n) - u^n\|^2 + \frac{1}{6}\|\widehat{e}_h^n\|_{a,h}^2 + \|e_h^n\|^2.$$

Step 6: Control of Q_4**.** The Cauchy–Schwarz inequality and Young's inequality reveal

$$Q_4 = (e_h^n, e_h^{n-1}) \leq \|e_h^n\| \|e_h^{n-1}\| \leq \frac{1}{2}\|e_h^n\|^2 + \frac{1}{2}\|e_h^{n-1}\|^2.$$

Step 7: Abstract error bounds**.** Substitute the bounds of Q_i $(i = 1,2,3,4)$ from Steps 3–6 in (6.8) and use elementary manipulations to show

$$\frac{1}{2}\|e_h^n\|^2 + \frac{\Delta t}{2}\|\widehat{e}_h^n\|_{a,h}^2 \leq C_4 \Delta t \left(\|\chi(u^n)\|^2 + \|u^n - \Pi_h^{k+2}(u^n)\|^2 + \sum_{K \in \mathscr{T}_h} \|u^n - \Pi_K^{k+2}(u^n)\|_{\#,K}^2 \right)$$
$$+ \Delta t \|e_h^n\|^2 + \frac{1}{2}\|e_h^{n-1}\|^2$$

with $C_4 = \max\{C_1, C_2, C_3\}$. Multiply the above inequality by 2, sum it from $n = 1$ to l (where l can be $1, 2, \cdots, m$), introduce $C_5 = 2C_4$, and utilize $\widehat{e}_h^0 = 0$ to observe

$$(1 - 2\Delta t)\|e_h^n\|^2 + \Delta t \sum_{n=1}^{l} \|\widehat{e}_h^n\|_{a,h}^2 \leq C_5 \Delta t \sum_{n=1}^{l} \left(\|\chi(u^n)\|^2 + \|u^n - \Pi_h^{k+2}(u^n)\|^2 + \sum_{K \in \mathscr{T}_h} \|u^n - \Pi_K^{k+2}(u^n)\|_{\#,K}^2 \right)$$
$$+ 2\Delta t \sum_{n=1}^{l-1} \|e_h^n\|^2.$$

For $0 < \Delta t < 1/2$, an application of discrete Gronwall's inequality ([37], Lem. 10.5) shows

$$\|e_h^l\| + \left(\Delta t \sum_{n=1}^{l} \|\widehat{e}_h^n\|_{a,h}^2 \right)^{1/2} \lesssim \left(\Delta t \sum_{n=1}^{l} \left(\|\chi(u^n)\|^2 + \|u^n - \Pi_h^{k+2}(u^n)\|^2 + \sum_{K \in \mathscr{T}_h} \|u^n - \Pi_K^{k+2}(u^n)\|_{\#,K}^2 \right) \right)^{1/2}.$$

Taking maximum as l varies from 1 to m, we obtain

$$\max_{1\le l\le m}\|e_h^l\|+\left(\Delta t\sum_{l=1}^{m}\|\widehat{e}_h^l\|_{a,h}^2\right)^{1/2}$$
$$\lesssim\left(\Delta t\sum_{l=1}^{m}\left(\|\chi(u^l)\|^2+\|u^l-\Pi_h^{k+2}(u^l)\|^2+\sum_{K\in\mathscr{T}_h}\|u^l-\Pi_K^{k+2}(u^l)\|_{\#,K}^2\right)\right)^{1/2}. \tag{6.13}$$

A triangle inequality applied to (6.6), and (6.13) lead to

$$\max_{1\le n\le m}\|u^n-u_h^n\|\lesssim\max_{1\le n\le m}\|u^n-\Pi_h^{k+2}(u^n)\|+\max_{1\le n\le m}\|e_h^n\|\lesssim\max_{1\le n\le m}\|u^n-\Pi_h^{k+2}(u^n)\|$$
$$+\left(\Delta t\sum_{n=1}^{m}\left(\|\chi(u^n)\|^2+\|u^n-\Pi_h^{k+2}(u^n)\|^2+\sum_{K\in\mathscr{T}_h}\|u^n-\Pi_K^{k+2}(u^n)\|_{\#,K}^2\right)\right)^{1/2}. \tag{6.14}$$

The definition of $\|\bullet\|_{a,h}$ reveals

$$\left(\sum_{K\in\mathscr{T}_h}\left(\gamma\|D^2\mathscr{R}_K^{\mathrm{i},2}(\widehat{e}_K^n)\|_K^2+\|D\mathscr{R}_K^{\mathrm{i},1}(\widehat{e}_K^n)\|_K^2\right)\right)^{1/2}\lesssim\|\widehat{e}_h^n\|_{a,h}. \tag{6.15}$$

Apply triangle inequality in (6.7), utilize (6.15), and (6.13) to obtain

$$\left(\Delta t\sum_{n=1}^{m}\left(\sum_{K\in\mathscr{T}_h}\left(\gamma\|D^2(u^n-\mathscr{R}_K^2(\widehat{u}_K^n))\|_K^2+\|D(u^n-\mathscr{R}_K^1(\widehat{u}_K^n))\|_K^2\right)\right)\right)^{1/2}$$
$$\lesssim\left(\Delta t\sum_{n=1}^{m}\left(\sum_{K\in\mathscr{T}_h}\left(\gamma\|D^2(u^n-\mathscr{E}_K^2(u^n))\|_K^2+\|D(u^n-\mathscr{E}_K^1(u^n))\|_K^2\right)\right)\right)^{1/2}+\left(\Delta t\sum_{n=1}^{m}\|\widehat{e}_h^n\|_{a,h}^2\right)^{1/2}$$
$$\lesssim\left(\Delta t\sum_{n=1}^{m}\left(\sum_{K\in\mathscr{T}_h}\left(\gamma\|D^2(u^n-\mathscr{E}_K^2(u^n))\|_K^2+\|D(u^n-\mathscr{E}_K^1(u^n))\|_K^2\right)\right)\right)^{1/2}$$
$$+\left(\Delta t\sum_{n=1}^{m}\left(\|\chi(u^n)\|^2+\|u^n-\Pi_h^{k+2}(u^n)\|^2+\sum_{K\in\mathscr{T}_h}\|u^n-\Pi_K^{k+2}(u^n)\|_{\#,K}^2\right)\right)^{1/2}.$$

A combination of (6.14) and above displayed result leads to an *abstract* bound for the error below.

$$\max_{1\le n\le m}\|u^n-u_h^n\|+\left(\Delta t\sum_{n=1}^{m}\left(\sum_{K\in\mathscr{T}_h}\left(\gamma\|D^2(u^n-\mathscr{R}_K^2(\widehat{u}_K^n))\|_K^2+\|D(u^n-\mathscr{R}_K^1(\widehat{u}_K^n))\|_K^2\right)\right)\right)^{1/2}$$
$$\lesssim\max_{1\le n\le m}\|u^n-\Pi_h^{k+2}(u^n)\|+\left(\Delta t\sum_{n=1}^{m}\left(\sum_{K\in\mathscr{T}_h}\left(\gamma\|D^2(u^n-\mathscr{E}_K^2(u^n))\|_K^2+\|D(u^n-\mathscr{E}_K^1(u^n))\|_K^2\right)\right)\right)^{1/2}$$
$$+\left(\Delta t\sum_{n=1}^{m}\left(\|\chi(u^n)\|^2+\|u^n-\Pi_h^{k+2}(u^n)\|^2+\sum_{K\in\mathscr{T}_h}\|u^n-\Pi_K^{k+2}(u^n)\|_{\#,K}^2\right)\right)^{1/2}. \tag{6.16}$$

Step 8: Conclusion**.** In this step, the terms on the right-hand side of (6.16) are controlled under the additional regularity assumptions on the exact solution.

An application of Theorem 4.1(d) yields

$$\max_{1\le n\le m}\|u^n-\Pi_h^{k+2}(u^n)\|\lesssim\begin{cases}h^{k+3}|u|_{L^\infty(0,T;H^{k+3}(\mathscr{T}_h))} & \text{for } k\ge 1,\\ h^3(|u|_{L^\infty(0,T;H^3(\mathscr{T}_h))}+h^\beta|u|_{L^\infty(0,T;H^{3+\beta}(\mathscr{T}_h))}) & \text{for } k=0.\end{cases}\tag{6.17}$$

Use Lemma 4.3(a), (c) to get

$$\left(\Delta t\sum_{n=1}^m\left(\sum_{K\in\mathscr{T}_h}\left(\gamma\|D^2(u^n-\mathscr{E}_K^2(u^n))\|_K^2+\|D(u^n-\mathscr{E}_K^1(u^n))\|_K^2\right)\right)\right)^{1/2}$$
$$\lesssim\left(\Delta t\sum_{n=1}^m\left(\sum_{K\in\mathscr{T}_h}\|u^n-\Pi_K^{k+2}(u^n)\|_{\#,K}^2\right)\right)^{1/2}.$$

Apply Lemma 4.4 and use the fact $m\Delta t=T$ on the right-hand side of the above inequality to obtain

$$\left(\Delta t\sum_{n=1}^m\left(\sum_{K\in\mathscr{T}_h}\|u^n-\Pi_K^{k+2}(u^n)\|_{\#,K}^2\right)\right)^{1/2}\lesssim\begin{cases}(\sum_{K\in\mathscr{T}_h}h^{k+2}\sigma_K^{\frac12})|u|_{L^\infty(0,T;H^{k+3}(\mathscr{T}_h))} & \text{for } k\ge1,\\ (\sum_{K\in\mathscr{T}_h}h^2\sigma_K^{\frac12})(|u|_{L^\infty(0,T;H^3(\mathscr{T}_h))} & \\ \quad+h^\beta|u|_{L^\infty(0,T;H^{3+\beta}(\mathscr{T}_h))}) & \text{for } k=0.\end{cases}\tag{6.18}$$

The definition of $\chi(\bullet)$ from (6.5) and Lemma 4.2 lead to

$$\left(\Delta t\sum_{n=1}^m\|\chi(u^n)\|^2\right)^{1/2}\lesssim\Delta t\|u_{tt}\|_{L^2(0,T;L^2(\Omega)}.\tag{6.19}$$

Use Theorem 4.1(d) and use the fact $m\Delta t=T$ to establish

$$\left(\Delta t\sum_{n=1}^m\|u^n-\Pi_h^{k+2}(u^n)\|^2\right)^{1/2}\lesssim\begin{cases}h^{k+3}|u|_{L^\infty(0,T;H^{k+3}(\mathscr{T}_h))} & \text{for } k\ge1,\\ h^3(|u|_{L^\infty(0,T;H^3(\mathscr{T}_h))}+h^\beta|u|_{L^\infty(0,T;H^{3+\beta}(\mathscr{T}_h))}) & \text{for } k=0.\end{cases}\tag{6.20}$$

A combination of (6.17)–(6.20) with (6.16) concludes the proof of Theorem 3.4(a).

6.3. Proof of Theorem 3.4 (b)

The proof is divided into five steps. The constants C_6, C_7, C_8 in Steps 2–3 are independent of γ but may depend on the constants from the discrete trace, discrete inverse, and discrete Poincaré inequalities from Theorem 4.1 and ε in the Young's inequality. Recall the settings from Section 6.2.

Step 1: Error inequality**.** For all $\widehat{v}_h=(v_h,v_{\mathscr{F}_h^{\mathrm{i}}},\zeta_{\mathscr{F}_h^{\mathrm{i}}})\in\widehat{V}_h$, (1.1) leads to

$$(u_t^n,v_h)+(\gamma\Delta^2u^n-\Delta u^n,v_h)+(f(u^n),v_h)=0.$$

The definitions of Π_h^{k+2} in (2.3) and $\widehat{E}_h$ in Section 3.1 applied to the first and second terms of the above expression, respectively, shows

$$(\Pi_h^{k+2}(u_t^n),v_h)+a_h(\widehat{E}_h(u^n),\widehat{v}_h)+(f(u^n),v_h)=0\quad\text{for all }\widehat{v}_h\in\widehat{V}_h.\tag{6.21}$$

The backward Euler HHO scheme (6.1), (6.21), the definition of $\bar\partial$, the abbreviation $\widehat{\theta}_h^n=\widehat{E}_h(u^n)-\widehat{u}_h^n:=(\theta_h^n,\theta_{\mathscr{F}_h^{\mathrm{i}}}^n,\tilde\theta_{\mathscr{F}_h^{\mathrm{i}}}^n)$ from (6.6), and elementary algebra lead to

$$(\bar\partial\theta_h^n,\widehat{v}_h)+a_h(\widehat{\theta}_h^n,\widehat{v}_h)=(f(u_h^n)-f(u^n),\widehat{v}_h)+(\bar\partial E_h(u^n)-\Pi_h^{k+2}(u_t^n),\widehat{v}_h)\quad\text{for all }\widehat{v}_h\in\widehat{V}_h.$$

Choose $\widehat{v}_h^n = \widehat{\theta}_h^n - \widehat{\theta}_h^{n-1}$ in the above equation. The definition of $\bar{\partial}$ yields $(\Delta t)^{-1}\|\theta_h^n - \theta_h^{n-1}\|^2 \le (\bar{\partial}\theta_h^n, \theta_h^n - \theta_h^{n-1})$ and Young's inequality helps to deduce $\frac{1}{2}\big(\|\widehat{\theta}_h^n\|_{a,h}^2 - \|\widehat{\theta}_h^{n-1}\|_{a,h}^2\big) \le a_h(\widehat{\theta}_h^n, \widehat{\theta}_h^n - \widehat{\theta}_h^{n-1})$. All these show

$$\begin{aligned}\frac{1}{\Delta t}\|\theta_h^n - \theta_h^{n-1}\|^2 + \frac{1}{2}\big(\|\widehat{\theta}_h^n\|_{a,h}^2 - \|\widehat{\theta}_h^{n-1}\|_{a,h}^2\big) &\le (f(u_h^n) - f(u^n), \theta_h^n - \theta_h^{n-1})\\ &\quad + (\bar{\partial}E_h(u^n) - \Pi_h^{k+2}(u_t^n), \theta_h^n - \theta_h^{n-1}) =: N_1 + N_2. \end{aligned} \tag{6.22}$$

Step 2: Control of N_1. Let $\widehat{E}_h = (E_h, E_{\mathscr{F}_h^{\mathrm{i}}}, E_{\mathscr{F}_h^{\mathrm{i}}})$. Introduce an intermediate term to obtain

$$\begin{aligned}N_1 := (f(u_h^n) - f(u^n), \theta_h^n - \theta_h^{n-1}) &= (f(u_h^n) - f(E_h(u^n)), \theta_h^n - \theta_h^{n-1})\\ &\quad + (f(E_h(u^n)) - f(u^n), \theta_h^n - \theta_h^{n-1}).\end{aligned} \tag{6.23}$$

The first term on the right-hand side of (6.23) is controlled using arguments similar to (6.9) and (6.10) with $u_\alpha^n = (1-\alpha)u_h^n + \alpha E_h(u^n)$ leading to

$$\begin{aligned}(f(u_h^n) - f(E_h(u^n)), \theta_h^n - \theta_h^{n-1}) &= -((3(u_\alpha^n)^2 - 1)\theta_h^n, \theta_h^n - \theta_h^{n-1})\\ &\le (3\|(u_\alpha^n)^2\theta_h^n\|) + \|\theta_h^n\|)\|\theta_h^n - \theta_h^{n-1}\| \quad \text{and} \end{aligned} \tag{6.24}$$

$$\|(u_\alpha^n)^2\theta_h^n\| \le \|u_\alpha^n\|_{L^8(\Omega)}^2\|\theta_h^n\|_{L^4(\Omega)} \le \tilde{C}_6^1\big(\|u_h^n\|_{L^8(\Omega)}^2 + \|E_h(u^n)\|_{L^8(\Omega)}^2\big)\|\theta_h^n\|_{L^4(\Omega)}. \tag{6.25}$$

An application of Lemma 3.3(a) (iii) leads to $\|u_h^n\|_{L^8(\Omega)} \le \tilde{C}_6^2$, since $\gamma \le 1$ and u_0 is sufficiently smooth. Theorem 4.1(f) and a triangle inequality show

$$\|E_h(u^n)\|_{L^8(\Omega)} \lesssim \|\widehat{E}_h(u^n)\|_{a,h} \lesssim \|\widehat{E}_h(u^n) - \widehat{I}_h^k(u^n)\|_{a,h} + \|\widehat{I}_h^k(u^n)\|_{a,h}. \tag{6.26}$$

Theorem 3.2, Lemma 4.4, and regularity of u^n reveal $\|\widehat{E}_h(u^n) - \widehat{I}_h^k(u^n)\|_{a,h} \lesssim \tilde{C}_6^{3,1}$. Lemmas 3.1 and 4.5, $\gamma \le 1$, and regularity of solution yield $\|\widehat{I}_h^k(u^n)\|_{L^8(\Omega)} \le \tilde{C}_6^{3,2}$. These bounds in (6.26) leads to $\|E_h(u^n)\|_{L^8(\Omega)} \le \tilde{C}_6^3$, where $\tilde{C}_6^3 = \max\{\tilde{C}_6^{3,1}, \tilde{C}_6^{3,2}\}$. Arguments analogous to (6.11) show $\|\theta_h^n\|_{L^4(\Omega)} \le \tilde{C}_6^4\|\widehat{\theta}_h^n\|_{a,h}$ and $\|\theta_h^n\| \le \tilde{C}_6^5\|\widehat{\theta}_h^n\|_{a,h}$. Apply all these bounds in (6.24) to derive

$$(f(u_h^n) - f(E_h(u^n)), \theta_h^n - \theta_h^{n-1}) \le \widehat{C}_6\|\widehat{\theta}_h^n\|_{a,h}\|\theta_h^n - \theta_h^{n-1}\| \text{ with } \widehat{C}_6 = 3\tilde{C}_6^1\tilde{C}_6^4((\tilde{C}_6^2)^2 + (\tilde{C}_6^3)^2) + \tilde{C}_6^5.$$

An application of (1.2) with $\varepsilon = 1/4$ leads to

$$(f(u_h^n) - f(E_h(u^n)), \theta_h^n - \theta_h^{n-1}) \le C_6\Delta t\|\widehat{\theta}_h^n\|_{a,h}^2 + \frac{1}{8\Delta t}\|\theta_h^n - \theta_h^{n-1}\|^2 \text{ with } C_6 = 2(\tilde{C}_6)^2. \tag{6.27}$$

The regularity of the solution with a Sobolev embedding result and arguments analogous to (6.26) establish $\|u^n\|$ and $\|E_h(u^n)\|$ are bounded. The definition of f and generalized Holder's inequality reveal

$$\begin{aligned}(f(E_h(u^n)) - f(u^n), \theta_h^n - \theta_h^{n-1}) &= (((E_h(u^n))^2 + (u^n)^2 + E_h(u^n)u^n - 1)(E_h(u^n) - u^n), \theta_h^n - \theta_h^{n-1})\\ &\le \left(\frac{3}{2}\|u^n\|^2 + \frac{3}{2}\|E_h(u^n)\|^2 + 1\right)\|E_h(u^n) - u^n\|\|\theta_h^n - \theta_h^{n-1}\|.\end{aligned}$$

A triangle inequality yields $\|E_h(u^n) - u^n\| \le \|E_h(u^n) - \Pi_h^{k+2}(u^n)\| + \|\Pi_h^{k+2}(u^n) - u^n\|$. Note that $\|E_h(u^n) - \Pi_h^{k+2}(u^n)\| \lesssim \|\widehat{\eta}_h^n\|_{a,h}$ from (6.6) and Theorem 4.1(f). These bounds and (1.2) with $\varepsilon = 1/4$ in the above displayed inequality lead to

$$(f(E_h(u^n)) - f(u^n), \theta_h^n - \theta_h^{n-1}) \le C_7\Delta t(\|\widehat{\eta}_h^n\|_{a,h}^2 + \|\Pi_h^{k+2}(u_h^n) - u^n\|^2) + \frac{1}{8\Delta t}\|\theta_h^n - \theta_h^{n-1}\|^2. \tag{6.28}$$

A substitution of (6.27) and (6.28) in (6.23) yields

$$N_1 \le C_6\Delta t\|\widehat{\theta}_h^n\|_{a,h}^2 + C_7\Delta t(\|\widehat{\eta}_h^n\|_{a,h}^2 + \|\Pi_h^{k+2}(u_h^n) - u^n\|^2) + \frac{1}{4\Delta t}\|\theta_h^n - \theta_h^{n-1}\|^2.$$

Step 3: Control of N_2**.** The triangle inequality and the Cauchy–Schwarz inequality show

$$N_2 = (\bar{\partial}E_h(u^n) - \Pi_h^{k+2}(u_t^n), \theta_h^n - \theta_h^{n-1}) \leq (\|\bar{\partial}E_h(u^n) - E_h(u_t^n)\| + \|E_h(u_t^n) - \Pi_h^{k+2}(u_t^n)\|)\|\theta_h^n - \theta_h^{n-1}\|.$$

Elementary manipulations, the definition of $\chi(\bullet)$ from (6.5), with the notation for the first component of $\widehat{\eta}_h^n$ defined by $\eta_h^n := \Pi_h^{k+2}(u^n) - E_h(u^n)$ reveal

$$\begin{aligned}\bar{\partial}E_h(u^n) - E_h(u_t^n) &= (\bar{\partial}u^n - u_t^n) - \bar{\partial}\eta_h^n + (\eta_h^n)_t + \bar{\partial}(\Pi_h^{k+2}(u^n) - u^n) - (\Pi_h^{k+2}(u^n) - u^n)_t \\ &= \chi(u^n) - \chi(\eta_h^n) + \chi(\Pi_h^{k+2}(u^n) - u^n).\end{aligned}$$

A combination of the last two displayed results and elementary algebra establish

$$N_2 \leq \big(\|\chi(u^n)\| + \|\chi(\eta_h^n)\| + \|\chi(\Pi_h^{k+2}(u^n) - u^n)\| + \|(\eta_h^n)_t\|^2\big)\|\theta_h^n - \theta_h^{n-1}\|.$$

An application of Theorem 4.1(f) to bound the second term on the right-hand side of the above expression, and Young's inequality reveal

$$N_2 \leq C_8\Delta t\big(\|\chi(u^n)\|^2 + \|\chi(\widehat{\eta}_h^n)\|_{a,h}^2 + \|\chi(\Pi_h^{k+2}(u^n) - u^n)\|^2 + \|(\eta_h^n)_t\|^2\big) + \frac{1}{4\Delta t}\|\theta_h^n - \theta_h^{n-1}\|^2.$$

Step 4: Abstract bound**.** The bounds of N_1 and N_2 from Steps 2 to 3 in (6.22) and algebraic manipulations show

$$\begin{aligned}\frac{1}{2\Delta t}\|\theta_h^n - \theta_h^{n-1}\|^2 + \frac{1}{2}(\|\widehat{\theta}_h^n\|_{a,h}^2 - \|\widehat{\theta}_h^{n-1}\|_{a,h}^2) &\leq C_9\Delta t\big(\|\chi(u^n)\|^2 + \|\chi(\widehat{\eta}_h^n)\|_{a,h}^2 + \|(\eta_h^n)_t\|^2 + \|\widehat{\eta}_h^n\|_{a,h}^2 \\ &\quad + \|\Pi_h^{k+2}(u^n) - u^n\|^2 + \|(\chi(\Pi_h^{k+2}(u^n) - u^n)\|^2 + \|\widehat{\theta}_h^n\|_{a,h}^2\big),\end{aligned}$$

where $C_9 = \max\{C_6, C_7, C_8\}$. Multiply the above inequality by 2, sum it for $n = 1$ to l (where l can be $1, 2, \cdots, m$), introduce $C_{10} = 2C_9$, and utilize $\widehat{\theta}_h^0 = 0$ to observe

$$\begin{aligned}(1 - C_{10}\Delta t)\|\widehat{\theta}_h^l\|_{a,h}^2 &\leq C_{10}\Delta t\sum_{n=1}^{l}\big(\|\chi(u^n)\|^2 + \|\chi(\widehat{\eta}_h^n)\|_{a,h}^2 + \|(\eta_h^n)_t\|^2 + \|\widehat{\eta}_h^n\|_{a,h}^2 \\ &\quad + \|\Pi_h^{k+2}(u^n) - u^n\|^2 + \|(\chi(\Pi_h^{k+2}(u^n) - u^n)\|^2\big) + C_{10}\Delta t\sum_{n=1}^{l-1}\|\widehat{\theta}_h^n\|_{a,h}^2.\end{aligned}$$

For $1 - C_{10}\Delta t > 0$, an application of the discrete Gronwall's inequality shows

$$\begin{aligned}\|\widehat{\theta}_h^l\|_{a,h} \lesssim \Bigg(\Delta t\sum_{n=1}^{l}\big(\|\chi(u^n)\|^2 + \|\chi(\widehat{\eta}_h^n)\|_{a,h}^2 + \|(\eta_h^n)_t\|^2 \\ + \|\widehat{\eta}_h^n\|_{a,h}^2 + \|\Pi_h^{k+2}(u^n) - u^n\|^2 + \|\chi(\Pi_h^{k+2}(u^n) - u^n)\|^2\big)\Bigg)^{1/2}.\end{aligned}$$

Taking maximum as l varies from 1 to m, we obtain

$$\begin{aligned}\max_{1\leq l\leq m}\|\widehat{\theta}_h^l\|_{a,h} \lesssim \Bigg(\Delta t\sum_{l=1}^{m}\big(\|\chi(u^l)\|^2 + \|\chi(\widehat{\eta}_h^l)\|_{a,h}^2 + \|(\widehat{\eta}_h^l)_t\|^2 \\ + \|\widehat{\eta}_h^l\|_{a,h}^2 + \|\Pi_h^{k+2}(u^l) - u^l\|^2 + \|\chi(\Pi_h^{k+2}(u^l) - u^l)\|^2\big)\Bigg)^{1/2}.\end{aligned}$$

Since $\widehat{e}_h^n := \widehat{I}_h^k(u^n) - \widehat{u}_h^n$ from (6.6), the above displayed result reveals

$$\max_{1\le n\le m}\|\widehat{I}_h^k(u^n)-\widehat{u}_h^n\|_{a,h} \lesssim \max_{1\le n\le m}\left(\|\widehat{\theta}_h^n\|_{a,h}+\|\widehat{\eta}_h^n\|_{a,h}\right) \lesssim \left(\Delta t\sum_{n=1}^m \left(\|\chi(u^n)\|^2+\|\chi(\widehat{\eta}_h^n)\|_{a,h}^2+\|(\widehat{\eta}_h^n)_t\|^2\right.\right.$$
$$\left.\left.+\|\widehat{\eta}_h^n\|_{a,h}^2+\|\Pi_h^{k+2}(u^n)-u^n\|^2+\|\chi(\Pi_h^{k+2}(u^n)-u^n)\|^2\right)\right)^{1/2}+\max_{1\le n\le m}\|\widehat{\eta}_h^n\|_{a,h}. \tag{6.29}$$

A triangle inequality in (6.7), (6.15), and (6.29) reveal

$$\max_{1\le n\le m}\left(\sum_{K\in\mathscr{T}_h}\left(\gamma^{1/2}\|D^2(u^n-\mathscr{R}_K^2(\widehat{u}_K^n))\|_K+\|D(u^n-\mathscr{R}_K^1(\widehat{u}_K^n))\|_K\right)\right) \tag{6.30}$$
$$\lesssim \max_{1\le n\le m}\left(\sum_{K\in\mathscr{T}_h}\left(\gamma^{1/2}\|D^2(u^n-\mathscr{E}_K^2(u^n))\|_K+\|D(u^n-\mathscr{E}_K^1(u^n))\|_K\right)\right)+\max_{1\le n\le m}\|\widehat{e}_h^n\|_{a,h}$$
$$\lesssim \max_{1\le n\le m}\left(\sum_{K\in\mathscr{T}_h}\left(\gamma^{1/2}\|D^2(u^n-\mathscr{E}_K^2(u^n))\|_K+\|D(u^n-\mathscr{E}_K^1(u^n))\|_K\right)\right)$$
$$+\left(\Delta t\sum_{n=1}^m\left(\|\chi(u^n)\|^2+\|\chi(\widehat{\eta}_h^n)\|_{a,h}^2+\|(\widehat{\eta}_h^n)_t\|^2+\|\widehat{\eta}_h^n\|_{a,h}^2\right.\right.$$
$$\left.\left.+\|\Pi_h^{k+2}(u^n)-u^n\|^2+\|\chi(\Pi_h^{k+2}(u^n)-u^n)\|^2\right)\right)^{1/2}+\max_{1\le n\le m}\|\widehat{\eta}_h^n\|_{a,h}. \tag{6.31}$$

Step 5: Conclusion**.** Several terms on the right-hand side of (6.31) are already estimated in Step 8 of Theorem 3.4(a). Here we provide estimates for the remaining terms. Apply the definitions of $\chi(\bullet)$ from (6.5) and $\widehat{\eta}_h^n$ from (6.6), Lemma 4.2, Theorem 3.2, and Lemma 4.4 lead to

$$\left(\Delta t\sum_{n=1}^m\|\chi(\widehat{\eta}_h^n)\|_{a,h}^2\right)^{1/2}\lesssim\Delta t\begin{cases}\int_0^T\|(\widehat{\eta}_h)_{tt}\|_{a,h}\,dt \text{ for } k\ge1\\ \int_0^T\|(\widehat{\eta}_h)_{tt}\|_{a,h}\,dt \text{ for } k=0\end{cases}\lesssim\Delta t\begin{cases}(\sum_{K\in\mathscr{T}_h}h^{k+2}\sigma_K^{\frac12})|u_{tt}|_{L^2(0,T;H^{k+3}(\mathscr{T}_h))}\\ \qquad\text{for } k\ge1,\\ (\sum_{K\in\mathscr{T}_h}h^2\sigma_K^{\frac12})(|u_{tt}|_{L^2(0,T;H^3(\mathscr{T}_h))}\\ +h^\beta|u_{tt}|_{L^2(0,T;H^{3+\beta}(\mathscr{T}_h))}) \text{ for } k=0.\end{cases}$$

Apply Theorem 4.1(f) and proceed as above to bound the term $\|(\widehat{\eta}_h^n)_t)\|_{a,h}$ with the fact $m\Delta t=T$ to derive

$$\left(\Delta t\sum_{n=1}^m\|(\widehat{\eta}_h^n)_t\|^2\right)^{1/2}\lesssim\left(\Delta t\sum_{n=1}^m\|(\widehat{\eta}_h^n)_t\|_{a,h}^2\right)^{1/2}\lesssim\begin{cases}(\sum_{K\in\mathscr{T}_h}h^{k+2}\sigma_K^{\frac12})|u_t|_{L^\infty(0,T;H^{k+3}(\mathscr{T}_h))} \text{ for } k\ge1,\\ (\sum_{K\in\mathscr{T}_h}h^2\sigma_K^{\frac12})(|u_t|_{L^\infty(0,T;H^3(\mathscr{T}_h))}\\ \qquad+h^\beta|u_t|_{L^\infty(0,T;H^{3+\beta}(\mathscr{T}_h))}) \text{ for } k=0,\end{cases}$$

$$\left(\Delta t\sum_{n=1}^m\|\widehat{\eta}_h^n\|_{a,h}^2\right)^{1/2}\lesssim\begin{cases}(\sum_{K\in\mathscr{T}_h}h^{k+2}\sigma_K^{\frac12})|u|_{L^\infty(0,T;H^{k+3}(\mathscr{T}_h))} \text{ for } k\ge1,\\ (\sum_{K\in\mathscr{T}_h}h^2\sigma_K^{\frac12})(|u|_{L^\infty(0,T;H^3(\mathscr{T}_h))}+h^\beta|u|_{L^\infty(0,T;H^{3+\beta}(\mathscr{T}_h))}) \text{ for } k=0,\end{cases}$$

and

$$\max_{1\le n\le m}\|\widehat{\eta}_h^n\|_{a,h}\le\begin{cases}(\sum_{K\in\mathscr{T}_h}h^{k+2}\sigma_K^{\frac12})|u|_{L^\infty(0,T;H^{k+3}(\mathscr{T}_h))} \text{ for } k\ge1,\\ (\sum_{K\in\mathscr{T}_h}h^2\sigma_K^{\frac12})(|u|_{L^\infty(0,T;H^3(\mathscr{T}_h))}+h^\beta|u|_{L^\infty(0,T;H^{3+\beta}(\mathscr{T}_h))}) \text{ for } k=0.\end{cases}$$

Use the definition of $\chi(\bullet)$ from (6.5), Lemma 4.2, and Theorem 4.1(d) to obtain

$$\left(\Delta t\sum_{n=1}^{m}\|\chi(\Pi_h^{k+2}(u^n)-u^n)\|^2\right)^{1/2}\lesssim\begin{cases}h^{k+3}|u_{tt}|_{L^2(0,T;H^{k+3}(\mathscr{T}_h))} & \text{for } k\geq 1,\\ h^3(|u_{tt}|_{L^2(0,T;H^3(\mathscr{T}_h))}+h^\beta|u_{tt}|_{L^2(0,T;H^{3+\beta}(\mathscr{T}_h))}) & \text{for } k=0.\end{cases}$$

A combination of all these in (6.31) concludes the proof of Theorem 3.4 (b).

7. Crank Nicolson scheme

This section has two subsections: the proof of Lemma 3.5 is presented in Section 7.1, Theorem 3.6 is proved in Section 7.2.

For $1\leq n\leq m$, recall the *Crank-Nicolson HHO scheme* from Section 3.3 that seeks $\widehat{u}_h^n=(u_h^n,u_{\mathscr{F}_h^{\mathrm{i}}}^n,\sigma_{\mathscr{F}_h^{\mathrm{i}}}^n)\in\widehat{V}_h$ such that

$$(\bar{\partial}u_h^n,v_h)+a_h(\widehat{u}_h^{n-\frac{1}{2}},\widehat{v}_h)+(\widetilde{f}(u_h^{n-1},u_h^n),v_h)=0\ \text{ for all } \widehat{v}_h\in\widehat{V}_h\ \text{ with }\ \widehat{u}_h^0=\widehat{I}_h^k(u_0),\tag{7.1}$$

where $\widetilde{f}(u_h^{n-1},u_h^n)=\frac{1}{4}((u_h^{n-1})^3+(u_h^{n-1})^2u_h^n+u_h^{n-1}(u_h^n)^2+(u_h^n)^3)-\frac{1}{2}(u_h^{n-1}+u_h^n)$.

7.1. Proof of Lemma 3.5

Proof of Lemma 3.5(a)(i). It is enough to establish that $L(\widehat{u}_h^n)$ is a decreasing sequence for all $0\leq n\leq m$. The choice $\widehat{v}_h=\widehat{u}_h^n-\widehat{u}_h^{n-1}$ in (7.1) and $a_h(\widehat{u}_h^{n-\frac{1}{2}},\widehat{u}_h^n-\widehat{u}_h^{n-1})=\frac{1}{2}(\|\widehat{u}_h^n\|_{a,h}^2-\|\widehat{u}_h^{n-1}\|_{a,h}^2)$, $(\widetilde{f}(u_h^{n-1},u_h^n),u_h^n-u_h^{n-1})=(F(u_h^n)-F(u_h^{n-1}),1)$ from the definitions of $\|\cdot\|_{a,h}$ and $\widetilde{f}$, respectively, lead to

$$(\Delta t)^{-1}\|\widehat{u}_h^n-\widehat{u}_h^{n-1}\|^2+\frac{1}{2}(\|\widehat{u}_h^n\|_{a,h}^2-\|\widehat{u}_h^{n-1}\|_{a,h}^2)+(F(u_h^n)-F(u_h^{n-1}),1)=0.$$

The definition of $L(\bullet)$ from (3.3) and above result show $L(\widehat{u}_h^n)-L(\widehat{u}_h^{n-1})=\frac{1}{2}(\|\widehat{u}_h^n\|_{a,h}^2-\|\widehat{u}_h^{n-1}\|_{a,h}^2)+(F(u_h^n)-F(u_h^{n-1}),1)=-(\Delta t)^{-1}\|\widehat{u}_h^n-\widehat{u}_h^{n-1}\|^2\leq 0$. This establishes that $L(\widehat{u}_h^n)\leq L(\widehat{u}_h^{n-1})$ for all $0\leq n\leq m$. □

Proof of Lemma 3.5(a)(ii)–(iii), (b). The proofs follow analogous to Lemmas 3.3(a)(ii)–(iii) and 3.3(b) and are skipped. □

7.2. Proof of Theorem 3.6

The proof of the theorem utilizes the lemmas stated below.

Lemma 7.1. *Let u^n be the solution of (1.1) and $\widehat{u}_h^n$ with $1\leq n\leq m$ be the solution of the Crank-Nicolson HHO scheme (7.1). Then, for $u^{n-\frac{1}{2}}:=\frac{u^n+u^{n-1}}{2}$, it holds*

$$\|f(u(t^{n-\frac{1}{2}}))-\widetilde{f}(u_h^{n-1},u_h^n)\|\lesssim\|u(t^{n-\frac{1}{2}})-u^{n-\frac{1}{2}}\|+\|u^n-u^{n-1}\|^2+\|u^n-u_h^n\|+\|u^{n-1}-u_h^{n-1}\|.\tag{7.2}$$

Proof. A triangle inequality and elementary algebra show

$$\begin{aligned}\|f(u(t^{n-\frac{1}{2}}))-\widetilde{f}(u_h^{n-1},u_h^n)\|&\leq\|f(u(t^{n-\frac{1}{2}}))-f(u^{n-\frac{1}{2}})\|+\|f(u^{n-\frac{1}{2}})-\widetilde{f}(u^{n-1},u^n)\|\\&\quad+\|\widetilde{f}(u^{n-1},u^n)-\widetilde{f}(u^{n-1},u_h^n)\|+\|\widetilde{f}(u^{n-1},u_h^n)-\widetilde{f}(u_h^{n-1},u_h^n)\|:=\sum_{i=1}^{4}T_i.\end{aligned}\tag{7.3}$$

The terms on the right-hand side of (7.3) are estimated in Steps 1–4 below.

Step 1: Control of T_1. The mean value theorem shows $f(u(t^{n-\frac{1}{2}})) - f(u^{n-\frac{1}{2}}) = f'(u_\alpha^n)(u(t^{n-\frac{1}{2}}) - u^{n-\frac{1}{2}})$ with $u_\alpha^n = (1-\alpha)u(t^{n-\frac{1}{2}}) + \alpha u^{n-\frac{1}{2}}$ for some $\alpha \in (0,1)$. The regularity of u_n^α plus the definition of $f'(\bullet)$ leads to

$$T_1 = \|f'(u_\alpha^n)(u(t^{n-\frac{1}{2}}) - u^{n-\frac{1}{2}})\| \le \|f'(u_\alpha^n)\|_{L^\infty(\Omega)}\|u(t^{n-\frac{1}{2}}) - u^{n-\frac{1}{2}}\| \lesssim \|u(t^{n-\frac{1}{2}}) - u^{n-\frac{1}{2}}\|.$$

Step 2: Control of T_2. The definitions of $f(\bullet)$ and $\widetilde{f}(\bullet,\bullet)$ and elementary algebra establish

$$T_2 = (1/8)\|(u^n - u^{n-1})((u^n)^2 - (u^{n-1})^2)\| \le (1/8)\|u^n + u^{n-1}\|_{L^\infty(\Omega)}\|u^n - u^{n-1}\|^2 \lesssim \|u^n - u^{n-1}\|^2,$$

where the regularity of u^n and u^{n-1} are used in last step.

Step 3: Control of T_3. The definition of $\widetilde{f}(\bullet,\bullet)$ and elementary algebra reveal

$$|\widetilde{f}(z,w) - \widetilde{f}(z,v)| \le (1/2)|(z^2 + w^2 + v^2 - 1)(w - v)|. \tag{7.4}$$

The choice $z := u^{n-1}$, $w := u^n$, and $v := u_h^n$ in (7.4) reveal

$$T_3 \le (1/2)\|(u^{n-1})^2 + (u^n)^2 + (u_h^n)^2 - 1\|\|u^n - u_h^n\| \lesssim \|u^n - u_h^n\|$$

with regularity of u^{n-1} and u^n, $\gamma \le 1$, and Theorem 4.1(f) in the last step.

Step 4: Control of T_4. The symmetry of $\widetilde{f}(\bullet,\bullet)$ leads to $T_4 = \|\widetilde{f}(u_h^n, u^{n-1}) - \widetilde{f}(u_h^n, u_h^{n-1})\|$. The choice $z := u_h^n$, $w := u^{n-1}$, and $v := u_h^{n-1}$ in (7.4) and similar arguments in T_3 show $T_4 \lesssim \|u^{n-1} - u_h^{n-1}\|$. A combination of Steps 1–4 in (7.3) concludes the proof.

□

Lemma 7.2 ([12,39]). *For given $v_{tt}, v_{ttt} \in L^2(t^{n-1}, t^n; L^2(\Omega))$ and $v_t \in L^\infty(t^{n-1}, t^n; L^2(\Omega))$, it holds*

$$\|\bar\partial v^n - v_t(t^{n-\frac{1}{2}})\| \lesssim (\Delta t)^{\frac{3}{2}}\|v_{ttt}\|_{L^2(t^{n-1},t^n;L^2(\Omega))}, \quad \|v(t^{n-\frac{1}{2}}) - v^{n-\frac{1}{2}}\| \lesssim (\Delta t)^{\frac{3}{2}}\|v_{tt}\|_{L^2(t^{n-1},t^n;L^2(\Omega))},$$
$$\text{and} \quad \|v^n - v^{n-1}\| \lesssim \Delta t\|v_t\|_{L^\infty(t^{n-1},t^n;L^2(\Omega))}.$$

Proof of Theorem 3.6. The proof is divided into seven steps below.

Step 1: Settings. Define

$$\widetilde{\chi}(v^n) = \bar\partial v^n - v_t(t^{n-\frac{1}{2}}) \tag{7.5}$$

and $\widetilde{u}^n = u^{n-\frac{1}{2}} - u(t^{n-\frac{1}{2}})$. Recall the split from (6.6):

$$\widehat{e}_h^n := \widehat{\eta}_h^n + \widehat{\theta}_h^n, \text{ where } \widehat{\eta}_h^n = \widehat{I}_h^k(u^n) - \widehat{E}_h(u^n) \text{ and } \widehat{\theta}_h^n = \widehat{E}_h(u^n) - \widehat{u}_h^n, \text{ and let } \widehat{E}_h(u_0) = \widehat{I}_h^k(u_0) = \widehat{u}_h^0.$$

Step 2: Error equation. For all $\widehat{v}_h \in \widehat{V}_h$, the definition of $\widehat{E}_h$ from Section 3.1 shows

$$(\gamma\Delta^2 u^{n-\frac{1}{2}} - \Delta u^{n-\frac{1}{2}}, v_h) = a_h(\widehat{E}_h(u^{n-\frac{1}{2}}), \widehat{v}_h) \text{ and } (\gamma\Delta^2\widetilde{u}^n - \Delta\widetilde{u}^n, v_h) = a_h(\widehat{E}_h(\widetilde{u}^n), \widehat{v}_h). \tag{7.6}$$

The continuous formulation in (1.1), (7.6), and elementary algebra show

$$(u_t(t^{n-\frac{1}{2}}), v_h) + a_h(\widehat{E}_h(u^{n-\frac{1}{2}}), \widehat{v}_h) + (f(u(t^{n-\frac{1}{2}})), v_h) = a_h(\widehat{E}_h(\widetilde{u}^n), \widehat{v}_h) \text{ for all } \widehat{v}_h \in \widehat{V}_h.$$

Recall $\theta_h^n = E_h(u^n) - u_h^n$, $\widehat{\theta}_h^{n-1/2} = \widehat{E}_h(u^{n-1/2}) - \widehat{u}_h^{n-1/2}$ from Step 1. This, (7.1), the above displayed equation, and elementary algebra lead to

$$\begin{aligned}(\bar\partial\theta_h^n, v_h) + a_h(\widehat{\theta}_h^{n-\frac{1}{2}}, \widehat{v}_h) = (\widetilde{f}(u_h^{n-1}, u_h^n) - f(u(t^{n-\frac{1}{2}})), v_h) + (\bar\partial E_h(u^n) - \Pi_h^{k+2}(u_t(t^{n-\frac{1}{2}})), v_h)\\ + a_h(\widehat{E}_h(\widetilde{u}^n), \widehat{v}_h),\end{aligned} \tag{7.7}$$

where $(\Pi_h^{k+2}(u_t(t^{n-\frac{1}{2}})), v_h) = (u_t(t^{n-\frac{1}{2}}), v_h)$ is utilized in the last step. Choose $\widehat{v}_h := \bar{\partial}\widehat{\theta}_h^n$ in the above equation and observe $a_h(\widehat{\theta}_h^{n-\frac{1}{2}}, \bar{\partial}\widehat{\theta}_h^n) = \frac{1}{2}\bar{\partial}\|\widehat{\theta}_h^n\|_{a,h}^2$ from elementary manipulations to arrive at

$$\|\bar{\partial}\theta_h^n\|^2 + \frac{1}{2}\bar{\partial}\|\widehat{\theta}_h^n\|_{a,h}^2 = (\widetilde{f}(u_h^{n-1}, u_h^n) - f(u^{n-\frac{1}{2}}), \bar{\partial}\theta_h^n) + (\bar{\partial}E_h(u^n) - \Pi_h^{k+2}(u_t^{n-\frac{1}{2}}), \bar{\partial}\theta_h^n)$$
$$+ a_h(\widehat{E}_h(\widetilde{u}^n), \bar{\partial}\widehat{\theta}_h^n) := \sum_{i=1}^{3}\mathcal{T}_i. \tag{7.8}$$

Step 3: Control of $\mathcal{T}_1$**.** The Cauchy–Schwarz inequality and (1.2) with $\varepsilon = 1/3$ lead to

$$\mathcal{T}_1 \le \|\widetilde{f}(u_h^{n-1}, u_h^n) - f(u^{n-\frac{1}{2}})\|\|\bar{\partial}\theta_h^n\| \le \frac{3}{2}\|\widetilde{f}(u_h^{n-1}, u_h^n) - f(u^{n-\frac{1}{2}})\|^2 + \frac{1}{6}\|\bar{\partial}\theta_h^n\|^2$$
$$\le \frac{3}{2}\tilde{C}_{11}\big(\|\widetilde{u}^n\|^2 + \|u^n - u^{n-1}\|^4 + \|u^n - u_h^n\|^2 + \|u^{n-1} - u_h^{n-1}\|^2\big) + \frac{1}{6}\|\bar{\partial}\theta_h^n\|^2,$$

where Lemma 7.1 used in the last step and the coefficient absorbed in (7.2) is denoted by $\tilde{C}_{11}$. For $i \in \{n, n-1\}$, the notations from Step 1 with the first component of $\widehat{\eta}_h^i$ denoted by $\eta_h^i = \Pi_h^{k+2}(u^i) - E_h(u^i)$ and elementary manipulations lead to

$$\|u^i - u_h^i\|^2 \le 3\big(\|u^i - \Pi_h^{k+2}(u^i)\|^2 + \|\eta_h^i\|^2 + \|\theta_h^i\|^2\big) \lesssim \|u^i - \Pi_h^{k+2}(u^i)\|^2 + \|\widehat{\eta}_h^i\|_{a,h}^2 + \|\widehat{\theta}_h^i\|_{a,h}^2,$$

where Theorem 4.1(f) is used in the last step. The last two displayed inequalities establish

$$\mathcal{T}_1 \le C_{11}\big(\|\widetilde{u}^n\|^2 + \|u^n - u^{n-1}\|^4 + \sum_{i=n-1}^{n}\big(\|u^i - \Pi_h^{k+2}(u^i)\|^2 + \|\widehat{\eta}_h^i\|_{a,h}^2 + \|\widehat{\theta}_h^i\|_{a,h}^2\big)\big) + \frac{1}{6}\|\bar{\partial}\theta_h^n\|^2,$$

where C_{11} depends on $\tilde{C}_{11}$ and the constant from Theorem 4.1(f).

Step 4: Control of $\mathcal{T}_2$**.** The notations $\widetilde{\chi}(v^n) = \bar{\partial}v^n - v_t(t^{n-\frac{1}{2}})$, $\eta_h^n = \Pi_h^{k+2}(u^n) - E_h(u^n)$, and $(\eta_h(t^{n-\frac{1}{2}}))_t = \Pi_h^{k+2}(u_t(t^{n-\frac{1}{2}})) - E_h(u_t(t^{n-\frac{1}{2}}))$, and elementary manipulations reveal

$$\bar{\partial}E_h(u^n) - \Pi_h^{k+2}(u_t(t^{n-\frac{1}{2}})) = \widetilde{\chi}(u^n) - \widetilde{\chi}(\eta_h^n) + \widetilde{\chi}(\Pi_h^{k+2}(u^n) - u^n) - (\eta_h(t^{n-\frac{1}{2}}))_t.$$

Apply Cauchy–Schwarz inequality and (1.2) with $\varepsilon = 1/3$ to obtain

$$\mathcal{T}_2 \le \frac{3}{2}\big(\|\widetilde{\chi}(u^n)\|^2 + \|\widetilde{\chi}(\eta_h^n)\|^2 + \|\widetilde{\chi}(\Pi_h^{k+2}(u^n) - u^n)\|^2 + \|(\eta_h(t^{n-\frac{1}{2}}))_t\|^2\big) + \frac{1}{6}\|\bar{\partial}\theta_h^n\|^2.$$

Theorem 4.1(f) shows $\|\widetilde{\chi}(\eta_h^n)\| \lesssim \|\widetilde{\chi}(\widehat{\eta}_h^n)\|_{a,h}$ and $\|(\eta_h(t^{n-\frac{1}{2}}))_t\| \lesssim \|(\widehat{\eta}_h(t^{n-\frac{1}{2}}))_t\|_{a,h}$. These bounds and above displayed inequality establish

$$\mathcal{T}_2 \le C_{12}\big(\|\widetilde{\chi}(u^n)\|^2 + \|\widetilde{\chi}(\widehat{\eta}_h^n)\|_{a,h}^2 + \|\widetilde{\chi}(\Pi_h^{k+2}(u^n) - u^n)\|^2 + \|(\widehat{\eta}_h(t^{n-\frac{1}{2}}))_t\|_{a,h}^2\big) + \frac{1}{6}\|\bar{\partial}\theta_h^n\|^2.$$

where C_{12} depends on the absorbed constant from Theorem 4.1(f).

Step 5: Control of $\mathcal{T}_3$**.** An application of (7.6), Cauchy–Schwarz inequality, and (1.2) with $\varepsilon = 1/3$ leads to

$$\mathcal{T}_3 \le \frac{3}{2}\|\gamma\Delta^2\widetilde{u}^n - \Delta\widetilde{u}^n\|^2 + \frac{1}{6}\|\bar{\partial}\theta_h^n\|^2.$$

Step 6: Abstract bound**.** The bounds of $\mathcal{T}_1$-$\mathcal{T}_3$ from Steps 3-5 in (7.8) and algebraic manipulations show

$$\frac{1}{2}\|\bar{\partial}\theta_h^n\|^2 + \frac{1}{2}\bar{\partial}\|\widehat{\theta}_h^n\|_{a,h}^2 \le C_{13}\big(\|\widetilde{u}^n\|^2 + \|u^n - u^{n-1}\|^4 + \|u^{n-1} - \Pi_h^{k+2}(u^{n-1})\|^2 + \|\widehat{\eta}_h^{n-1}\|_{a,h}^2$$

$$+\|\widehat{\theta}_h^{n-1}\|_{a,h}^2+\|u^n-\Pi_h^{k+2}(u^n)\|^2+\|\widehat{\eta}_h^n\|_{a,h}^2+\|\widehat{\theta}_h^n\|_{a,h}^2+\|\widetilde{\chi}(u^n)\|^2+\|\widetilde{\chi}(\widehat{\eta}_h^n)\|_{a,h}^2$$
$$+\|\widetilde{\chi}(\Pi_h^{k+2}(u^n)-u^n)\|^2+\|(\widehat{\eta}_h(t^{n-\frac{1}{2}}))_t\|_{a,h}^2+\|\gamma\Delta^2\widetilde{u}^n-\Delta\widetilde{u}^n\|^2\big) \text{ with } C_{13}=\max\{3/2,C_{11},C_{12}\}.$$

Multiply the above inequality by 2, sum it for $n=1$ to l (where l can be $1,2,\cdots,m$), introduce $C_{14}=4C_{13}$, and utilize $\widehat{\theta}_h^0=0$ to observe

$$\begin{aligned}(1-C_{14}\Delta t)\|\widehat{\theta}_h^l\|_{a,h}^2\le C_{14}\Delta t\sum_{n=1}^{l}\big(&\|\widetilde{u}^n\|^2+\|u^n-u^{n-1}\|^4+\|u^{n-1}-\Pi_h^{k+2}(u^{n-1})\|^2+\|\widehat{\eta}_h^{n-1}\|_{a,h}^2\\&+\|u^n-\Pi_h^{k+2}(u^n)\|^2+\|\widehat{\eta}_h^n\|_{a,h}^2+\|\widetilde{\chi}(u^n)\|^2+\|\widetilde{\chi}(\widehat{\eta}_h^n)\|_{a,h}^2+\|\widetilde{\chi}(\Pi_h^{k+2}(u^n)-u^n)\|^2\\&+\|(\widehat{\eta}_h(t^{n-\frac{1}{2}}))_t\|_{a,h}^2+\|\gamma\Delta^2\widetilde{u}^n-\Delta\widetilde{u}^n\|^2\big)+C_{14}\Delta t\sum_{n=1}^{l-1}\|\widehat{\theta}_h^n\|_{a,h}^2.\end{aligned}$$

Manipulations analogous to Theorem 3.4(b) with $1-C_{14}\Delta t>0$ in above inequality leads to

$$\begin{aligned}\max_{1\le l\le m}\|\widehat{\theta}_h^l\|_{a,h}\lesssim\Bigg(\Delta t\sum_{l=1}^{m}\big(&\|\widetilde{u}^l\|^2+\|u^l-u^{l-1}\|^2+\|u^{l-1}-\Pi_h^{k+2}(u^{l-1})\|^2+\|\widehat{\eta}_h^{l-1}\|_{a,h}+\|u^l-\Pi_h^{k+2}(u^l)\|^2\\&+\|\widehat{\eta}_h^l\|_{a,h}+\|\widetilde{\chi}(u^l)\|^2+\|\widetilde{\chi}(\widehat{\eta}_h^l)\|_{a,h}^2+\|\widetilde{\chi}(\Pi_h^{k+2}(u^l)-u^l)\|^2+\|(\widehat{\eta}_h(t^{l-\frac{1}{2}}))_t\|_{a,h}^2+\|\gamma\Delta^2\widetilde{u}^l-\Delta\widetilde{u}^l\|^2\big)\Bigg)^{1/2}.\end{aligned}$$

The definition of $\widehat{e}_h^n$ from (6.6) and above displayed result reveal

$$\begin{aligned}\max_{1\le n\le m}\|\widehat{I}_h^k(u^n)-\widehat{u}_h^n\|_{a,h}\lesssim\Bigg(\Delta t\sum_{n=1}^{m}\big(&\|\widetilde{u}^n\|^2+\|u^n-u^{n-1}\|^4+\|u^{n-1}-\Pi_h^{k+2}(u^{n-1})\|^2+\|\widehat{\eta}_h^{n-1}\|_{a,h}^2\\&+\|u^n-\Pi_h^{k+2}(u^n)\|^2+\|\widehat{\eta}_h^n\|_{a,h}^2+\|\widetilde{\chi}(u^n)\|^2+\|\widetilde{\chi}(\widehat{\eta}_h^n)\|_{a,h}^2+\|\widetilde{\chi}(\Pi_h^{k+2}(u^n)-u^n)\|^2\\&+\|(\widehat{\eta}_h(t^{n-\frac{1}{2}}))_t\|_{a,h}^2+\|\gamma\Delta^2\widetilde{u}^n-\Delta\widetilde{u}^n\|^2\big)\Bigg)^{1/2}+\max_{1\le n\le m}\|\widehat{\eta}_h^n\|_{a,h}.\end{aligned}\tag{7.9}$$

Use triangle inequality in (6.7), (6.15), and (7.9) to establish

$$\begin{aligned}&\max_{1\le n\le m}\Bigg(\sum_{K\in\mathscr{T}_h}\big(\gamma^{1/2}\|D^2(u^n-\mathscr{R}_K^2(\widehat{u}_K^n))\|_K+\|D(u^n-\mathscr{R}_K^1(\widehat{u}_K^n))\|_K\big)\Bigg)\\&\lesssim\max_{1\le n\le m}\Bigg(\sum_{K\in\mathscr{T}_h}\big(\gamma^{1/2}\|D^2(u^n-\mathscr{E}_K^2(u^n))\|_K+\|D(u^n-\mathscr{E}_K^1(u^n))\|_K\big)\Bigg)+\max_{1\le n\le m}\|\widehat{e}_h^n\|_{a,h}\\&\lesssim\max_{1\le n\le m}\Bigg(\sum_{K\in\mathscr{T}_h}\big(\gamma^{1/2}\|D^2(u^n-\mathscr{E}_K^2(u^n))\|_K+\|D(u^n-\mathscr{E}_K^1(u^n))\|_K\big)\Bigg)+\Bigg(\Delta t\sum_{n=1}^{m}\big(\|\widetilde{u}^n\|^2\\&\quad+\|u^n-u^{n-1}\|^4+\|u^{n-1}-\Pi_h^{k+2}(u^{n-1})\|^2+\|\widehat{\eta}_h^{n-1}\|_{a,h}^2+\|u^n-\Pi_h^{k+2}(u^n)\|^2+\|\widehat{\eta}_h^n\|_{a,h}^2+\|\widetilde{\chi}(u^n)\|^2\\&\quad+\|\widetilde{\chi}(\widehat{\eta}_h^n)\|_{a,h}^2+\|\widetilde{\chi}(\Pi_h^{k+2}(u^n)-u^n)\|^2+\|(\widehat{\eta}_h(t^{n-\frac{1}{2}}))_t\|_{a,h}^2+\|\gamma\Delta^2\widetilde{u}^n-\Delta\widetilde{u}^n\|^2\big)\Bigg)^{1/2}\\&\quad+\max_{1\le n\le m}\|\widehat{\eta}_h^n\|_{a,h}.\end{aligned}\tag{7.10}$$

Step 7: Conclusion. Several terms on the right-hand side of (7.10) are already estimated in Step 8 and Step 5 of Theorem 3.4(a) and (b), respectively. Here we provide estimates for the remaining terms. An application of Lemma 7.2 yields

$$\left(\Delta t\sum_{n=1}^{m}\|\widetilde{u}^n\|^2\right)^{1/2}\lesssim(\Delta t)^2\|u_{ttt}\|_{L^2(0,T;L^2(\Omega))},\quad\left(\Delta t\sum_{n=1}^{m}\|u^n-u^{n-1}\|^4\right)^{1/2}\lesssim(\Delta t)^2\|u_t\|_{L^\infty(0,T;L^2(\Omega))},$$

$$\left(\Delta t\sum_{n=1}^{m}\|\gamma\Delta^2\widetilde{u}^n-\Delta\widetilde{u}^n\|^2\right)^{1/2}\lesssim\begin{cases}(\Delta t)^2|u_{ttt}|_{L^2(0,T;H^{k+3}(\mathscr{T}_h))} & \text{for } k\geq 1,\\ (\Delta t)^2(|u_{ttt}|_{L^2(0,T;H^3(\mathscr{T}_h))}+|u_{ttt}|_{L^2(0,T;H^{3+\beta}(\mathscr{T}_h))}) & \text{for } k=0,\end{cases}$$

and $(\Delta t\sum_{n=1}^{m}\|\widetilde{\chi}(u^n)\|^2)^{1/2}\lesssim(\Delta t)^2\|u_{tt}\|_{L^2(0,T;L^2(\Omega))}$, where $\gamma\leq 1$ is used in the second last result and definition of $\widetilde{\chi}(\bullet)$ from (7.5) is used in the last result. Recall the definitions of $\widetilde{\chi}(\bullet)$ and $\widehat{\eta}_h^n$ from Step 1. This and Lemma 7.2 show

$$\left(\Delta t\sum_{n=1}^{m}\|\widetilde{\chi}(\widehat{\eta}_h^n)\|_{a,h}^2\right)^{1/2}\lesssim(\Delta t)^2\begin{cases}\int_0^T\|(\widehat{\eta}_h)_{ttt}\|_{a,h}\,\mathrm{d}t & \text{for } k\geq 1\\ \int_0^T\|(\widehat{\eta}_h)_{ttt}\|_{a,h}\,\mathrm{d}t & \text{for } k=0\end{cases}$$

$$\lesssim(\Delta t)^{\frac12}\begin{cases}(\sum_{K\in\mathscr{T}_h}h^{k+2}\sigma_K^{\frac12})|u_{ttt}|_{L^2(0,T;H^{k+3}(\mathscr{T}_h))} & \text{for } k\geq 1,\\ (\sum_{K\in\mathscr{T}_h}h^2\sigma_K^{\frac12})(|u_{ttt}|_{L^2(0,T;H^3(\mathscr{T}_h))}\\ \quad+h^\beta|u_{ttt}|_{L^2(0,T;H^{3+\beta}(\mathscr{T}_h))}) & \text{for } k=0,\end{cases}$$

where Theorem 3.2 and Lemma 4.4 are used in the last step. Use the definition of $\widetilde{\chi}(\bullet)$ from 7.5, Lemma 7.2, and Theorem 4.1(d) to obtain

$$\left(\Delta t\sum_{n=1}^{m}\|\widetilde{\chi}(\Pi_h^{k+2}(u^n)-u^n)\|^2\right)^{1/2}\lesssim\begin{cases}h^{k+3}|u_{ttt}|_{L^2(0,T;H^{k+3}(\mathscr{T}_h))} & \text{for } k\geq 1,\\ h^3(|u_{ttt}|_{L^2(0,T;H^3(\mathscr{T}_h))}+h^\beta|u_{ttt}|_{L^2(0,T;H^{3+\beta}(\mathscr{T}_h))}) & \text{for } k=0.\end{cases}$$

The definition of $\widehat{\eta}_h^n$ from (6.6), Theorem 3.2, and Lemma 4.4 lead to

$$\left(\Delta t\sum_{n=1}^{m}\|(\widehat{\eta}_h(t^{n-\frac12}))_t\|^2\right)^{1/2}\lesssim\left(\Delta t\sum_{n=1}^{m}\|(\widehat{\eta}_h(t^{n-\frac12}))_t\|_{a,h}\right)^{1/2}$$

$$\lesssim\begin{cases}(\sum_{K\in\mathscr{T}_h}h^{k+2}\sigma_K^{\frac12})|u_t|_{L^\infty(0,T;H^{k+3}(\mathscr{T}_h))} & \text{for } k\geq 1,\\ (\sum_{K\in\mathscr{T}_h}h^2\sigma_K^{\frac12})(|u_t|_{L^\infty(0,T;H^3(\mathscr{T}_h))}\\ \quad+h^\beta|u_t|_{L^\infty(0,T;H^{3+\beta}(\mathscr{T}_h))}) & \text{for } k=0,\end{cases}$$

where $m\Delta t=T$ is used in the last step. A combination of all these bounds in (7.10) concludes the proof of Theorem 3.6.

□

Remark 7.3 (Sufficiently small Δt in Crank-Nocolson scheme)**.** The nonlinear contributions are accounted in $\mathscr{T}_1$. This is substituted in Step 6 of Theorem 3.6 and leads to the assumption that Δt is sufficiently small in the *Crank–Nicolson scheme.* Moreover, in Theorem 3.4(b) (resp. Thm. 3.6), the condition $\Delta t<\frac{1}{C_{10}}$ (resp. $\Delta t<\frac{1}{C_{14}}$) is required. This provides a precise quantification of the notion of *sufficiently small* Δt in time discretization.

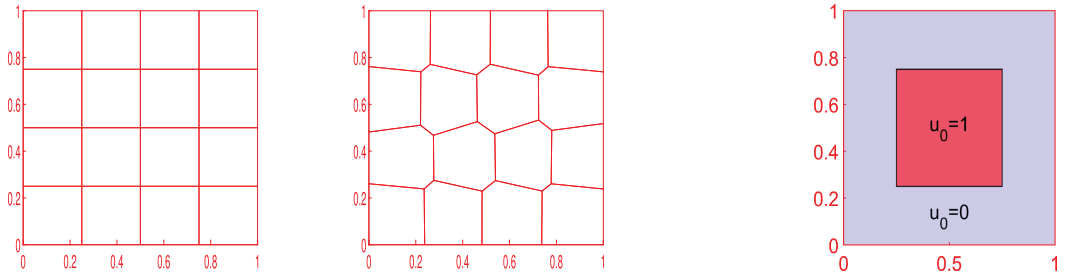

(a) (b) (c)

FIGURE 2. (a) Cartesian mesh. (b) Polygonal mesh. (c) Initial condition $u_0(x)$ for Example 8.2.

8. Numerical implementation

This section discusses results of numerical experiments that validate the theoretical estimates derived in Theorems 3.4 and 3.6. The convergence rates and robustness of the HHO and *backward Euler* (resp. *Crank-Nicolson*) *scheme* for the spatial and time variables, respectively, with respect to γ are demonstrated.

Two h-refined mesh families (Cartesian and polygonal Voronoi-like) meshes have been used for the HHO method in the spatial direction, see Figures 2a and 2b. The HHO scheme in space direction is implemented for the polynomial degrees $k \in \{0, 1, 2, 3\}$ and with $\{16, 64, 256, 1024, 4096\}$ elements.

To observe the convergence rates in the spatial direction, the time discretization parameter is chosen as $\Delta t = h^{k+2} \sum_{K\in\mathscr{T}_h} \sigma_K^{1/2}$ (resp. $(\Delta t)^2 = h^{k+2} \sum_{K\in\mathscr{T}_h} \sigma_K^{1/2}$) for *backward Euler* (resp. *Crank-Nicolson*) *scheme*. With this choice, the restriction that the time discretization parameter needs to be *sufficiently small*, seems to be taken care of in the implementations. The decay in the error for *backward Euler* (resp. *Crank-Nicolson*) *schemes* in the time direction for a fixed mesh size is presented in Table A.23.

The errors in $L^2(H^2)$ and $L^\infty(H^2)$-norms are denoted in the tables as

$$\|\mathfrak{E}_h\|_{L^2(H^2)} := \left(\Delta t \sum_{n=1}^{m} \sum_{K\in\mathscr{T}_h} \left(\gamma \|D^2(u^n - \mathscr{R}_K^2(\widehat{u}_K^n))\|_K^2 + \|D(u^n - \mathscr{R}_K^1(\widehat{u}_K^n))\|_K^2 \right) \right)^{1/2} \quad \text{and}$$

$$\|\mathfrak{E}_h\|_{L^\infty(H^2)} := \max_{1\le n\le m} \left(\sum_{K\in\mathscr{T}_h} \left(\gamma^{\frac{1}{2}} \|D^2(u^n - \mathscr{R}_K^2(u_K^n))\|_K + \|D(u^n - \mathscr{R}_K^1(u_K^n))\|_K \right) \right).$$

8.1. Example 1 – Manufactured solution

Choose $\Omega \times (0, T] = (0, 1)^2 \times (0, 0.1]$ and a manufactured solution as $u_{\text{ex}}(x, y, t) = e^{-t} x^2 y^2 \ (x - 1)^2 (y - 1)^2$. This leads to a nonhomogeneous right-hand side in (1.1). Consider the case of EFK equation, that is, $\gamma \in (0, 1]$. The source function and initial data that corresponds to the exact solutions u_{ex} are obtained as $g(x, t) = (u_{\text{ex}})_t + \gamma \Delta^2 u_{\text{ex}} - \Delta u_{\text{ex}} + f(u_{\text{ex}})$ with $u_0(x) = u_{\text{ex}}(x, 0)$. The initial-boundary value problem (1.1) is linearized with the Newton scheme: for details of the algorithm we refer to [15]. The deviation in this article is that the space discretization is performed using HHO method whereas the time discretization is using both backward Euler and Crank Nicolson schemes. Table 1 summarizes the details of tables where the results from this numerical experiment are presented.

The tables that demonstrate the experimental order of convergence (EOC) and discrete errors in various norms are presented in Appendix A. The convergence rates for the Cartesian and polygonal meshes compare well and they agree with the theoretical estimates derived in Theorems 3.4 and 3.6. In Tables A.1 and A.2 (resp. Tabs. A.3 and A.4), the errors in $L^2(H^2)$ (resp. $L^\infty(H^2)$)-norm for the backward Euler scheme (3.2) are shown

TABLE 1. Summary for Example 8.1.

Example 8.1	Backward Euler		Crank-Nicolson	
	Cartesian	Polygonal	Cartesian	Polygonal
$\|\mathfrak{E}_h\|_{L^2(H^2)}$	Table A.1	Table A.2	–	–
$\|\mathfrak{E}_h\|_{L^\infty(H^2)}$	Table A.3	Table A.4	Table A.5	Table A.6

TABLE 2. Summary for Example 8.2 with Cartesian meshes.

Example 8.2	Backward Euler	Crank-Nicolson
$\|E_h^{\mathrm{Re}}\|_{L^2(H^2)} := \frac{\|\mathfrak{E}_h\|_{L^2(H^2)}}{\|\widehat{u}_h\|_{L^2(H^2)}}$	Table A.7	–
$\|E_h^{\mathrm{Re}}\|_{L^\infty(H^2)} := \frac{\|\mathfrak{E}_h\|_{L^\infty(H^2)}}{\|\widehat{u}_h\|_{L^\infty(H^2)}}$	Table A.8	Tables A.9 and A.10

for Cartesian and polygonal meshes, respectively. For the Crank Nicolson scheme (3.4), the numerical results for errors in $L^\infty(H^2)$-norm are presented in Table A.5 (resp. Tab. A.6) for Cartesian (resp. polygonal) meshes. The convergence rates and errors for the schemes (3.2) and (3.4) are tabulated for $\gamma \in \{1, 0.125, 10^{-2}, 10^{-4}, 10^{-6}\}$ and $k \in \{0, 1, 2, 3\}$. The rates $\mathscr{O}(h^{k+1})$ are observed initially; however as γ transitions to smaller values (see for example, $\gamma = 10^{-6}$) the convergence rate improves to that for the second-order problem, that is, $\mathscr{O}(h^{k+2})$. This concludes that between two extreme values of γ $(0 < \gamma \leq 1)$, a transition in convergence rate from $k+1$ to $k+2$ is observed.

In Table A.23, the decay of the errors in $L^\infty(H^2)$-norm for the time direction with 1024 polygonal elements is displayed for $\gamma = 1$ and $k \in \{0, 2\}$ for the *backward Euler* and *Crank-Nicolson* time discretizations. As Δt decreases, as expected, a faster error decay is observed for the *Crank-Nicolson scheme* in comparison to the *backward Euler scheme*.

8.2. Example 2 – Discontinuous initial data

In this example, we choose the initial data in (1.1) to be discontinuous, $\gamma \in (0, 1]$, and the domain to be $\Omega \times (0, T] := (0, 1)^2 \times (0, 0.1]$. Let $u_0 : \Omega \to \mathbb{R}$ be defined by $u_0(x) := \begin{cases} 1 & \text{if } (x, y) \in [\frac{1}{4}, \frac{3}{4}]^2, \\ 0 & \text{if } (x, y) \in \Omega \setminus [\frac{1}{4}, \frac{3}{4}]^2. \end{cases}$ The computational mesh $\mathscr{T}_h$ is aligned with the discontinuity interface at the square $[1/4, 3/4]^2$, so each cell $K \in \mathscr{T}_h$ lies entirely within one region where u_0 is constant. The cell unknowns are initialized *via* the L^2 projection $u_K^0 = \Pi_K^{k+2}(u_0)|_K$ (Sect. 2.3), which yields either u_K^0=1 or u_K^0=0 depending on whether K is in the interior or exterior of the square. The face unknowns on the discontinuity interface are initialized as $u_F^0 = \frac{1}{2}\Big(\frac{1}{|F|}\int_F u_{K^+}^0 \,\mathrm{d}s + \frac{1}{|F|}\int_F u_{K^-}^0 \,\mathrm{d}s\Big)$ (for the Newton algorithm). Though the theoretical results assume more *regularity* for the initial data, the observations in the numerical experiments demonstrate that the scheme is robust even for *discontinuous* initial data. Since the exact solution is not available, the errors $\mathfrak{E}_h$ are calculated by choosing the exact solution as the computed solution in the finest mesh with 4096 elements. Table 2 summarizes the details of tables where the numerical outcomes from this example are demonstrated.

In Table A.7 (resp. Tab. A.8), the relative errors in $L^2(H^2)$ (resp. $L^\infty(H^2)$)-norm for the *backward Euler scheme* (3.2) are shown for Cartesian meshes. For the *Crank-Nicolson scheme* (3.4), the numerical rates in $L^\infty(H^2)$-norm are presented in Table A.9. The numerical rates and relative errors for both schemes (3.2) and (3.4) are tabulated for $\gamma \in \{1, 0.125, 10^{-2}, 10^{-4}\}$ and $k \in \{0, 1, 2, 3\}$. The rates of $\mathscr{O}(h^{k+2})$ are obtained initially; however as γ approaches smaller values (see for example $\gamma = 10^{-6}$) the numerical convergence rate improves

TABLE 3. Summary for Example 8.3.

Example 8.3	Backward Euler		Crank-Nicolson	
Case I	Cartesian	Polygonal	Cartesian	Polygonal
$\|\mathfrak{E}_h\|_{L^2(H^2)}$	Table A.11	Table A.12	–	–
$\|\mathfrak{E}_h\|_{L^\infty(H^2)}$	Table A.13	Table A.14	Table A.15	Table A.16
Case II	Cartesian	Polygonal	Cartesian	Polygonal
$\|\mathfrak{E}_h\|_{L^2(H^2)}$	Table A.17	Table A.18	–	–
$\|\mathfrak{E}_h\|_{L^\infty(H^2)}$	Table A.19	Table A.20	Table A.21	Table A.22

to that for the second-order problem, that is, $\mathcal{O}(h^{k+2})$. Moreover, for $\gamma = 0$, an optimal convergence rate of $\mathcal{O}(h^{k+2})$ is observed for $k \in \{0, 1, 2, 3\}$.

8.3. Example 3 – Fisher-Kolmogorov equation

This example considers the FK equation with $\gamma = 0$ in Example 8.1 and discusses the two types of numerical simulations. In Case I, we consider the same discrete setting as in the EFK model and approximate u in the interior of element $K \in \mathcal{T}_h$, the trace and normal derivative of u on the faces F of K. In Case II, u is approximated in the interior of the element $K \in \mathcal{T}_h$ and the trace of u is approximated on the faces F of K as in second-order problems [20]. The modifications in the settings are listed below and a summary of details of tables for this numerical experiment are presented in Table 3.

– The modified *global HHO space* reads

$$\widehat{V}_h := \mathscr{P}_{k+2}(\mathcal{T}_h) \times \mathscr{P}_{k+2}(\mathcal{F}_h^{\mathrm{i}}).$$

A generic element of $\widehat{V}_h$ is denoted as $\widehat{v}_h := (v_h, v_{\mathcal{F}_h^{\mathrm{i}}})$ with $v_h = (v_K)_{K\in\mathcal{T}_h}$ and $v_{\mathcal{F}_h^{\mathrm{i}}} := (v_F)_{F\in\mathcal{F}_h^{\mathrm{i}}}$. The restriction of $\widehat{v}_h \in \widehat{V}_h$ to $K \in \mathcal{T}_h$ is denoted by $(v_K, v_{\mathcal{F}_K^{\mathrm{i}}}) \in \widehat{V}_K$. Note that $v_{\mathcal{F}_K^{\mathrm{i}}}|_F := v_F \in \mathscr{P}_{k+2}(F)$.

– The *reduction operator* $\widehat{I}_h^k(\bullet)$ is defined as $\widehat{I}_h^k(v) := (\Pi_h^{k+2}(v), \Pi_{\mathcal{F}_h^{\mathrm{i}}}^{k+2}(v))$ for all $v \in H^1(\Omega)$.

– For all $\widehat{v}_K = (v_K, v_{\mathcal{F}_K^{\mathrm{i}}})$, $\widehat{w}_K = (w_K, w_{\mathcal{F}_K^{\mathrm{i}}}) \in \widehat{V}_K$, the *local stabilization* bilinear form $\mathscr{S}_K : \widehat{V}_K \times \widehat{V}_K \to \mathbb{R}$ is defined as $\mathscr{S}_K(\widehat{v}_K, \widehat{w}_K) := \sum_{F\in\mathcal{F}_K} h_K^{-1}(v_F - v_K, w_F - w_K)_F$.

For Case I (resp. Case II), the numerical results are presented in Tables A.11–A.16 (resp. Tabs. A.17–A.22). For the Case I, Tables A.11 and A.12 (resp. Tabs. A.13 and A.14) represent the errors in $L^2(H^2)$ (resp. $L^\infty(H^2)$)-norm for the *backward Euler scheme* (3.2) with Cartesian and polygonal meshes, respectively. For the *Crank Nicolson scheme* (3.4), the numerical results for errors in $L^\infty(H^2)$-norm are shown in Table A.15 (resp. Tab. A.16) for Cartesian (resp. polygonal) meshes. For the Case II, Tables A.17 and A.18 (resp. Tabs. A.19 and A.20) demonstrate the errors in $L^2(H^2)$ (resp. $L^\infty(H^2)$)-norm for scheme (3.2) with Cartesian and polygonal meshes, respectively. For scheme (3.4), the numerical results for errors in $L^\infty(H^2)$-norm are presented in Table A.21 (resp. Tab. A.22) for Cartesian (resp. polygonal) meshes. Both schemes (3.2)–(3.4) achieve optimal error bounds of $\mathcal{O}(h^{k+2})$ in the Cases I and II, respectively.

For the Case I, Table A.23 illustrates the decay of errors in $L^\infty(H^2)$-norm for the time direction with 1024 polygonal elements, where $\gamma = 0$ and $k \in \{0, 2\}$. Using *backward Euler* and *Crank-Nicolson schemes* for time discretization, the results demonstrate a faster error decay for the *Crank-Nicolson scheme* than the *backward Euler scheme* as Δt decreases.

Remark 8.1. In Example 8.3, for the FK model ($\gamma = 0$ in EFK model (1.1)), optimal error bounds for both schemes (3.2)–(3.4) have been observed using modified HHO space discretization for Case II, where u is

approximated only in the interior of the element $K \in \mathscr{T}_h$ and the trace of u is approximated on the faces F of K as in second-order problems [20]. Case II has the advantage that the exact solution is expected to have only the regularity $u \in H^{1+r}(\Omega)$ $r > 1/2$. A unified framework for EFK (resp. FK) models with the regularity $u \in H^{2+r}(\Omega)$ $r > 3/2$ (resp. $u \in H^{1+r}(\Omega)$ $r > 1/2$), *is an interesting future work.*

Acknowledgments

The authors extend their sincere gratitude to Professor Zhaonan Dong for generously sharing the HHO code for the biharmonic problem. The authors acknowledge the fruitful suggestions from the referees and Professor Jérôme Droniou that have improved the paper considerably. Raman Kumar acknowledges the funding by the European Union (ERC Synergy, NEMESIS, project number 101115663). Views and opinions expressed are, however, those of the authors only and do not necessarily reflect those of the European Union or the European Research Council Executive Agency. Neither the European Union nor the granting authority can be held responsible for them. Neela Nataraj acknowledges the J.C. Bose grant ANRF/JBG/2025/000209/HAA.

References

[1] M. Abbas, A. Ern and N. Pignet, Hybrid high-order methods for finite deformations of hyperelastic materials. *Comput. Mech.* **62** (2018) 909–928.

[2] D.G. Aronson and H.F. Weinberger, Multidimensional nonlinear diffusion arising in population genetics. *Adv. in Math.* **30** (1978) 33–76.

[3] L. Botti, D.A. Di Pietro and J. Droniou, A hybrid high-order method for the incompressible Navier–Stokes equations based on Temam's device. *J. Comput. Phys.* **376** (2019) 786–816.

[4] M. Botti, D.A. Di Pietro and P. Sochala, A hybrid high-order discretization method for nonlinear poroelasticity. *Comput. Methods Appl. Math.* **20** (2020) 227–249.

[5] E. Burman, O. Duran, A. Ern and M. Steins, Convergence analysis of hybrid high-order methods for the wave equation. *J. Sci. Comput.* **87** (2021) 91.

[6] E. Burman, O. Duran and A. Ern, Hybrid high-order methods for the acoustic wave equation in the time domain. *Commun. Appl. Math. Comput.* **4** (2022) no. 2, 597–633.

[7] F. Chave, D.A. Di Pietro, F. Marche and F. Pigeonneau, A hybrid high-order method for the Cahn–Hilliard problem in mixed form. *SIAM J. Numer. Anal.* **54** (2016) 1873–1898.

[8] F. Chave, D.A. Di Pietro and S. Lemaire, A discrete Weber inequality on three-dimensional hybrid spaces with application to the HHO approximation of magnetostatics. *Math. Models Methods Appl. Sci.* **32** (2022) 175–207.

[9] M. Cicuttin, A. Ern and N. Pignet, Hybrid High-Order Methods: A Primer with Applications to Solid Mechanics. Springer (2021).

[10] M. Corti, F. Bonizzoni, L. Dede', A.M. Quarteroni and P.F. Antonietti, Discontinuous Galerkin methods for Fisher-Kolmogorov equation with application to α-synuclein spreading in Parkinson's disease. *Comput. Methods Appl. Mech. Eng.* **417** (2023) 116450.

[11] P. Coullet, C. Elphick and D. Repaux, Nature of spatial chaos. *Phys. Rev. Lett.* **58** (1987) 431.

[12] P. Danumjaya and A.K. Pani, Numerical methods for the extended Fisher-Kolmogorov (EFK) equation. *Int. J. Numer. Anal. Model.* **3** (2006) 186–210.

[13] P. Danumjaya, A.K. Pany and A.K. Pani, Morley FEM for the fourth-order nonlinear reaction-diffusion problems. *Comput. Math. Appl.* **99** (2021) 229–245.

[14] A. Das, B.P. Lamichhane and N. Nataraj, A unified mixed finite element method for fourth-order time-dependent problems using biorthogonal systems. *Comput. Math. Appl.* **165** (2024) 52–69.

[15] A. Das, N. Nataraj and G.C. Ramesan, Semi and fully-discrete analysis of extended Fisher-Kolmogorov equation with nonstandards FEMs for space discretization. *J. Sci. Comput.* **104** (2025) 14.

[16] G.T. Dee and W. van Saarloos, Bistable systems with propagating fronts leading to pattern formation. *Phys. Rev. Lett.* **60** (1988) 2641.

[17] D.A. Di Pietro and J. Droniou, A hybrid high-order method for Leray-Lions elliptic equations on general meshes. *Math. Comput.* **86** (2017) 2159–2191.

[18] D.A. Di Pietro and A. Ern, A hybrid high-order locking-free method for linear elasticity on general meshes. *Comput. Methods Appl. Mech. Eng.* **283** (2015) 1–21.
[19] D.A. Di Pietro and S. Krell, A hybrid high-order method for the steady incompressible Navier–Stokes problem. *J. Sci. Comput.* **74** (2018) 1677–1705.
[20] D.A. Di Pietro, A. Ern and S. Lemaire, An arbitrary-order and compact-stencil discretization of diffusion on general meshes based on local reconstruction operators. *Comput. Methods Appl. Math.* **14** (2014) 461–472.
[21] D.A. Di Pietro, A. Ern, A. Linke and F. Schieweck, A discontinuous skeletal method for the viscosity-dependent Stokes problem. *Comput. Methods Appl. Mech. Eng.* **306** (2016) 175–195.
[22] Z. Dong and A. Ern, Hybrid high-order method for singularly perturbed fourth-order problems on curved domains. *ESAIM Math. Model. Numer. Anal.* **55** (2021) 3091–3114.
[23] Z. Dong and A. Ern, Hybrid high-order and weak Galerkin methods for the biharmonic problem. *SIAM J. Numer. Anal.* **60** (2022) 2626–2656.
[24] Z. Dong and A. Ern, C^0-hybrid high-order methods for biharmonic problems. *IMA J. Numer. Anal.* **44** (2024) 24–57.
[25] A. Ern and M. Steins, Convergence analysis for the wave equation discretized with hybrid methods in space (HHO, HDG and WG) and the leapfrog scheme in time. *J. Sci. Comput.* **101** (2024) 7.
[26] T. Gudi and H.S. Gupta, A fully discrete C^0 interior penalty Galerkin approximation of the extended Fisher-Kolmogorov equation. *J. Comput. Appl. Math.* **247** (2013) 1–16.
[27] T. Gudi, G. Mallik and T. Pramanick, A hybrid high-order method for quasilinear elliptic problems of nonmonotone type. *SIAM J. Numer. Anal.* **60** (2022) 2318–2344.
[28] Z. Guozhen, Experiments on director waves in nematic liquid crystals. *Phys. Rev. Lett.* **49** (1982) 1332.
[29] R.M. Hornreich, M. Luban and S. Shtrikman, Critical behavior at the onset of k-space instability on the λ line. *Phys. Rev. Lett.* **35** (1975) 1678.
[30] S. Kesavan, Topics in Functional Analysis and Applications. Wiley Eastern Limited, New Delhi (1989).
[31] G. Mallik and T. Gudi, A hybrid high-order method for a class of strongly nonlinear elliptic boundary value problems. *J. Sci. Comput.* **98** (2024) 6.
[32] L. Pei, C. Zhang and M. Li, Dissipative nonconforming virtual element method for the fourth order nonlinear extended Fisher-Kolmogorov equation. *Comput. Math. Appl.* **152** (2023) 28–45.
[33] L.A. Peletier and W.C. Troy, Chaotic spatial patterns described by the extended Fisher-Kolmogorov equation. *J. Differ. Equ.* **129** (1996) 458–508.
[34] L.A. Peletier and W.C. Troy, Spatial patterns described by the extended Fisher-Kolmogorov equation: periodic solutions. *SIAM J. Math. Anal.* **28** (1997) 1317–1353.
[35] G.C. Remesan, Convergence analysis of semilinear elliptic evolution equations with rough source terms. Preprint (2026).
[36] R. Temam, Navier–Stokes Equations: Theory and Numerical Analysis. Vol. 343. American Mathematical Society (2024).
[37] V. Thomée, Galerkin Finite Element Methods for Parabolic Problems. *Springer Series in Computational Mathematics*, 2nd edition. Vol. 25. Springer-Verlag, Berlin (2006).
[38] C.-M. Xie, M.-F. Feng and Y. Luo, A hybrid high-order method for the Sobolev equation. *Appl. Numer. Math.* **178** (2022) 84–97.
[39] C.-M. Xie, M.-F. Feng, Y. Luo and L. Zhang, A hybrid high-order method for Sobolev equation with convection-dominated term. *Comput. Math. Appl.* **118** (2022) 85–94.

Appendix A. Example 8.1

Table A.1. Convergence and discrete $L^2(H^2)$ errors for *backward Euler scheme* with Cartesian meshes.

$k=0$	$\gamma=1$		$\gamma=0.125$		$\gamma=10^{-2}$		$\gamma=10^{-4}$		$\gamma=10^{-6}$	
# of cells	$\|\mathfrak{E}_h\|_{L^2(H^2)}$	EOC	$\|\mathfrak{E}_h\|_{L^2(H^2)}$	EOC	$\|\mathfrak{E}_h\|_{L^2(H^2)}$	EOC	$\|\mathfrak{E}_h\|_{L^2(H^2)}$	EOC	$\|\mathfrak{E}_h\|_{L^2(H^2)}$	EOC
16	9.75e−02	–	3.72e−01	–	1.08e−01	–	7.50e−02	–	1.78e−01	–
64	5.10e−02	0.93	1.95e−01	0.93	5.50e−02	0.97	3.94e−02	0.93	9.00e−02	1.73
256	2.59e−02	0.98	9.90e−02	0.97	2.76e−02	0.99	1.99e−02	0.97	4.49e−02	1.91
1024	1.30e−02	0.99	4.94e−02	0.99	1.38e−02	0.99	1.00e−02	1.00	2.24e−02	1.96
4096	6.48e−03	1.00	2.46e−02	1.00	6.91e−03	1.00	5.02e−03	1.00	1.12e−02	1.97
$k=1$	$\gamma=1$		$\gamma=0.125$		$\gamma=10^{-2}$		$\gamma=10^{-4}$		$\gamma=10^{-6}$	
16	6.00e−02	–	6.36e−03	–	1.26e−02	–	1.53e−02	–	7.35e−05	–
64	1.54e−02	1.95	6.18e−03	1.94	2.70e−04	1.93	8.51e−04	2.41	9.31e−06	2.98
256	3.87e−03	1.99	1.56e−03	1.98	1.57e−05	2.39	5.06e−05	2.55	1.17e−06	2.99
1024	9.72e−04	2.00	3.92e−04	2.00	8.57e−07	2.41	3.10e−06	2.22	1.46e−07	2.99
4096	2.43e−04	2.00	9.80e−05	2.00	4.96e−08	2.22	1.91e−07	2.06	1.82e−08	2.99
$k=2$	$\gamma=1$		$\gamma=0.125$		$\gamma=10^{-2}$		$\gamma=10^{-4}$		$\gamma=10^{-6}$	
16	1.60e−02	–	1.89e−03	–	1.28e−03	–	8.99e−02	–	5.03e−05	–
64	2.04e−03	2.97	2.34e−04	3.01	1.55e−04	3.04	9.09e−03	3.30	3.93e−05	3.56
256	2.56e−04	2.99	2.87e−05	3.02	1.90e−05	3.02	8.77e−04	3.37	2.46e−06	3.99
1024	3.13e−05	3.03	3.38e−06	3.08	2.34e−06	3.02	8.93e−05	3.09	1.54e−07	3.99
4096	3.83e−06	3.03	4.07e−07	3.05	2.89e−07	3.01	9.99e−06	3.16	9.62e−09	4.00
$k=3$	$\gamma=1$		$\gamma=0.125$		$\gamma=10^{-2}$		$\gamma=10^{-4}$		$\gamma=10^{-6}$	
16	9.17e−01	–	7.63e−04	–	9.49e−04	–	8.38e−04	–	4.30e−05	–
64	5.40e−02	4.08	4.56e−05	4.06	5.93e−05	4.00	5.26e−05	3.99	1.33e−06	5.01
256	3.27e−03	4.04	2.87e−06	3.99	3.70e−06	4.00	3.31e−06	3.99	4.08e−08	5.02
1024	1.97e−04	4.05	1.80e−07	3.99	2.30e−07	4.01	2.05e−07	4.01	1.27e−09	5.00
4096	1.18e−05	4.06	9.98e−09	4.10	1.39e−08	4.04	1.28e−08	4.00	3.97e−11	5.00

Table A.2. Convergence and discrete $L^2(H^2)$ errors for *backward Euler scheme* with polygonal meshes.

$k=0$	$\gamma=1$		$\gamma=0.125$		$\gamma=10^{-2}$		$\gamma=10^{-4}$		$\gamma=10^{-6}$	
# of cells	$\|\mathfrak{E}_h\|_{L^2(H^2)}$	EOC	$\|\mathfrak{E}_h\|_{L^2(H^2)}$	EOC	$\|\mathfrak{E}_h\|_{L^2(H^2)}$	EOC	$\|\mathfrak{E}_h\|_{L^2(H^2)}$	EOC	$\|\mathfrak{E}_h\|_{L^2(H^2)}$	EOC
16	5.88e+00	–	1.41e-01	–	8.16e-02	–	1.79e-02	–	5.31e-02	–
64	2.96e-01	0.99	7.10e-02	0.99	4.10e-02	0.98	9.10e-03	0.98	1.41e-02	1.90
256	1.48e-01	0.99	3.54e-02	1.00	2.05e-02	0.99	4.56e-03	0.99	3.61e-03	1.96
1024	7.41e-02	0.99	1.77e-02	1.00	1.03e-02	0.99	2.28e-03	1.00	9.11e-04	1.99
4096	3.69e-02	1.00	8.83e-03	1.00	5.15e-03	1.00	1.14e-03	1.00	2.28e-04	2.00
$k=1$	$\gamma=1$		$\gamma=0.125$		$\gamma=10^{-2}$		$\gamma=10^{-4}$		$\gamma=10^{-6}$	
16	1.46e−02	–	4.68e−03	–	4.28e−03	–	1.75e−02	–	1.06e−03	–
64	3.66e−03	1.98	1.22e−03	1.93	1.08e−03	1.99	4.37e−03	2.00	1.37e−04	2.94
256	9.18e−04	1.99	3.08e−04	1.98	2.51e−04	2.10	1.02e−03	2.09	1.72e−05	2.98
1024	2.30e−04	1.99	7.74e−05	1.99	5.94e−05	2.32	2.45e−04	2.06	2.17e−06	2.99
4096	5.76e−05	1.99	1.94e−05	2.00	1.20e−05	2.31	5.69e−05	2.10	2.72e−07	3.00
$k=2$	$\gamma=1$		$\gamma=0.125$		$\gamma=10^{-2}$		$\gamma=10^{-4}$		$\gamma=10^{-6}$	
16	3.87e−03	–	6.20e−03	–	2.04e−04	–	2.63e−04	–	8.29e−05	–
64	4.98e−04	2.96	7.88e−04	2.97	2.63e−05	2.96	3.33e−05	2.98	5.42e−06	3.93
256	6.30e−05	2.99	9.88e−05	2.99	3.30e−06	2.99	4.24e−06	2.97	3.42e−07	3.98
1024	7.92e−06	2.99	1.23e−05	3.00	4.14e−07	3.00	4.91e−07	3.10	2.15e−08	4.00
4096	9.93e−07	3.00	1.54e−06	3.00	5.17e−08	3.00	5.82e−08	3.07	1.35e−09	4.00
$k=3$	$\gamma=1$		$\gamma=0.125$		$\gamma=10^{-2}$		$\gamma=10^{-4}$		$\gamma=10^{-6}$	
16	5.33e−04	–	1.49e−04	–	2.85e−05	–	1.88e−05	–	1.36e−04	–
64	3.42e−05	3.96	9.98e−06	3.90	1.83e−06	3.95	1.19e−06	3.99	5.13e−06	4.73
256	2.16e−06	3.99	6.34e−07	3.97	1.16e−07	3.98	7.42e−08	3.99	1.69e−07	4.92
1024	1.35e−07	3.99	3.98e−08	3.99	7.27e−09	3.99	4.64e−09	3.99	5.39e−09	4.98
4096	8.43e−09	4.00	2.49e−09	4.00	4.55e−10	3.99	2.90e−10	4.00	1.68e−10	4.99

TABLE A.3. Convergence and discrete $L^\infty(H^2)$ errors for *backward Euler scheme* with Cartesian meshes.

$k=0$	$\gamma=1$		$\gamma=0.125$		$\gamma=10^{-2}$		$\gamma=10^{-4}$		$\gamma=10^{-6}$	
# of cells	$\|\mathfrak{E}_h\|_{L^\infty(H^2)}$	EOC	$\|\mathfrak{E}_h\|_{L^\infty(H^2)}$	EOC	$\|\mathfrak{E}_h\|_{L^\infty(H^2)}$	EOC	$\|\mathfrak{E}_h\|_{L^\infty(H^2)}$	EOC	$\|\mathfrak{E}_h\|_{L^\infty(H^2)}$	EOC
16	1.30e−01	–	5.56e−02	–	5.17e−02	–	1.19e−01	–	1.32e−02	–
64	6.09e−02	1.09	2.96e−02	0.99	2.67e−02	0.94	6.05e−02	0.98	3.36e−03	1.97
256	2.84e−02	1.10	1.52e−02	0.96	1.36e−02	0.98	3.03e−02	0.99	8.49e−04	1.99
1024	1.39e−02	1.03	7.63e−03	0.98	6.80e−03	1.00	1.51e−02	1.00	2.13e−04	2.00
4096	6.63e−03	1.06	3.82e−03	1.00	3.41e−03	1.00	7.60e−03	1.00	5.32e−05	2.00
$k=1$	$\gamma=1$		$\gamma=0.125$		$\gamma=10^{-2}$		$\gamma=10^{-4}$		$\gamma=10^{-6}$	
16	1.97e−02	–	4.64e−03	–	4.38e−03	–	1.10e−02	–	1.57e−03	–
64	5.34e−03	1.88	1.17e−03	1.99	1.02e−03	2.09	2.59e−03	2.08	1.99e−04	2.98
256	1.37e−03	1.97	2.90e−04	2.00	2.39e−04	2.08	6.22e−04	2.05	2.49e−05	3.00
1024	3.42e−04	1.99	7.30e−05	2.00	5.87e−05	2.02	1.29e−04	2.26	3.11e−06	3.00
4096	8.58e−05	2.00	1.82e−05	2.00	1.20e−05	2.24	2.67e−05	2.27	3.89e−07	3.00
$k=2$	$\gamma=1$		$\gamma=0.125$		$\gamma=10^{-2}$		$\gamma=10^{-4}$		$\gamma=10^{-6}$	
16	3.81e−03	–	3.44e−04	–	1.99e−04	–	2.55e−04	–	1.30e−04	–
64	4.89e−04	2.96	4.52e−05	2.93	2.54e−05	2.96	3.21e−05	2.99	8.41e−06	3.95
256	6.15e−05	2.99	5.72e−06	2.98	3.19e−06	2.99	4.02e−06	3.00	5.31e−07	3.99
1024	7.71e−06	3.00	7.18e−07	3.00	4.00e−07	3.00	5.03e−07	3.00	3.32e−08	4.00
4096	9.66e−07	3.00	8.98e−08	3.00	5.02e−08	3.00	6.28e−08	3.00	2.07e−09	4.00
$k=3$	$\gamma=1$		$\gamma=0.125$		$\gamma=10^{-2}$		$\gamma=10^{-4}$		$\gamma=10^{-6}$	
16	3.84e−03	–	3.10e−04	–	2.96e−04	–	1.17e−05	–	3.68e−03	–
64	2.48e−04	3.95	2.46e−05	3.66	3.29e−05	3.90	7.49e−06	3.96	1.35e−04	4.77
256	1.56e−05	3.99	1.62e−06	3.93	2.14e−06	3.98	4.71e−08	3.99	4.41e−06	4.94
1024	9.75e−07	4.00	1.02e−07	3.98	1.28e−07	4.00	2.93e−09	4.00	1.40e−07	4.98
4096	6.09e−08	4.00	6.42e−09	4.00	4.88e−09	4.00	1.83e−10	4.00	4.37e−09	5.00

TABLE A.4. Convergence and discrete $L^\infty(H^2)$ errors for *backward Euler scheme* with polygonal meshes.

$k=0$	$\gamma=1$		$\gamma=0.125$		$\gamma=10^{-2}$		$\gamma=10^{-4}$		$\gamma=10^{-6}$	
# of cells	$\|\mathfrak{E}_h\|_{L^\infty(H^2)}$	EOC	$\|\mathfrak{E}_h\|_{L^\infty(H^2)}$	EOC	$\|\mathfrak{E}_h\|_{L^\infty(H^2)}$	EOC	$\|\mathfrak{E}_h\|_{L^\infty(H^2)}$	EOC	$\|\mathfrak{E}_h\|_{L^\infty(H^2)}$	EOC
16	1.41e−01	–	8.02e−02	–	3.20e−02	–	4.95e−03	–	2.07e−02	–
64	7.38e−02	0.93	4.16e−02	0.94	1.62e−02	0.98	1.25e−03	1.00	5.33e−03	1.96
256	3.75e−02	0.98	2.10e−02	0.98	8.15e−03	0.99	3.12e−04	1.00	1.34e−03	1.99
1024	1.89e−02	0.99	1.06e−02	0.99	4.07e−03	0.99	7.81e−05	1.00	3.36e−04	2.00
4096	9.42e−03	1.00	5.30e−03	1.00	2.03e−03	1.00	1.95e−05	1.00	8.41e−05	2.00
$k=1$	$\gamma=1$		$\gamma=0.125$		$\gamma=10^{-2}$		$\gamma=10^{-4}$		$\gamma=10^{-6}$	
16	4.59e−02	–	1.84e−02	–	3.61e−02	–	2.65e−02	–	2.05e−02	–
64	1.17e−02	1.97	4.96e−03	1.89	9.16e−03	1.98	6.96e−04	1.00	2.73e−03	2.92
256	2.96e−03	1.99	1.27e−03	1.97	2.29e−03	1.99	1.75e−04	1.02	3.51e−04	2.96
1024	7.41e−04	2.00	3.18e−04	1.99	5.74e−05	1.99	4.40e−05	1.04	4.42e−06	2.99
4096	1.85e−04	2.00	7.98e−05	2.00	1.42e−05	2.00	1.10e−05	1.00	5.54e−07	3.00
$k=2$	$\gamma=1$		$\gamma=0.125$		$\gamma=10^{-2}$		$\gamma=10^{-4}$		$\gamma=10^{-6}$	
16	7.71e−03	–	6.62e−04	–	1.79e−03	–	2.22e−04	–	3.50e−04	–
64	9.99e−04	2.94	8.42e−05	2.98	2.36e−04	2.92	2.90e−05	2.94	2.72e−05	3.69
256	1.26e−04	2.99	1.06e−05	2.99	3.05e−05	2.96	3.67e−06	2.99	1.78e−06	3.94
1024	1.58e−05	3.00	1.32e−06	3.00	3.84e−06	2.99	4.59e−07	3.00	1.12e−07	3.99
4096	1.98e−06	3.00	1.65e−07	3.00	4.81e−07	3.00	5.75e−08	3.00	7.03e−09	4.00
$k=3$	$\gamma=1$		$\gamma=0.125$		$\gamma=10^{-2}$		$\gamma=10^{-4}$		$\gamma=10^{-6}$	
16	7.53e−04	–	4.78e−05	–	2.38e−04	–	1.82e−04	–	4.47e−04	–
64	5.82e−05	3.69	3.04e−06	3.97	1.48e−06	3.99	1.18e−06	3.95	1.73e−06	4.68
256	3.81e−06	3.94	1.91e−07	3.99	9.36e−08	3.99	7.46e−08	3.99	5.74e−08	4.94
1024	2.41e−07	3.99	1.19e−08	4.00	5.84e−09	4.00	4.29e−09	4.00	1.79e−09	4.99
4096	1.51e−08	4.00	7.46e−10	4.00	3.64e−10	4.00	2.92e−10	4.00	5.63e−11	5.00

TABLE A.5. Convergence and discrete $L^\infty(H^2)$ errors for *Crank-Nicolson scheme* with Cartesian meshes.

$k=0$	$\gamma=1$		$\gamma=0.125$		$\gamma=10^{-2}$		$\gamma=10^{-4}$		$\gamma=10^{-6}$	
# of cells	$\|\mathfrak{E}_h\|_{L^\infty(H^2)}$	EOC	$\|\mathfrak{E}_h\|_{L^\infty(H^2)}$	EOC	$\|\mathfrak{E}_h\|_{L^\infty(H^2)}$	EOC	$\|\mathfrak{E}_h\|_{L^\infty(H^2)}$	EOC	$\|\mathfrak{E}_h\|_{L^\infty(H^2)}$	EOC
16	2.99e−01	–	6.54e−02	0.91	4.03e−02	0.94	1.97e−02	–	2.00e−02	–
64	1.52e−01	0.97	3.34e−02	0.96	2.04e−02	0.98	1.00e−02	0.97	5.46e−03	1.88
256	7.68e−02	0.99	1.692e−02	0.98	1.02e−02	0.99	5.05e−03	0.99	1.39e−03	1.97
1024	3.84e−02	1.00	8.480e−03	1.00	5.14e−03	1.00	2.53e−03	1.00	3.51e−04	1.99
4096	1.92e−02	1.00	4.24e−03	1.00	2.56e−03	1.00	1.26e−03	1.00	8.79e−05	2.00
$k=1$	$\gamma=1$		$\gamma=0.125$		$\gamma=10^{-2}$		$\gamma=10^{-4}$		$\gamma=10^{-6}$	
16	1.77e−02	–	8.48e−03	–	2.03e−03	–	5.16e−03	–	5.99e−04	–
64	4.44e−03	1.99	2.22e−03	1.93	5.20e−04	1.97	1.28e−03	2.01	7.92e−05	2.92
256	1.12e−03	1.99	5.64e−04	1.98	1.30e−04	1.99	1.25e−04	2.01	1.00e−05	2.98
1024	2.80e−04	1.99	1.41e−04	1.99	3.26e−05	2.00	3.06e−05	2.03	1.26e−06	2.99
4096	6.99e−05	2.00	3.53e−05	2.00	8.17e−06	2.00	6.37e−06	2.26	1.57e−07	3.00
$k=2$	$\gamma=1$		$\gamma=0.125$		$\gamma=10^{-2}$		$\gamma=10^{-4}$		$\gamma=10^{-6}$	
16	2.19e−03	–	7.26e−04	–	7.02e−04	–	3.13e−04	–	6.03e−04	–
64	2.78e−04	2.98	9.48e−05	2.93	8.58e−05	3.03	3.90e−05	3.00	4.38e−05	3.78
256	3.48e−05	2.99	1.20e−05	2.99	1.04e−05	3.04	4.73e−06	3.04	2.88e−06	3.92
1024	4.35e−06	2.99	1.50e−06	3.00	1.10e−06	3.23	5.59e−07	3.08	1.75e−07	4.04
4096	5.43e−07	3.00	1.88e−07	3.00	1.17e−07	3.22	6.55e−08	3.09	1.09e−08	4.00
$k=3$	$\gamma=1$		$\gamma=0.125$		$\gamma=10^{-2}$		$\gamma=10^{-4}$		$\gamma=10^{-6}$	
16	1.27e−03	–	1.06e−04	–	6.10e−05	–	1.06e−04	–	1.28e−04	–
64	9.27e−05	3.77	6.70e−06	3.98	3.85e−06	3.98	6.50e−06	4.02	5.11e−06	4.64
256	6.13e−06	3.92	4.20e−07	4.00	2.41e−07	3.99	3.56e−07	4.18	1.66e−07	4.94
1024	3.87e−07	3.98	2.62e−08	4.00	1.51e−08	4.00	2.10e−08	4.08	5.25e−09	4.99
4096	2.44e−08	4.00	1.64e−09	4.00	9.44e−10	4.00	1.26e−09	4.06	1.64e−10	5.00

TABLE A.6. Convergence and discrete $L^\infty(H^2)$ errors for *Crank-Nicolson scheme* with polygonal meshes.

$k=0$	$\gamma=1$		$\gamma=0.125$		$\gamma=10^{-2}$		$\gamma=10^{-4}$		$\gamma=10^{-6}$	
# of cells	$\|\mathfrak{E}_h\|_{L^\infty(H^2)}$	EOC	$\|\mathfrak{E}_h\|_{L^\infty(H^2)}$	EOC	$\|\mathfrak{E}_h\|_{L^\infty(H^2)}$	EOC	$\|\mathfrak{E}_h\|_{L^\infty(H^2)}$	EOC	$\|\mathfrak{E}_h\|_{L^\infty(H^2)}$	EOC
16	2.07e−01	–	1.55e−01	–	7.87e−02	–	7.56e−02	–	1.30e−02	–
64	1.05e−01	0.97	7.98e−02	0.96	4.02e−02	0.96	3.98e−02	0.93	3.33e−03	1.96
256	5.28e−02	0.99	4.02e−02	0.98	2.01e−02	0.99	2.02e−02	0.98	8.41e−04	1.99
1024	2.66e−02	1.00	2.00e−02	0.99	1.01e−02	1.00	1.01e−02	0.99	2.10e−04	2.00
4096	1.33e−02	1.00	1.01e−02	1.00	5.04e−03	1.00	5.07e−03	1.00	5.28e−05	2.00
$k=1$	$\gamma=1$		$\gamma=0.125$		$\gamma=10^{-2}$		$\gamma=10^{-4}$		$\gamma=10^{-6}$	
16	8.31e−02	–	2.80e−02	–	5.38e−03	–	4.99e−03	–	1.18e−02	
64	2.15e−02	1.95	7.52e−03	1.89	1.36e−03	1.99	1.25e−03	1.99	1.50e−03	2.96
256	5.40e−03	1.98	1.92e−03	1.97	3.40e−04	1.99	3.12e−04	2.00	1.86e−04	3.00
1024	1.36e−03	1.99	4.82e−04	1.99	8.50e−05	2.00	7.79e−05	2.00	2.34e−05	3.00
4096	3.39e−04	2.00	1.21e−04	2.00	2.12e−05	2.00	1.94e−05	2.00	2.93e−06	3.00
$k=2$	$\gamma=1$		$\gamma=0.125$		$\gamma=10^{-2}$		$\gamma=10^{-4}$		$\gamma=10^{-6}$	
16	8.31e−02	–	2.80e−02	–	5.38e−03	–	5.00e−03	–	1.18e−02	–
64	2.15e−02	1.95	7.52e−03	1.89	1.36e−03	1.99	1.25e−03	1.99	1.50e−03	2.96
256	5.40e−03	1.98	1.92e−03	1.97	3.10e−04	1.99	3.12e−04	2.00	1.87e−04	3.00
1024	1.36e−03	1.99	4.82e−04	1.99	8.50e−05	2.00	7.78e−05	2.00	2.34e−05	3.00
4096	3.39e−04	2.00	1.21e−04	2.00	2.13e−05	2.00	1.94e−05	2.00	2.93e−06	3.00
$k=3$	$\gamma=1$		$\gamma=0.125$		$\gamma=10^{-2}$		$\gamma=10^{-4}$		$\gamma=10^{-6}$	
16	2.74e−03	–	1.10e−03	–	3.82e−05	–	3.91e−05	–	5.50e−05	–
64	2.11e−04	3.70	7.00e−05	3.97	2.42e−06	3.98	2.47e−06	3.98	1.86e−06	4.88
256	1.69e−05	3.65	4.38e−06	3.99	1.51e−07	4.00	1.55e−07	4.00	6.35e−08	4.97
1024	1.13e−06	3.90	2.74e−07	3.99	9.44e−09	4.00	9.67e−09	4.00	1.85e−09	4.99
4096	7.17e−08	3.99	1.72e−08	4.00	5.90e−10	4.00	7.76e−11	4.00	5.82e−11	5.00

Example 8.2

TABLE A.7. Convergence and discrete $L^2(H^2)$ relative errors for *backward Euler scheme* with discontinuous $u_0(x)$.

$k=0$	$\gamma=1$		$\gamma=0.125$		$\gamma=10^{-2}$		$\gamma=10^{-4}$		$\gamma=10^{-6}$	
# of cells	$\|E_h^{\mathrm{Re}}\|_{L^2(H^2)}$	EOC	$\|E_h^{\mathrm{Re}}\|_{L^2(H^2)}$	EOC	$\|E_h^{\mathrm{Re}}\|_{L^2(H^2)}$	EOC	$\|E_h^{\mathrm{Re}}\|_{L^2(H^2)}$	EOC	$\|E_h^{\mathrm{Re}}\|_{L^2(H^2)}$	EOC
16	1.44e−01	–	5.04e−02	–	2.34e−02	–	1.38e−02	–	6.09e−03	–
64	7.56e−02	0.92	2.62e−02	0.94	1.20e−02	0.96	7.32e−03	0.92	1.57e−03	1.94
256	3.84e−02	0.97	1.33e−02	0.97	6.02e−03	0.99	3.72e−03	0.97	3.97e−04	1.98
1024	1.94e−02	0.99	6.70e−03	0.99	3.01e−03	1.00	1.87e−03	0.99	9.97e−05	2.00
$k=1$	$\gamma=1$		$\gamma=0.125$		$\gamma=10^{-2}$		$\gamma=10^{-4}$		$\gamma=10^{-6}$	
16	8.52e−03	–	4.18e−03	–	1.84e−03	–	2.72e−03	–	6.55e−04	–
64	2.16e−03	1.97	1.08e−03	1.96	4.74e−04	1.95	7.00e−04	1.96	8.36e−05	2.96
256	5.40e−04	1.99	2.70e−04	1.99	1.20e−04	1.99	2.70e−04	1.99	1.05e−05	2.99
1024	1.36e−04	2.00	6.80e−05	2.00	3.00e−05	2.00	6.80e−05	2.00	1.31e−06	3.00
$k=2$	$\gamma=1$		$\gamma=0.125$		$\gamma=10^{-2}$		$\gamma=10^{-4}$		$\gamma=10^{-6}$	
16	9.36e−04	–	4.48e−04	–	1.60e−04	–	1.33e−04	–	2.66e−05	–
64	1.19e−04	2.97	5.68e−05	2.97	2.03e−05	2.98	1.68e−05	2.98	1.71e−06	3.96
256	1.50e−05	2.99	7.12e−06	2.99	2.53e−06	2.99	2.11e−06	2.99	1.07e−07	3.99
1024	1.88e−06	3.00	8.88e−07	3.00	3.18e−07	3.00	2.64e−07	3.00	6.72e−09	4.00
$k=3$	$\gamma=1$		$\gamma=0.125$		$\gamma=10^{-2}$		$\gamma=10^{-4}$		$\gamma=10^{-6}$	
16	1.31e−04	–	6.42e−05	–	1.72e−05	–	3.08e−05	–	4.17e−06	–
64	8.43e−06	3.96	4.26e−06	3.91	1.10e−06	3.96	1.95e−06	3.97	1.34e−07	4.96
256	5.31e−07	3.99	2.70e−07	3.98	6.92e−08	3.99	1.23e−07	3.99	4.21e−09	4.99
1024	3.30e−08	4.00	1.70e−08	4.00	4.33e−09	4.00	7.71e−09	4.00	1.32e−10	5.00

TABLE A.8. Convergence and discrete $L^\infty(H^2)$ relative errors for *backward Euler scheme* with *discontinuous* $u_0(x)$.

$k=0$	$\gamma=1$		$\gamma=0.125$		$\gamma=10^{-2}$		$\gamma=10^{-4}$		$\gamma=10^{-6}$	
# of cells	$\|E_h^{\mathrm{Re}}\|_{L^\infty(H^2)}$	EOC	$\|E_h^{\mathrm{Re}}\|_{L^2(H^2)}$	EOC	$\|E_h^{\mathrm{Re}}\|_{L^\infty(H^2)}$	EOC	$\|E_h^{\mathrm{Re}}\|_{L^\infty(H^2)}$	EOC	$\|E_h^{\mathrm{Re}}\|_{L^\infty(H^2)}$	EOC
16	9.87e−02	–	9.46e−02	–	3.05e−02	–	1.77e−02	–	7.32e−03	–
64	6.03e−02	0.71	4.94e−02	0.93	1.58e−02	0.94	6.15e−03	1.52	2.45e−03	1.57
256	3.18e−02	0.91	2.51e−02	0.98	8.09e−03	0.97	2.56e−03	1.20	6.76e−04	1.85
1024	1.63e−02	0.97	1.26e−02	0.99	4.07e−03	0.99	1.21e−03	1.08	1.74e−04	1.95
$k=1$	$\gamma=1$		$\gamma=0.125$		$\gamma=10^{-2}$		$\gamma=10^{-4}$		$\gamma=10^{-6}$	
16	7.62e−02	–	2.92e−02	–	1.32e−02	–	7.81e−03	–	1.86e−03	–
64	3.96e−02	0.94	7.66e−03	1.93	3.54e−03	1.90	2.09e−03	1.90	2.34e−04	2.99
256	2.02e−02	0.97	1.94e−03	1.98	9.07e−04	1.97	5.31e−04	1.97	2.94e−05	2.99
1024	1.02e−02	0.90	4.86e−04	1.99	2.28e−04	1.99	1.34e−04	1.99	3.67e−06	2.99
$k=2$	$\gamma=1$		$\gamma=0.125$		$\gamma=10^{-2}$		$\gamma=10^{-4}$		$\gamma=10^{-6}$	
16	7.50e−03	–	5.66e−03	–	1.75e−03	–	7.38e−04	–	1.16e−04	–
64	9.81e−04	2.93	7.22e−04	2.97	2.23e−04	2.97	9.78e−05	2.93	7.70e−06	3.90
256	1.24e−04	2.99	9.09e−05	2.99	2.82e−05	2.99	1.24e−05	2.98	4.89e−07	3.97
1024	1.55e−05	3.00	1.14e−05	2.99	3.53e−06	3.00	1.55e−06	3.00	3.05e−08	4.00
$k=3$	$\gamma=1$		$\gamma=0.125$		$\gamma=10^{-2}$		$\gamma=10^{-4}$		$\gamma=10^{-6}$	
16	5.82e−04	–	8.22e−04	–	1.78e−05	–	9.95e−06	–	2.59e−06	–
64	3.66e−05	3.98	5.24e−05	3.97	1.13e−06	3.97	3.91e−07	4.66	8.32e−08	4.96
256	2.31e−06	3.99	3.30e−06	3.99	7.10e−08	3.99	1.85e−08	4.39	2.60e−09	4.99
1024	1.44e−07	4.00	2.06e−07	4.00	4.44e−09	4.00	1.04e−09	4.15	8.18e−11	5.00

TABLE A.9. Convergence and discrete $L^\infty(H^2)$ relative errors for *Crank-Nicolson scheme* with *discontinuous* $u_0(x)$.

$k=0$	$\gamma=1$		$\gamma=0.125$		$\gamma=10^{-2}$		$\gamma=10^{-4}$		$\gamma=10^{-6}$	
# of cells	$\|E_h^{\mathrm{Re}}\|_{L^\infty(H^2)}$	EOC	$\|E_h^{\mathrm{Re}}\|_{L^\infty(H^2)}$	EOC	$\|E_h^{\mathrm{Re}}\|_{L^\infty(H^2)}$	EOC	$\|E_h^{\mathrm{Re}}\|_{L^\infty(H^2)}$	EOC	$\|E_h^{\mathrm{Re}}\|_{L^\infty(H^2)}$	EOC
16	7.77e−02	–	4.90e−02	–	4.38e−02	–	2.74e−02	–	5.12e−03	–
64	4.08e−02	0.92	2.52e−02	0.92	2.29e−02	0.93	1.54e−02	0.93	1.36e−03	1.91
256	2.10e−02	0.96	1.18e−02	1.09	1.17e−02	0.98	8.02e−03	0.95	3.47e−04	1.97
1024	1.06e−02	1.00	5.62e−03	1.07	5.87e−03	0.99	4.06e−03	0.99	8.76e−05	1.99
$k=1$	$\gamma=1$		$\gamma=0.125$		$\gamma=10^{-2}$		$\gamma=10^{-4}$		$\gamma=10^{-6}$	
16	6.99e−03	–	4.58e−02	–	1.63e−02	–	4.15e−03	–	2.04e−04	–
64	1.94e−03	1.85	1.21e−02	1.92	4.22e−03	1.95	1.07e−03	1.96	2.62e−05	2.96
256	5.07e−04	1.93	3.06e−03	1.98	1.07e−03	1.98	2.68e−04	1.99	3.30e−06	2.98
1024	1.21e−04	1.97	7.70e−04	1.99	2.68e−04	1.99	6.73e−05	1.99	4.16e−07	2.99
$k=2$	$\gamma=1$		$\gamma=0.125$		$\gamma=10^{-2}$		$\gamma=10^{-4}$		$\gamma=10^{-6}$	
16	6.84e-03	–	2.14e-03	–	6.40e-04	–	2.15e-04	–	1.68e-05	–
64	8.94e-04	2.94	2.74e-04	2.97	8.34e-05	2.94	2.73e-05	2.97	1.10e-06	3.94
256	1.13e-04	2.98	3.44e-05	2.99	1.06e-05	2.98	3.43e-06	2.99	6.96e-08	3.97
1024	1.43e-05	2.99	4.32e-06	3.00	1.32e-06	2.99	4.30e-07	3.00	4.38e-09	3.99
$k=3$	$\gamma=1$		$\gamma=0.125$		$\gamma=10^{-2}$		$\gamma=10^{-4}$		$\gamma=10^{-6}$	
16	4.53e−04	–	4.64e−05	–	7.69e−05	–	5.15e−05	–	4.84e−05	–
64	2.95e−05	3.95	2.98e−06	3.95	4.89e−06	3.98	3.63e−06	3.92	1.63e−06	4.90
256	1.86e−06	3.99	1.89e−07	3.99	3.06e−07	3.99	2.31e−07	3.96	5.15e−08	4.97
1024	1.16e−07	4.00	1.19e−08	4.00	1.91e−08	3.99	1.45e−08	3.99	1.61e−09	4.99

TABLE A.10. Convergence and discrete $L^\infty(H^2)$ relative errors for *Crank-Nicolson scheme* with *discontinuous* $u_0(x)$ for $\gamma=0$.

# of cells	$k=0$		$k=1$		$k=2$		$k=3$	
	$\|\mathfrak{E}_h\|_{L^\infty(H^2)}$	EOC	$\|\mathfrak{E}_h\|_{L^\infty(H^2)}$	EOC	$\|\mathfrak{E}_h\|_{L^\infty(H^2)}$	EOC	$\|\mathfrak{E}_h\|_{L^\infty(H^2)}$	EOC
16	1.51e−02	–	2.51e−03	–	1.53e−04	–	5.91e−06	–
64	3.89e−03	1.96	3.23e−04	2.96	9.78e−06	3.97	1.88e−07	4.97
256	9.84e−04	1.99	4.08e−05	2.99	6.15e−07	3.99	5.91e−09	4.99
1024	2.47e−04	1.99	5.11e−06	3.00	3.84e−08	4.00	1.84e−10	5.00

Example 8.3

TABLE A.11. Convergence and discrete $L^2(H^2)$ errors for *backward Euler scheme* with Cartesian meshes: Case I.

# of cells	$k=0$		$k=1$		$k=2$		$k=3$	
	$\|\mathfrak{E}_h\|_{L^2(H^2)}$	EOC	$\|\mathfrak{E}_h\|_{L^2(H^2)}$	EOC	$\|\mathfrak{E}_h\|_{L^2(H^2)}$	EOC	$\|\mathfrak{E}_h\|_{L^2(H^2)}$	EOC
16	7.26e−01	–	1.01e−01	–	8.98e−03	–	1.18e−03	–
64	1.79e−01	2.01	1.35e−02	2.90	6.18e−04	3.86	4.12e−05	4.83
256	4.47e−02	2.00	1.71e−03	2.98	3.95e−05	3.96	1.33e−06	4.95
1024	1.12e−02	2.00	2.14e−04	2.99	2.47e−06	3.99	4.17e−08	4.98
4096	2.81e−03	2.00	2.68e−05	3.00	1.55e−07	4.00	1.00e−09	5.00

TABLE A.12. Convergence and discrete $L^2(H^2)$ errors for *backward Euler scheme* with polygonal meshes: Case I.

# of cells	$k=0$		$k=1$		$k=2$		$k=3$	
	$\|\mathfrak{E}_h\|_{L^2(H^2)}$	EOC	$\|\mathfrak{E}_h\|_{L^2(H^2)}$	EOC	$\|\mathfrak{E}_h\|_{L^2(H^2)}$	EOC	$\|\mathfrak{E}_h\|_{L^2(H^2)}$	EOC
16	1.94e−01	–	2.80e−02	–	3.25e−03	–	5.21e−04	–
64	4.89e−02	1.98	3.92e−03	2.83	2.36e−04	3.78	1.94e−05	4.74
256	1.23e−02	1.99	5.04e−04	2.95	1.54e−05	3.94	6.38e−07	4.92
1024	3.09e−03	1.99	6.36e−05	2.98	9.72e−07	3.98	2.01e−08	4.98
4096	7.75e−04	2.00	7.96e−06	3.00	6.08e−08	4.00	6.34e−10	5.00

TABLE A.13. Convergence and discrete $L^\infty(H^2)$ errors for *backward Euler scheme* with Cartesian meshes: Case I.

# of cells	$k=0$		$k=1$		$k=2$		$k=3$	
	$\|\mathfrak{E}_h\|_{L^\infty(H^2)}$	EOC	$\|\mathfrak{E}_h\|_{L^\infty(H^2)}$	EOC	$\|\mathfrak{E}_h\|_{L^\infty(H^2)}$	EOC	$\|\mathfrak{E}_h\|_{L^\infty(H^2)}$	EOC
16	6.69e−02	–	5.68e−03	–	1.64e−04	–	1.07e−05	–
64	1.80e−02	1.89	7.33e−04	2.95	1.06e−05	3.96	3.37e−07	4.98
256	4.62e−03	1.96	9.27e−05	2.99	6.69e−07	3.99	1.06e−08	4.99
1024	1.17e−03	1.99	1.16e−05	2.99	4.18e−08	3.99	3.30e−10	4.99
4096	2.93e−04	2.00	1.45e−06	3.00	2.62e−09	4.00	1.06e−11	5.00

TABLE A.14. Convergence and discrete $L^\infty(H^2)$ errors for *backward Euler scheme* with polygonal meshes: Case I.

# of cells	$k=0$		$k=1$		$k=2$		$k=3$	
	$\|\mathfrak{E}_h\|_{L^\infty(H^2)}$	EOC	$\|\mathfrak{E}_h\|_{L^\infty(H^2)}$	EOC	$\|\mathfrak{E}_h\|_{L^\infty(H^2)}$	EOC	$\|\mathfrak{E}_h\|_{L^\infty(H^2)}$	EOC
16	1.53e−02	–	1.24e−03	–	8.84e−05	–	1.77e−05	–
64	3.99e−03	1.93	1.61e−04	2.94	6.41e−06	3.78	5.85e−07	4.91
256	1.02e−03	1.96	2.02e−05	2.98	4.13e−07	3.95	1.85e−08	4.98
1024	2.58e−04	1.98	2.40e−06	2.99	2.59e−08	3.99	5.81e−10	4.99
4096	6.45e−05	2.00	3.16e−07	3.00	1.62e−09	4.00	1.82e−11	4.99

TABLE A.15. Convergence and discrete $L^\infty(H^2)$ errors for *Crank-Nicolson scheme* with Cartesian meshes: Case I.

# of cells	$k=0$		$k=1$		$k=2$		$k=3$	
	$\|\mathfrak{E}_h\|_{L^\infty(H^2)}$	EOC	$\|\mathfrak{E}_h\|_{L^\infty(H^2)}$	EOC	$\|\mathfrak{E}_h\|_{L^\infty(H^2)}$	EOC	$\|\mathfrak{E}_h\|_{L^\infty(H^2)}$	EOC
16	1.07e−01	–	1.98e−02	–	1.58e−03	–	3.56e−04	–
64	2.64e−02	2.01	2.54e−03	2.95	1.16e−04	3.77	1.28e−05	4.80
256	6.55e−03	2.00	3.22e−04	2.98	7.52e−06	3.94	4.09e−07	4.95
1024	1.64e−03	2.00	4.03e−05	2.99	4.74e−07	3.98	1.29e−08	4.99
4096	4.07e−04	2.00	5.03e−06	3.00	2.97e−08	4.00	4.05e−10	5.00

TABLE A.16. Convergence and discrete $L^\infty(H^2)$ errors for *Crank-Nicolson scheme* with polygonal meshes: Case I.

# of cells	$k=0$		$k=1$		$k=2$		$k=3$	
	$\|\mathfrak{E}_h\|_{L^\infty(H^2)}$	EOC	$\|\mathfrak{E}_h\|_{L^\infty(H^2)}$	EOC	$\|\mathfrak{E}_h\|_{L^\infty(H^2)}$	EOC	$\|\mathfrak{E}_h\|_{L^\infty(H^2)}$	EOC
16	1.68e−02	–	3.40e−03	–	5.20e−04	–	7.33e−05	–
64	4.29e−03	1.96	4.88e−04	2.80	3.54e−05	3.87	2.38e−06	4.94
256	1.09e−03	1.98	6.27e−05	2.95	2.26e−06	3.97	7.50e−08	4.98
1024	2.73e−04	1.99	7.88e−06	2.99	1.42e−07	3.99	2.34e−09	4.99
4096	6.84e−05	2.00	9.86e−07	3.00	8.86e−09	4.00	7.28e−11	5.00

TABLE A.17. Convergence and discrete $L^2(H^2)$ errors for *backward Euler scheme* with Cartesian meshes: Case II.

# of cells	$k=0$		$k=1$		$k=2$		$k=3$	
	$\|\mathfrak{E}_h\|_{L^2(H^2)}$	EOC	$\|\mathfrak{E}_h\|_{L^2(H^2)}$	EOC	$\|\mathfrak{E}_h\|_{L^2(H^2)}$	EOC	$\|\mathfrak{E}_h\|_{L^2(H^2)}$	EOC
16	2.64e−01	–	1.15e−03	–	4.49e−06	–	2.46e−05	–
64	2.30e−01	1.98	1.42e−04	3.00	2.84e−07	3.98	8.40e−07	4.97
256	5.74e−02	2.00	1.77e−05	3.00	1.79e−08	3.99	2.68e−08	4.97
1024	1.42e−02	1.99	2.20e−06	3.00	1.12e−09	3.99	8.44e−10	4.99
4096	3.45e−03	2.03	2.76e−07	2.99	7.01e−11	4.00	2.64e−11	5.00

TABLE A.18. Convergence and discrete $L^2(H^2)$ errors for *backward Euler scheme* with polygonal meshes: Case II.

# of cells	$k=0$		$k=1$		$k=2$		$k=3$	
	$\|\mathfrak{E}_h\|_{L^2(H^2)}$	EOC	$\|\mathfrak{E}_h\|_{L^2(H^2)}$	EOC	$\|\mathfrak{E}_h\|_{L^2(H^2)}$	EOC	$\|\mathfrak{E}_h\|_{L^2(H^2)}$	EOC
16	1.54e−03	–	1.09e−04	–	4.98e−06	–	2.61e−04	–
64	1.44e−02	2.07	1.28e−04	3.13	3.62e−06	4.19	3.08e−04	5.17
256	3.81e−03	2.00	1.68e−05	3.03	2.26e−07	4.10	4.07e−05	5.08
1024	9.81e−04	2.02	2.02e−06	3.05	1.34e−08	4.06	4.52e−06	5.07
4096	2.52e−04	2.03	2.46e−07	3.04	8.15e−10	4.05	5.51e−07	5.06

TABLE A.19. Convergence and discrete $L^\infty(H^2)$ errors for *backward Euler scheme* with Cartesian meshes: Case II.

# of cells	$k=0$		$k=1$		$k=2$		$k=3$	
	$\|\mathfrak{E}_h\|_{L^\infty(H^2)}$	EOC	$\|\mathfrak{E}_h\|_{L^\infty(H^2)}$	EOC	$\|\mathfrak{E}_h\|_{L^\infty(H^2)}$	EOC	$\|\mathfrak{E}_h\|_{L^\infty(H^2)}$	EOC
16	2.96e−02	–	1.04e−02	–	1.10e−04	–	2.18e−04	–
64	7.44e−03	1.99	1.30e−03	3.00	7.08e−06	3.96	7.76e−06	4.81
256	1.87e−03	2.00	1.58e−04	3.03	4.44e−07	3.99	2.51e−07	4.95
1024	4.65e−04	2.00	1.95e−05	3.02	2.78e−08	4.00	7.92e−09	4.99
4096	1.17e−04	2.00	2.42e−06	3.00	1.74e−09	4.00	2.47e−10	5.00

TABLE A.20. Convergence and discrete $L^\infty(H^2)$ errors for *backward Euler scheme* with polygonal meshes: Case II.

# of cells	$k=0$		$k=1$		$k=2$		$k=3$	
	$\|\mathfrak{E}_h\|_{L^\infty(H^2)}$	EOC	$\|\mathfrak{E}_h\|_{L^\infty(H^2)}$	EOC	$\|\mathfrak{E}_h\|_{L^\infty(H^2)}$	EOC	$\|\mathfrak{E}_h\|_{L^\infty(H^2)}$	EOC
16	8.43e−03	–	6.44e−04	–	2.47e−04	–	5.32e−05	–
64	2.15e−03	1.96	8.14e−05	2.99	1.66e−05	3.69	1.64e−06	5.01
256	5.40e−04	1.99	1.02e−05	2.96	1.07e−06	3.95	5.15e−08	4.99
1024	1.35e−04	2.00	1.28e−06	3.00	6.77e−08	3.99	1.61e−09	5.00
4096	3.39e−05	2.00	1.60e−07	3.00	4.24e−09	4.00	5.03e−11	5.00

TABLE A.21. Convergence and discrete $L^\infty(H^2)$ errors for *Crank-Nicolson scheme* with Cartesian meshes: Case II.

# of cells	$k=0$		$k=1$		$k=2$		$k=3$	
	$\|\mathfrak{E}_h\|_{L^\infty(H^2)}$	EOC	$\|\mathfrak{E}_h\|_{L^\infty(H^2)}$	EOC	$\|\mathfrak{E}_h\|_{L^\infty(H^2)}$	EOC	$\|\mathfrak{E}_h\|_{L^\infty(H^2)}$	EOC
16	1.77e−02	–	8.56e−04	–	5.17e−04	–	1.18e−04	–
64	4.44e−03	1.99	1.13e−04	2.92	3.76e−05	3.78	4.75e−06	4.64
256	1.12e−03	1.99	1.43e−05	2.98	2.47e−06	3.92	1.55e−07	4.94
1024	2.80e−04	1.99	1.80e−06	2.99	5.46e−08	3.02	4.88e−09	4.99
4096	6.99e−05	2.00	2.24e−07	3.00	9.85e−09	4.00	1.52e−10	5.00

TABLE A.22. Convergence and discrete $L^\infty(H^2)$ errors for *Crank-Nicolson scheme* with polygonal meshes: Case II.

# of cells	$k=0$		$k=1$		$k=2$		$k=3$	
	$\|\mathfrak{E}_h\|_{L^\infty(H^2)}$	EOC	$\|\mathfrak{E}_h\|_{L^\infty(H^2)}$	EOC	$\|\mathfrak{E}_h\|_{L^\infty(H^2)}$	EOC	$\|\mathfrak{E}_h\|_{L^\infty(H^2)}$	EOC
16	1.13e−02	–	1.58e−03	–	9.22e−05	3.95	7.81e−05	–
64	2.93e−03	1.96	2.01e−04	2.96	5.73e−06	4.00	2.51e−06	4.95
256	7.41e−04	1.99	2.56e−05	2.99	3.59e−07	4.00	7.93e−08	4.98
1024	1.86e−04	2.00	3.21e−06	3.00	2.24e−08	4.00	2.49e−09	5.00
4096	4.62e−05	2.00	4.02e−07	3.00	1.40e−09	4.00	7.74e−11	5.00

Decay of errors

TABLE A.23. (Examples 8.1 (for $\gamma=1$) and 8.3 (for $\gamma=0$)). Decay of errors in $L^\infty(H^2)$-norm in time direction for fixed 1024 mesh elements.

Time-level	$\gamma=1,k=0$		$\gamma=1,k=2$		$\gamma=0,k=0$		$\gamma=0,k=2$	
	CN-Scheme	BE-Scheme	CN-Scheme	BE-Scheme	CN-Scheme	BE-Scheme	CN-Scheme	BE-Scheme
Level 1	1.15e−04	3.88e−03	6.28e−03	2.12e−01	8.49e−04	2.86e−02	3.12e−04	1.05e−02
Level 2	2.88e−05	1.85e−03	1.57e−03	1.01e−01	2.13e−04	1.36e−02	7.82e−05	5.02e−03
Level 3	7.17e−06	9.00e−04	3.92e−04	4.91e−02	5.30e−05	6.65e−03	1.95e−05	2.45e−03
Level 4	1.77e−06	4.44e−04	9.67e−05	2.42e−02	1.31e−05	3.28e−03	4.82e−06	1.21e−03
Level 5	4.21e−07	2.20e−04	2.30e−05	1.20e−02	3.11e−06	1.63e−03	1.14e−06	5.99e−04